



US Army Corps
of Engineers®

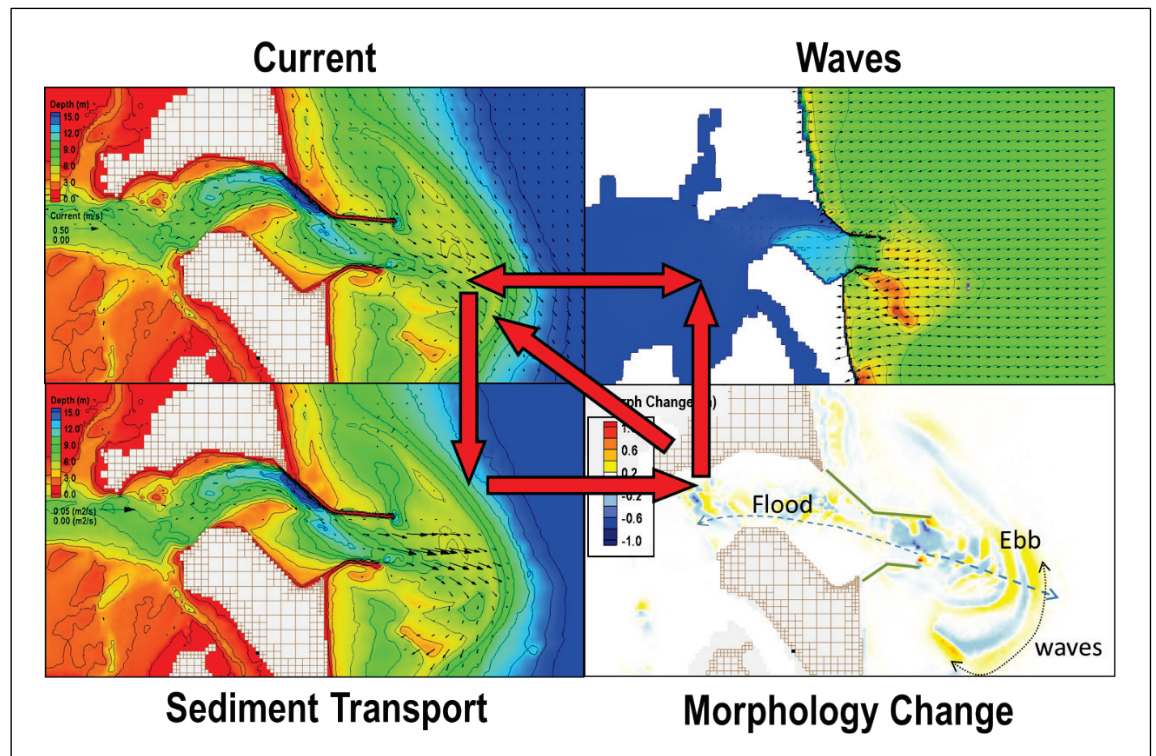


Coastal Inlets Research Program

Coastal Modeling System User's Manual

Honghai Li, Mitchell E. Brown, Lihwa Lin, Yan Ding, Tanya M. Beck,
Alejandro Sánchez, Weiming Wu, Christopher W. Reed, and
Alan K. Zundel

Month 2024



The US Army Engineer Research and Development Center (ERDC) solves the nation's toughest engineering and environmental challenges. ERDC develops innovative solutions in civil and military engineering, geospatial sciences, water resources, and environmental sciences for the Army, the Department of Defense, civilian agencies, and our nation's public good. Find out more at www.erdclibrary.on.worldcat.org/discovery.

To search for other technical reports published by ERDC, visit the ERDC online library at <http://www.erdclibrary.on.worldcat.org/discovery>.

Coastal Modeling System User's Manual

Honghai Li, Mitchell E. Brown, Lihwa Lin, Yan Ding, and Tanya M. Beck

*US Army Engineer Research and Development Center
Coastal and Hydraulics Laboratory
3909 Halls Ferry Road
Vicksburg, MS 39180-6199*

Alejandro Sánchez

*Hydrologic Engineering Center, US Army Corps of Engineers
609 Second Street
Davis, CA 95616-4687*

Weiming Wu

*Department of Civil and Environmental Engineering
Wallace H. Coulter School of Engineering
Clarkson University
8 Clarkson Avenue
Potsdam, New York 13699*

Christopher W. Reed

*Reed and Reed Consulting, LLC
1400 Village Square Blvd Unit 3-146
Tallahassee, FL 32312*

Alan K. Zundel

*Aquaveo, LLC
3210 N. Canyon Road
Provo, UT 84604*

Final Special Report (SR)

Distribution Statement A. Approved for public release: distribution is unlimited.

Prepared for US Army Engineer Research and Development Center
Coastal and Hydraulics Laboratory
3909 Halls Ferry Road
Vicksburg, MS 39180-6199

Under Funding Account Code U4391283; AMSCO Code 060000

Abstract

The Coastal Modeling System (CMS) is a suite of coupled 2D numerical models for simulating nearshore waves, currents, water levels, sediment transport, morphology change, and salinity and temperature. Developed by the Coastal Inlets Research Program of the US Army Corps of Engineers, the CMS provides coastal engineers and scientists a PC-based, easy-to-use, accurate, and efficient tool for understanding of coastal processes and for designing and managing of coastal inlets research, navigation projects, and sediment exchange between inlets and adjacent beaches. The present technical report acts as a user guide for the CMS, which contains comprehensive information on model theory, model setup, and model features. The detailed descriptions include creation of a new project, configuration of model grid, various types of boundary conditions, representation of coastal structures, numerical methods, and coupled simulations of waves, hydrodynamics, and sediment transport. Pre- and post-model data processing and CMS modeling procedures are also described through operation within a graphic user interface—the Surface-water Modeling System.

DISCLAIMER: The contents of this report are not to be used for advertising, publication, or promotional purposes. Citation of trade names does not constitute an official endorsement or approval of the use of such commercial products. All product names and trademarks cited are the property of their respective owners. The findings of this report are not to be construed as an official Department of the Army position unless so designated by other authorized documents.

DESTROY THIS REPORT WHEN NO LONGER NEEDED. DO NOT RETURN IT TO THE ORIGINATOR.

Contents

Abstract	ii
Figures and Tables.....	viii
Preface.....	xi
1 Introduction.....	1
1.1 Background.....	1
1.1.1 The Surface-water Modeling System (SMS)	2
1.1.2 Coastal Modeling System–Wave (CMS-Wave)	3
1.1.3 Coastal Modeling System-Flow (CMS-Flow).....	3
1.2 Objective.....	4
1.3 Approach	4
2 Hydrodynamics	6
2.1 Governing Equations	6
2.2 Model Forcing	7
2.2.1 Bed Shear Stress	7
2.2.2 Wind Surface Stress	9
2.2.3 Wave Radiation Stresses.....	11
2.2.4 Surface Roller Stresses	11
2.2.5 Eddy Viscosity.....	12
2.2.5.1 Subgrid Model	12
2.2.5.2 Falconer Equation	13
2.2.5.3 Depth-averaged Parabolic Model	13
2.2.5.4 Mixing Length Model	13
2.2.6 Wave Flux Velocity.....	14
2.3 Boundary Conditions	15
2.3.1 Wall Boundary	15
2.3.2 Flux Boundary.....	16
2.3.3 Water Level Boundary.....	17
2.3.4 Cross-Shore Boundary	18
3 Wave Transformation	20
3.1 Governing Equations	20
3.2 Wave Characteristics.....	21
3.2.1 Wave Diffraction.....	21
3.2.2 Wave-Current Interaction.....	22
3.2.3 Wave-Breaking Formulas.....	22
3.2.4 Bottom Friction Loss	23
3.2.5 Wave Runup	24
3.2.6 Wave Transmission and Overtopping at Structures.....	25
3.3 Wind Forcing	26

3.3.1	Wind Input Function.....	27
3.3.2	Whitecapping Dissipation Function	28
3.3.3	Wave Generation with Arbitrary Wind Direction	28
3.4	Model features.....	28
3.4.1	Variable-Rectangular-Cell Grid	28
3.4.2	Grid Nesting.....	29
3.4.3	Nonlinear Wave-Wave Interaction.....	29
3.4.4	Infragravity Wave Effect at Inlets	30
3.4.5	Wave Dissipation over Muddy Bed	30
3.4.6	Full-Plane and Wind-Field Input Capabilities.....	30
3.4.7	Fast-Mode Calculation	31
4	Sediment Transport	32
4.1	Governing Equations	32
4.1.1	Nonequilibrium Total-Load Transport Model.....	32
4.1.1.1	Total-Load Transport Equation	32
4.1.1.2	Fraction of Suspended Sediment.....	33
4.1.1.3	Adaptation Coefficient.....	33
4.1.1.4	Total-Load Correction Factor	34
4.1.1.5	Bed Change Equation.....	35
4.1.2	Equilibrium Concentrations and Transport Rates.....	36
4.1.2.1	Lund-Coastal Inlets Research Program (CIRP)	36
4.1.2.2	van Rijn	37
4.1.2.3	Soulsby-van Rijn	38
4.1.2.4	Watanabe.....	39
4.1.2.5	Cross-SHORE (CSHORE).....	40
4.2	Bed Material Layering and Sorting	41
4.3	Sediment Characteristics	43
4.3.1	Sediment Fall Velocity	43
4.3.2	Hiding and Exposure.....	43
4.3.3	Ripple Dimensions.....	45
4.3.4	Scaling Factors.....	45
4.3.4.1	Transport Scaling Factors	45
4.3.4.2	Morphologic Acceleration Factor	45
4.3.5	Hard Bottom	46
4.3.5.1	Bed-Slope.....	46
4.3.5.2	Avalanching.....	46
4.3.6	Horizontal Sediment Mixing Coefficient.....	46
4.3.7	Multiple-Sized Sediment Transport.....	47
4.3.7.1	Sediment Size Classes	47
4.3.7.2	Fractional Bed Composition.....	47
4.3.7.2.1	D50 Dataset and Geometric Standard Deviation.....	48
4.3.7.2.2	D16, D50, and D84 Datasets.....	48
4.3.7.2.3	D35, D50, and D90 Datasets.....	48
4.3.7.2.4	Cumulative Grain Size Distribution.....	49
4.3.7.2.5	Size Class Fractions	49

4.3.7.3	Bed Layer Thickness	49
4.3.7.4	Mixing Layer	49
4.4	Boundary Conditions	50
5	Salinity and Temperature Calculations.....	51
5.1	Governing Equations	51
5.1.1	Salinity Calculations.....	51
5.1.2	Temperature Calculations	52
5.1.2.1	Short-Wave Solar Radiation, <i>JSW</i>	53
5.1.2.2	Long-Wave Atmospheric Radiation, <i>JLW</i>	53
5.1.2.3	Latent Heat Flux, <i>JE</i>	53
5.1.2.4	Sensible Heat Flux, <i>J</i> , <i>JS</i>	53
5.2	Initial Condition	54
5.3	Boundary Conditions	54
6	Coastal Modeling System (CMS) Features.....	55
6.1	Model Hot Start.....	55
6.2	Grid Nesting	55
6.3	Sea Level Change	55
6.4	Coastal Structures	56
6.4.1	Rubble Mound.....	56
6.4.2	Weir.....	58
6.4.3	Culvert	59
6.4.4	Tide Gate	61
6.5	Dredging Operation.....	62
6.6	Sediment Mapping	66
7	Numerical Methods	67
7.1	Computational Grid.....	67
7.2	Model Discretization	70
7.3	Solver Options.....	71
7.4	Skewness Correction	71
7.5	Advection Schemes	72
7.6	Wetting and Drying	72
7.7	Parallelization	72
8	CMS-Flow Model Setup	74
8.1	Overview of Input and Output	74
8.1.1	Input Files.....	74
8.1.2	Output Files	75
8.2	Display Projections	76
8.3	Load Bathymetric Information for Project	77
8.4	Combining Multiple Datasets for Final Bathymetry	79
8.4.1	Changing Vertical Datums.....	80
8.4.1.1	Datum Conversion.....	81

8.4.1.2	Unit Conversion	83
8.4.1.3	Sign Change	84
8.4.2	Merging Data from Surveys	84
8.4.2.1	Merge All Scatter Points	84
8.4.2.2	Removing Triangulated Elements	86
8.4.2.3	Merge Scatter Sets with Priority	87
8.5	Using Dynamic Images	89
8.6	Building a Conceptual Model for Project	89
8.6.1	Create the Necessary Coverages	90
8.6.2	Create Quadtree Project Domain	92
8.6.3	Defining the Interface Between Land and Water Interface (Activity Classification)	94
8.6.4	Defining Grid Resolution	100
8.6.5	Creating the Quadtree Grid	102
8.6.6	Defining CMS Forcing (Boundary Conditions)	106
8.6.6.1	Water Level Boundary Condition	106
8.6.6.2	River Flux Boundary Condition	108
8.7	Running CMS-Flow	109
8.7.1	Create a CMS-Flow simulation	109
8.7.2	Defining CMS-Flow Model Control	110
8.7.2.1	General Tab	110
8.7.2.2	Flow Tab	110
8.7.2.3	Sediment Transport Tab	111
8.7.2.4	Salinity/Temperature Tab	111
8.7.2.5	Wave Tab	111
8.7.2.6	Wind Tab	111
8.7.2.7	Output Tab	111
8.7.3	Bottom Roughness	111
8.7.4	Sediment D50 Dataset	112
8.7.5	Hard Bottom Dataset	113
8.7.6	Assign Spatially Varying Datasets to Model Control	114
8.7.7	Viewing the Corresponding CMS cells for Boundary Conditions	115
8.7.8	Save Simulation	116
8.7.9	Changing Version of Model, If Needed	117
8.7.10	Launch Simulation	117
9	CMS-Wave Model Setup	119
9.1	Overview of Input and Output	119
9.1.1	Input Files	119
9.1.2	Output Files	120
9.2	Grid Generation	121
9.2.1	Importing the Scatter Set Data File	121
9.2.2	Setting the Global Projection and Background Maps	122
9.2.3	Creating the Cartesian Grid for CMS-Wave	124
9.3	Generating Wave Spectral Input for CMS-Wave	131
9.4	Create a New CMS-Wave Simulation	136

9.5	Model Control and CMS-Wave Parameters.....	137
9.6	Selecting Special Output Stations	140
9.7	Specifying Optional Structure Features.....	141
9.8	Running CMS-Wave	143
9.8.1	Export CMS-Wave files.....	143
9.8.2	Running from SMS.....	144
9.9	Specifications of Advanced CMS-Wave Features	144
9.9.1	Fast Mode Versus Standard Mode	145
9.9.2	Full-Plane.....	145
9.9.3	Wave Run-Up, Infragravity Wave, Nonlinear Wave-Wave Interaction, Muddy Bed, Spatial Wind Input.....	145
9.9.4	Permeable Structures.....	146
9.9.5	Grid Nesting.....	146
9.9.6	Spatially Varied Spectral Wave Input.....	146
9.9.7	Wave Roller in Surf Zone	146
10	CMS Dynamic Coupling (Steering)	147
10.1	Modify Flow Model Control for steering.....	147
10.2	Start the Steering Run.....	148
11	Summary.....	151
	References	152
	Abbreviations	163
	Report Documentation Page (SF 298)	165

Figures and Tables

Figures

1-1. Coastal Modeling System (CMS) framework and its components.....	2
2-1. Cross-shore and longshore coordinate.	19
4-1. Multiple bed layer model of bed material sorting.....	42
4-2. Schematic of the exposure height of bed sediment grains.	44
6-1. Sketch of culvert flow.	59
6-2. Schematic showing flow through a tide gate.	62
7-1. Examples of invalid Cartesian computational grids.	68
7-2. Types of Cartesian and telescoping grids supported by the Surface-water Modeling System (SMS) interface and CMS-Flow.	69
7-3. Computational stencils and control volumes for two types of Cartesian grids: nonuniform Cartesian (<i>left</i>) and telescoping grid (<i>right</i>).	69
8-1. Display Projection dialog window.	76
8-2. Horizontal Projection dialog window. Setting the Display Projection.	77
8-3. File Import Wizard dialog window—Step 1 of 2.....	78
8-4. File Import Wizard dialog window—Step 2 of 2.....	79
8-5. NOAA benchmark sheet for Long Branch Fishing Pier, New Jersey. (Image reproduced from NOAA, “Tides and Currents,” n.d. Public domain.).....	80
8-6. Graphical representation of datum relationships from benchmark sheet (Figure 8-5). (Image adapted from NOAA, “Tides and Currents,” n.d. Public domain.).	81
8-7. Diagram of datum changes.	82
8-8. Dataset Toolbox dialog window.	83
8-9. Merge Scatter Points dialog window.	85
8-10. Triangulated elements for merged scatter set.	86
8-11. Merge Scatter Sets window. Reordered list of scatter sets to be merged with priority.	88
8-12. Scatter points and contours for the final merged scatter set.	89
8-13. New Coverage dialog window for Coastal Modeling System-Flow (CMS-Flow) boundary conditions.....	91
8-14. Updated coverages in Surface-water Modeling System (SMS) data tree.	92
8-15. Point locations to define the extents of the grid frame.....	93
8-16. Grid Frame Properties dialog window.	94
8-17. Data access section of the NOAA website mentioned above. (Image reproduced from NOAA, “Shoreline Website,” n.d. Public domain.).....	95
8-18. Geographic Information System (GIS) to Feature Objects Wizard dialog window.	96
8-19. Create Contour Arcs dialog window.....	97
8-20. Bathymetry contour converted to feature arc.	97
8-21. Example of extra arcs to delete.....	98

8-22. Before and after extra resolution is removed from feature arcs.....	99
8-23. Enclosed set of feature arcs for defining land (inactive) area.....	99
8-24. Activity Classification Coverage dialog window. Activity Classification type selection for polygon.	100
8-25. Example of resolution zones defined for a CMS grid.	101
8-26. Polygon Attributes dialog window. Setting a resolution value for a polygon.....	102
8-27. Map → Quadtree UGrid dialog window. Data needed for generating the quadtree grid.....	103
8-28. Two resolution variations on a quadtree grid with increasing complexity.	104
8-29. Select Intersecting Objects dialog window. Making the proper selection of cells to turn off.	105
8-30. Display after selected cells were turned off.	105
8-31. Example placement of the water level forcing arc.	107
8-32. XY Series Editor dialog window. Properly completed XY Series Editor for water level curve.....	108
8-33. Data tree after adding options to the new simulation.	110
8-34. Location of scalar entry point denoted by S.	112
8-35. Snapped Preview indicator for boundary cells.	116
8-36. Folder structure on disk for each SMS 13.2 project.	117
8-37. Simulation Run Queue dialog window for a CMS-Flow simulation.....	118
9-1. Scatter dataset appearance in the SMS screen.....	122
9-2. Display projection dialogs.	123
9-3. Add online dynamic image in the SMS screen.	123
9-4. Creating the Cartesian grid frame.	124
9-5. The origin is shown at the <i>upper right corner</i> of the grid.....	125
9-6. Display Grid Frame Properties dialog window.	126
9-7. Display Feature Point properties menu window.	126
9-8. Specifying refine base cell size in the Refine Point window.	127
9-9. Grid Frame Properties dialog window. Specifying refine point maximum cell size and growth factor.....	128
9-10. Display Map → 2D Grid dialog window.....	129
9-11. Display Interpolation dialog window.....	129
9-12. CMS-Wave grid with variable cell size.....	130
9-13. CMS-Wave grid with bathymetry contours.	130
9-14. Display Information dialog window.	131
9-15. Display New Coverage window.....	132
9-16. Display Spectral Energy dialog window.....	133
9-17. Display Create Spectral Energy Grid dialog window.....	133
9-18. Display Generate Spectra dialog window.	135
9-19. Display spectral contours in Spectral Energy dialog window.....	136

9-20. Choices to create a new CMS-Wave simulation.	137
9-21. Display CMS-Wave Model Control dialog window.....	138
9-22. Display Boundary Control page from Model Control dialog window.....	139
9-23. Model Control dialog window. Display CMS-Wave simulation Options page.	140
9-24. Assign Structure selection window from the right-click menu.....	142
9-25. Assign Structure dialog window.....	142
9-26. Simulation Run Queue dialog window for a CMS-Wave simulation.	144
10-1. CMS-Flow Model Control dialog window, Wave tab.....	148
10-2. Example of the SMS interface for CMS-Flow and CMS-Wave steering.	149
10-3. CMS-Flow Simulation Run Queue dialog window for steering.	150

Tables

7-1. Card format for the selection of the advection scheme.....	72
8-1. List of CMS-Flow input files.....	74
8-2. List of CMS-Flow output files.	75
8-3. Types of grid solution output files.....	75
9-1 CMS-Wave input files.	120
9-2. CMS-Wave output files.	121
9-3. Example of incident wave parameters.	134
9-4. List of column contents for selhts.out file.....	141

Preface

This study was conducted for the US Army Engineer Research and Development Center (ERDC), Coastal and Hydraulics Laboratory (CHL), under the Coastal Inlets Research Program (CIRP), Coastal Modeling System Work Unit CMS Development, V&V, Tech Transfer, and User Support; Funding Account Code U4391283, AMSCO Code o60000.

The work was performed by the Coastal Engineering Branch of the Navigation Division and the Coastal Processes Branch of the Flood and Storm Protection Division, ERDC-CHL. At the time of publication of this report, Ms. Lauren M. Dunkin was chief, Coastal Engineering Branch, and Mr. Victor Gonzalez was chief, Coastal Processes Branch; Ms. Ashley E. Frey was chief, Navigation Division, and Mr. David May was chief, Flood and Storm Protection Division; Dr. Tanya M. Beck was CIRP program manager; Ms. Tiffany Burroughs was chief, Headquarters, US Army Corps of Engineers, Navigation Branch and Navigation business line manager; and Mr. Charles E. Wiggins, CHL, was ERDC technical director for Navigation. Mr. Keith W. Flowers was deputy director of CHL, and Dr. Ty V. Wamsley was the director.

The commander of ERDC was COL Christian Patterson, and the director was Dr. David W. Pittman.

This page intentionally left blank.

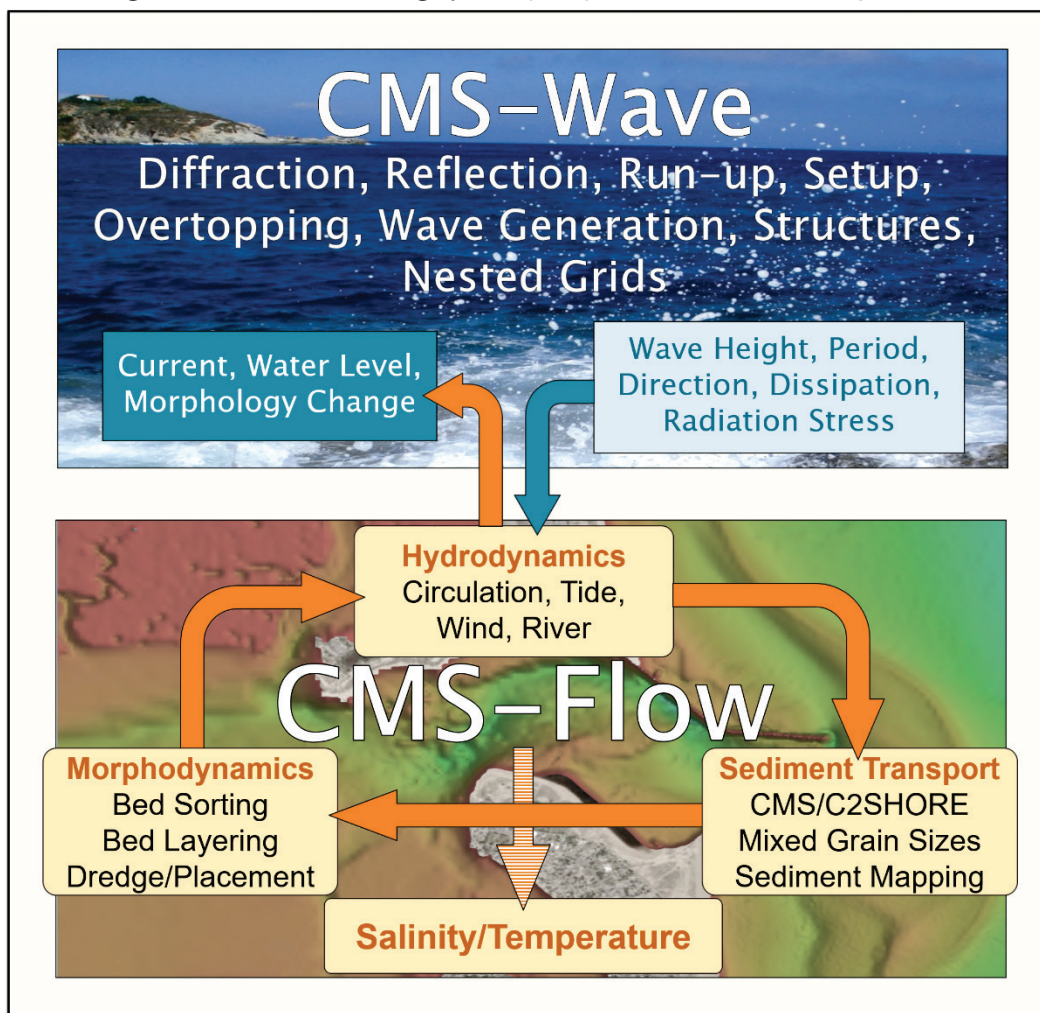
1 Introduction

1.1 Background

The Coastal Modeling System (CMS) is a numerical modeling system for nearshore waves, currents, water levels, sediment transport, and morphology change (Buttolph et al. 2006; Lin et al. 2008; Reed et al. 2011; Wu et al. 2011; Sánchez et al. 2014; Sánchez et al. 2016). The system was developed and continues to be supported by the Coastal Inlets Research Program (CIRP), a research and development program of the US Army Corps of Engineers (USACE) that is funded by the Operation and Maintenance Navigation Business Line of the USACE. The CMS is designed for coastal inlets and navigation applications, including channel performance and sediment exchange between inlets and adjacent beaches. Modeling provides planners and engineers with essential information for reducing costs of USACE Operation and Maintenance activities. CIRP is developing, testing, improving, transferring the CMS to USACE districts, industry, and academia and assisting users with engineering and scientific studies.

The overall framework of the CMS and its components is presented in Figure 1-1. The CMS includes a flow model (CMS-Flow) that calculates hydrodynamics, salinity and temperature, sediment transport, and morphology change and a spectral wave transformation model (CMS-Wave). The CMS-Wave and CMS-Flow models are tightly coupled within one inline code and may have the same or different computational grids. CMS takes advantage of the Surface-water Modeling System (SMS) interface versions 13.2 and newer (Aquaveo 2023).

Figure 1-1. Coastal Modeling System (CMS) framework and its components.



1.1.1 The Surface-water Modeling System (SMS)

The SMS was developed by a vendor, Aquaveo, and allows access to a full range of coastal and riverine models. There has been substantial funding from US Army Engineer Research and Development Center (ERDC) to also implement some of its numerical models, including the CMS-Flow and Wave models, as well as others. The SMS user interface allows a very flexible modeling approach using the idea of a conceptual modeling setup, with which a user can define a high-level representation of the region by creating a computational domain, boundary forcing conditions, and built-in tools to generate the necessary meshes and grids. The user interface utilizes optimized OpenGL graphics for rendering complex features and allows users to import a variety of data formats and imagery from other products, such as ArcGIS, TerraServer, and AutoCAD. SMS

also supports worldwide projection including both Cartesian and geographic systems.

The SMS is used for CMS flow and wave model configuration, input generation, and postprocessing of results. The SMS may also be used to extract boundary conditions from a larger-domain simulation (Buttolph et al. 2006). The SMS also provides a link between the CMS and the Lagrangian Particle Tracking Model (PTM) (MacDonald et al. 2006; Li and MacDonald 2012).

1.1.2 Coastal Modeling System-Wave (CMS-Wave)

CMS-Wave is a 2D spectral wave transformation model and solves the steady-state wave-action balance equation on a nonuniform Cartesian grid using a forward-marching finite difference method (Mase et al. 2005a; Lin et al. 2008). CMS-Wave includes physical processes such as wave shoaling, refraction, diffraction, reflection, wave-current interaction, wave breaking, wind wave generation, white capping of waves, and the influence of coastal structures on waves.

CMS-Wave is a phase-averaged model, which means that it neglects changes in the wave phase in calculating wave and other nearshore processes. This class of wave models represents changes that occur only in the wave energy density. CMS-Wave was originally built to represent theoretically developed approximations for both wave diffraction and reflection in a nearshore domain.

1.1.3 Coastal Modeling System-Flow (CMS-Flow)

CMS-Flow is a 2D horizontal (2DH) depth-integrated and wave-averaged nearshore hydrodynamic, salinity, temperature, sediment transport, and morphology change model. CMS-Flow calculates currents and water levels, including physical processes such as advection, turbulent mixing, combined wave-current bottom friction; wave mass flux; wind, atmospheric pressure, wave, river, and tidal forcing; Coriolis force; and the influence of coastal structures (Buttolph et al. 2006; Wu et al. 2011).

CMS-Flow has three noncohesive sediment transport models that differ mainly in the assumption of the local equilibrium transport for the bed and suspended loads (Buttolph et al. 2006; Sánchez and Wu 2011). CMS-Flow can simulate any number of sediment size fractions, the interactions

between size fractions, bed sorting and layering, and morphology change. The sediment transport model also includes processes such as avalanching, nonerodible surfaces (hard bottom), and bed-slope effects.

Typical applications of CMS-Flow include analyses of past and future navigation channel performance; wave, current, and wave-current interaction in channels and in the vicinity of navigation structures; and sediment management issues around coastal inlets and adjacent beaches. Some examples of CMS-Flow applications are as follows: Batten and Kraus (2006); Zarillo and Brehin (2007); Li et al. (2015, 2019); Beck and Kraus (2010); Byrnes et al. (2010); Dabees et al. (2011); Reed and Lin (2011); Rosati et al. (2011); Wang et al. (2011); Beck and Legault (2012); and Lin et al. (2013).

1.2 Objective

A never-published user's manual for the CMS was posted on the CIRP Wiki website (https://cirpwiki.info/wiki/CMS#Documentation_Portal) beginning in 2014. The draft manual provided the guidance for CMS users on how to set up, run, and postprocess results working with SMS Version 11.x. Extensive verification and validation tests against laboratory experiments, field cases, and analytical solutions were conducted for waves (Lin et al. 2011), hydrodynamics (Sánchez et al., "Report 3," 2011), and sediment transport and morphology change (Sánchez et al., "Report 4," 2011). Since the publication of the verification and validation reports, there have been a number of changes and added features and processes in the hydrodynamic and sediment transport models, and the SMS has been upgraded from SMS Version 11.x to SMS Version 13.2.

The purpose of the present report is to provide a description of the mathematical formulation and numerical methods. In addition, this report updates the unpublished CMS user's manual with focus on detailed information about model input parameters and coefficients, choice of methods, formulas, and scaling factors for model calculations, model features, and SMS Version 13.2 updates.

1.3 Approach

This report strives to present materials on the CMS to users as comprehensively as possible, which include basic model theories, numerical method, and graphical user interface. From a practical

perspective, the document also gives step-by-step instructions on how to pre- and post-process data for setting up and launching a model simulation, and how to conduct result post analysis for a final product.

The report is organized as follows. Section 2 through Section 5 present the governing equations, parameterizations, empirical equations, initial, and boundary conditions for hydrodynamics, wave transformation, sediment transport and bed change, temperature, and salinity. Variable definitions with units are also provided. Section 6 describes the CMS features. The numerical methods are presented in Section 7. The Finite Volume discretization is described for a general transport for hydrodynamics and total load sediment transport. The graphical user interface for CMS-Flow has experienced great changes in data tree structure and model setup from SMS Version 11.x to SMS Version 13.2. Section 8 through Section 10 describe on how to create input files and set up a model simulation for CMS-Flow, CMS-Wave, and CMS dynamic coupling, respectively, using SMS Version 13.2. Section 11 presents a summary, which is followed by the References section.

2 Hydrodynamics

2.1 Governing Equations

The hydrodynamic solutions of the CMS are obtained by the following depth-integrated and wave-averaged continuity and momentum equations (Phillips 1977; Svendsen 2006):

$$\frac{\partial h}{\partial t} + \frac{\partial(hV_j)}{\partial x_j} = S^m, \quad (2-1)$$

$$\begin{aligned} & \frac{\partial(hV_i)}{\partial t} + \frac{\partial(hV_jV_i)}{\partial x_j} - \varepsilon_{ij}f_c hV_j = -gh \frac{\partial \bar{\eta}}{\partial x_i} - \frac{h}{\rho} \frac{\partial p_a}{\partial x_i} \\ & + \frac{\partial}{\partial x_j} \left(v_t h \frac{\partial V_i}{\partial x_j} \right) - \frac{1}{\rho} \frac{\partial}{\partial x_j} (S_{ij} + R_{ij} - \rho h U_{wi} U_{wj}) + \frac{\tau_{si}}{\rho} - m_b \frac{\tau_{bi}}{\rho}, \end{aligned} \quad (2-2)$$

where

$h = \bar{\eta} - z_b$ = wave-averaged total water depth (m)¹ in which $\bar{\eta}$ is the wave-averaged water surface elevation (WSE) with respect to the still water level (SWL) (m), and z_b is the bed elevation with respect to the SWL, negative downwards (m),

t = time (s),

x_i and x_j = horizontal Cartesian coordinate in the i^{th} and j^{th} direction (m), i and $j=1, 2$ or x, y , respectively,

S^m = source or sink term (precipitation, evaporation, or other external input) (m/s),

V_i and V_j = total mean mass flux velocity, or simply total flux velocity, in the i^{th} and j^{th} direction (m/s), respectively,

$f_c = 2. \Omega \sin \phi$ = Coriolis parameter (rad/s) in which $\Omega = 7.29 \times 10^{-5}$ rad/s is the Earth's angular velocity of rotation, and ϕ is the latitude in degrees,

g = gravitational constant (approximately 9.81 m/s²),

p_a = atmospheric pressure (Pa),

ρ = water density (approximately 1,025 kg/m³),

v_t = total eddy viscosity (m²/s),

τ_{si} = wind surface stress (Pa),

S_{ij} = wave radiation stress (Pa),

1. For a full list of the spelled-out forms of the units of measure used in this document, please refer to *US Government Publishing Office Style Manual*, 31st ed. (Washington, DC: US Government Publishing Office 2016), 248-252, <https://www.govinfo.gov/content/pkg/GPO-STYLEMANUAL-2016/pdf/GPO-STYLEMANUAL-2016.pdf>.

R_{ij} = surface roller stress (Pa),
 U_{wi} and U_{wj} = depth-averaged wave flux velocity in the i^{th} and j^{th} direction (m/s), respectively,
 m_b = bed slope coefficient (-)², and
 τ_{bi} = combined wave and current mean bed shear stress (Pa).

Different from those derived by Svendsen (2006), the preceding equations include the water source or sink term in the continuity equation, and the atmospheric pressure, surface roller terms, and the bed slope coefficient in the momentum equation. Besides that, the horizontal mixing term is formulated slightly differently as a function of the total flux velocity. This approach is arguably more physically meaningful (Andrews and McIntyre 1978; Walstra et al. 2000) and also simplifies the discretization in the case where the total flux velocity is used as the model prognostic variable.

2.2 Model Forcing

As shown in Equations (2-24) and (2-2), the forcing to drive the hydrodynamics includes the bottom stress, surface stress, wave radiation stress, surface roller stress, and eddy viscosity. In the CMS, the forcing terms and related parameters are calculated as follows.

2.2.1 Bed Shear Stress

The bed shear stress is the combination of current-related (τ_{ci}) and wave-related bed shear stresses (τ_w) (Jonsson 1966) for which

$$\tau_{ci} = \rho c_b U U_i = \rho c_b U U_i \quad (2-3)$$

and

$$\tau_w = \frac{1}{2} \rho f_w u_w^2, \quad (2-4)$$

where

ρ = water density (~1025 kg/m³),
 c_b = bed friction coefficient (-),
 $U = \sqrt{U_i U_i}$ = current magnitude (m/s),
 f_w = wave friction factor (-), and

2. (-) indicates a dimensionless variable

u_w = bottom wave orbital velocity amplitude (m/s).

To obtain bed friction coefficient, c_b , bed roughness needs to be specified for hydrodynamic calculations, which can be determined by either a Manning's roughness coefficient (n) or a Nikuradse roughness height (k_s).

Related to the Manning's roughness coefficient (n), the bed friction coefficient (c_b) can be calculated as (Soulsby 1997)

$$c_b = gn^2h^{-1/3}. \quad (2-5)$$

Related to the Nikuradse roughness (k_s), the bed friction coefficient is calculated by assuming a logarithmic velocity profile as (Graf and Altinakar 1998)

$$c_b = \left[\frac{\kappa}{\ln(z_0/h)+1} \right]^2, \quad (2-6)$$

where $\kappa = 0.4$ is Von Karman constant and $z_0 = k_s/30$ is the bed roughness length (hydraulically rough flow).

In the CMS, the default bottom shear stress is calculated as function of bed composition and bedforms (Soulsby 1997; Raudkivi 1998; Soulsby and Whitehouse 1997; Van Rijn 2007a,b). In practice, however, Equations (2-5) and (2-6) are often used under the assumption of constant bed roughness in time because of the lack of data to initialize the bed composition and the large error in estimating the bed composition evolution and bedforms. In addition, using a constant bottom roughness simplifies the model calibration.

To estimate the wave friction factor (f_w), three methods were selected from literature (Swart 1976; Nielsen 1992; Soulsby 1997). One of the methods was employed in the CMS calculations of waves and sediment transport depending upon specific sediment transport formula for estimating bed shear stresses or velocities.

Under combined waves and currents, the mean (wave-averaged) bed shear stress is enhanced compared to the case of currents only. This enhancement of the bed shear stress is due to the nonlinear interaction between waves

and currents in the bottom boundary layer. In Equation (2-2), the mean (short-wave averaged) bed shear stress (τ_{bi}) is calculated as

$$\tau_{bi} = \lambda_{wc} \tau_{ci}, \quad (2-7)$$

where

λ_{wc} = nonlinear bottom friction enhancement factor ($\lambda_{wc} \geq 1$) (-)
and

τ_{ci} = current-related bed shear stress (Pa).

The nonlinear bottom friction enhancement factor (λ_{wc}) is calculated using one of the following formulations (name abbreviations are given in parenthesis):

- The quadratic formula (QUAD) by Wu et al. (2010)
- The empirical two-coefficient data fit (DATA2) by Soulsby (1995)
- The empirical thirteen-coefficient data fit (DATA13) by Soulsby (1995)
- The analytical wave-current boundary layer model (F84) by Fredsoe (1984)
- The numerical wave-current boundary layer model (HT91) by Huynh-Thanh and Temperville (1991)
- The numerical wave-current boundary layer model (DSK88) by Davies et al. (1988)
- The analytical wave-current boundary layer model (GM79) by Grant and Madsen (1979)

The default formula in the CMS is the QUAD formula, in which λ_{wc} is calculated by

$$\lambda_{wc} = \frac{\sqrt{U^2 + c_w u_w^2}}{U}, \quad (2-8)$$

where c_w is an empirical coefficient and u_w is the bottom wave orbital velocity amplitude based on linear wave theory. The default value of c_w in the CMS is set to 1.33 for regular waves and 0.65 for random waves, respectively.

2.2.2 Wind Surface Stress

The wind surface stress is calculated as

$$\tau_{si} = \rho_a C_D W W_i, \quad (2-9)$$

where

ρ_a = air density at sea level ($\sim 1.2 \text{ kg/m}^3$),
 C_D = wind drag coefficient (-),
 W_i = 10 m wind velocity (m/s), and
 $W = \sqrt{W_i W_i}$ = 10 m wind velocity magnitude (m/s).

The wind drag coefficient is calculated using the formula of Hsu (1988) and modified for high wind speeds based on field data by Powell et al. (2003):

$$C_D = \begin{cases} \left(\frac{\kappa}{14.56 - 2 \ln W} \right)^2 & \text{for } W \leq 30 \text{ m/s} \\ 10^{-3} \max(3.86 - 0.04W, 1.5) & \text{for } W > 30 \text{ m/s} \end{cases}. \quad (2-10)$$

Wind measurements taken at heights other than 10 m are converted to 10 m wind speeds using the 1/7 rule (Department of the Army 1984; USACE 2002):

$$W_i = W_i^z \left(\frac{10}{z} \right)^{1/7}, \quad (2-11)$$

where z is the elevation above the sea surface of the wind measurement and W_i^z is the wind velocity at height z .

The wind velocity is calculated using either a Eulerian or Lagrangian reference frame as

$$W_i = W_i^E - \gamma_w U_i, \quad (2-12)$$

where

W_i^E = 10 m wind velocity relative to the solid earth (Eulerian wind velocity) (m/s),
 γ_w = equal to zero for the Eulerian reference frame or one for the Lagrangian reference frame, and
 U_i = current velocity (m/s).

Although the default wind stress calculation in the CMS is to use the Eulerian wind, using the Lagrangian wind can be more accurate and

realistic for field applications (Bye 1985; Pacanowski 1987; Dawe and Thompson 2006).

2.2.3 Wave Radiation Stresses

The wave radiation stresses (S_{ij}) are calculated using linear wave theory as (Longuet-Higgins and Stewart 1961; Dean and Dalrymple 1984)

$$S_{ij} = \iint E_w(f, \theta) \left[n_g w_i w_j + \delta_{ij} \left(n_g - \frac{1}{2} \right) \right] df d\theta, \quad (2-13)$$

where

- f = the wave frequency (1/s),
- θ = the wave direction (rad),
- E_w = wave energy = $\frac{1}{16} \rho g H_s^2$ (N/m),
- H_s = significant wave height (m),
- w_i = wave unit vector = $(\cos \theta, \sin \theta)$ (-),
- $\delta_{ij} = \begin{cases} 1 & \text{for } i = j \\ 0 & \text{for } i \neq j \end{cases}$,
- $n_g = \frac{c_g}{c} = \frac{1}{2} \left(1 + \frac{2kh}{\sinh 2kh} \right)$ (-),
- c_g = wave group velocity (m/s),
- c = wave celerity (m/s), and
- k = wave number (rad/m).

The wave radiation stresses and their gradients are computed within the wave model and interpolated in space and time in the flow model.

2.2.4 Surface Roller Stresses

The surface roller contribution to the wave stresses (R_{ij}) is given by

$$R_{ij} = 2E_{sr} w_i w_j, \quad (2-14)$$

where

- E_{sr} = surface roller energy density (N/m) and
- $w_j = (\cos \theta_m, \sin \theta_m)$ = wave unit vector (-).

The surface roller is calculated within CMS-Wave. An effect of the surface roller is to shift the peak alongshore current velocity closer to shore.

Another side effect of the surface roller is to improve model stability (Sánchez et al., “Report 3,” 2011).

2.2.5 Eddy Viscosity

In CMS-Flow, the total eddy viscosity (ν_t) is equal to the sum of three parts: (1) a base value (ν_0); (2) the current-related eddy viscosity (ν_c); and (3) the wave-related eddy viscosity (ν_w) defined as follows:

$$\nu_t = \nu_0 + \nu_c + \nu_w . \quad (2-15)$$

The base value (ν_0) is approximately equal to the kinematic viscosity ($\sim 1.0 \times 10^{-6} \text{ m}^2/\text{s}$) but may be changed by user.

The current-related eddy viscosity (ν_c) can be calculated by one of the four algebraic models: (1) Falconer Equation, (2) depth-averaged parabolic, (3) subgrid, and (4) mixing-length. The default turbulence model is the subgrid model.

2.2.5.1 Subgrid Model

For the current-related eddy viscosity (ν_c), the subgrid turbulence model is given by

$$\nu_c = c_v u_{*c} h + (c_h \Delta)^2 |\bar{S}| , \quad (2-16)$$

where

$$\begin{aligned} c_v &= \text{vertical shear coefficient (-),} \\ c_h &= \text{horizontal shear coefficient (-),} \\ u_{*c} &= \sqrt{\tau_c / \rho} = \text{the bed shear velocity (m/s),} \\ h &= \text{the total water depth (m),} \\ \Delta &= \text{(average) grid size (m),} \\ |\bar{S}| &= \sqrt{2 e_{ij} e_{ij}} \text{ (1/s), and} \\ e_{ij} &= \text{deformation (strain rate) tensor} = \frac{1}{2} \left(\frac{\partial v_i}{\partial x_j} + \frac{\partial v_j}{\partial x_i} \right). \end{aligned}$$

The empirical coefficients c_v and c_h are related to the turbulence produced by the bed shear and horizontal velocity gradients. The parameter c_v is approximately equal to $\kappa/6=0.067$ (default) but may vary from 0.01 to 0.2.

The variable c_h is equal to approximately the Smagorinsky coefficient (Smagorinsky 1963) and may vary between 0.1 and 0.3 (default is 0.2).

2.2.5.2 Falconer Equation

The Falconer (1980) equation was the default method used in earlier versions of CMS for the current-related eddy viscosity (Militello et al. 2004). The equation is given by

$$\nu_c = 0.575c_bUh, \quad (2-17)$$

where c_b is the bottom friction coefficient and U is the depth-averaged current velocity magnitude.

2.2.5.3 Depth-averaged Parabolic Model

The depth-averaged parabolic model is given by

$$\nu_c = c_v u_{*c} h, \quad (2-18)$$

where c_v is set as a calibrated parameter and can be up to 1.0 in irregular waterways with weak meanders or even larger for strongly curved waterways.

2.2.5.4 Mixing Length Model

The mixing length model implemented in the CMS for the current-related eddy viscosity includes a component due to the vertical shear and is given by (Wu 2007)

$$\nu_c = \sqrt{(c_v u_{*c} h)^2 + (l_h^2 |\bar{S}|)^2}, \quad (2-19)$$

where

$$l_h = \text{mixing length} = \kappa \min(c_h h, y') \text{ (m) and} \\ y' = \text{distance to the nearest wall (m).}$$

The empirical coefficient c_h here is usually between 0.3 and 1.2. The effects of bed shear and horizontal velocity gradients are considered through the first and second terms on the *right-hand side* of Equation (2-16), respectively. It has been found that the modified mixing length model is

better than the depth-averaged parabolic eddy viscosity model that accounts for only the bed shear effect (Wu et al. 2004).

The wave-related eddy viscosity is separated into two components

$$\nu_w = c_{wf} u_{ws} H_s + c_{br} h \left(\frac{D_{br}}{\rho} \right)^{1/3}, \quad (2-20)$$

where

- c_{wf} = wave bottom friction coefficient for eddy viscosity (-),
- u_{ws} = peak bottom orbital velocity (m/s) based on the significant wave height H_s (m) and peak wave period T_p (s),
- c_{br} = wave breaking coefficient for eddy viscosity (-), and
- D_{br} = wave breaking dissipation (N/m/s).

The first term on the *right-hand side* of Equation (2-20) represents the component due to wave bottom friction, and the second term represents the component due to wave breaking. The coefficient c_{wf} is approximately equal to 0.5 (default) and may vary from 0.5 to 2.0. The coefficient c_{br} is approximately equal to 0.1 (default) and may vary from 0.04 to 0.15.

2.2.6 Wave Flux Velocity

The oscillatory wave motion produces a net time-averaged mass (volume) transport referred to as Stokes drift. In the surf zone, the surface roller also provides a contribution to the mean wave mass flux. In general, the depth-averaged wave flux velocity (U_{wi} or U_{wj}) is defined as the mean wave volume flux divided by the local water depth and is written as (Phillips 1977; Svendsen 2006)

$$U_{wi} = \frac{(E_w + 2E_{sr})w_i}{\rho h c}, \quad (2-21)$$

where

- E_w = wave energy = $\frac{1}{16} \rho g H_s^2$ (N/m)
- H_s = significant wave height (m)
- E_{sr} = surface roller energy density (N/m)
- $w_i = (\cos \theta, \sin \theta)$ = wave unit vector (-)
- c = wave celerity (m/s).

The first component is due to the Stokes velocity while the second component is due to the surface roller (only present in the surf zone).

The bed slope coefficient in Equation (2-2) is calculated as

$$m_b = |\nabla z_b| = \sqrt{\left(\frac{\partial z_b}{\partial x}\right)^2 + \left(\frac{\partial z_b}{\partial y}\right)^2 + 1}, \quad (2-22)$$

where z_b is the bed elevation and $\nabla = \left(\frac{\partial}{\partial x}, \frac{\partial}{\partial y}, 1\right)$.

Because of the presence of a bed slope, the bottom friction acts on a larger surface area for the same horizontal area. The effect of the bed slope on bottom friction is included through the bed slope coefficient (Mei 1989; Wu 2007).

2.3 Boundary Conditions

There are two types of lateral (horizontal) boundaries in the hydrodynamic module: closed and open. Closed boundaries are any boundary between water and land, either at the edge or within the computational grid. Below is a summary of the boundary conditions available in the CMS.

2.3.1 Wall Boundary

The wall boundary condition is a closed boundary and is applied at any cell face between water and land cells. Any unassigned boundary cell at the edge of the model domain is assumed to be closed and is assigned a wall boundary. A zero normal flux to the boundary is applied at closed boundaries. Two boundary conditions are available for the tangential flow:

- Free-slip: no tangential shear stress (wall friction)
- Partial-slip: tangential shear stress (wall friction) calculated based on the log law

Assuming a log law for a rough wall, the partial-slip tangential shear stress is given by

$$\tau_{wall} = \rho c_{wall} U_{\parallel}^2, \quad (2-23)$$

where U_{\parallel} is the magnitude of the wall parallel current velocity and c_{wall} is the wall friction coefficient equal to

$$c_{wall} = \left[\frac{\kappa}{\ln(y_p/y_0)} \right]^2. \quad (2-24)$$

Here, y_0 is the roughness length of the wall and is assumed to be equal to that of the bed (i.e., $y_0 = z_0$). The distance from the wall to the cell center is y_p .

2.3.2 Flux Boundary

The flux boundary condition is typically applied to the upstream end of a river or stream and specified as either a constant or time series of total water volume flux (Q). In a 2DH model, the total volume flux needs to be distributed across the boundary to estimate the depth-averaged velocities. This is done using a conveyance approach in which the current velocity is assumed to be related to the local flow depth (h) and Manning's (n) as $U \propto h^r / n$. Here, r is an empirical conveyance coefficient equal to approximately two-thirds for uniform flow. The smaller the r value the more uniform the current velocities are across the flux boundary. The water volume flux (q_i) at each boundary cell (i) is calculated as

$$\vec{q}_i = h \vec{U}_i = \frac{f_{Ramp} Q}{\left| \sum_i (\hat{e} \cdot \hat{n}) \frac{h_i^{r+1}}{n_i} \Delta l_i \right|} \frac{h_i^{r+1}}{n_i} \hat{e}, \quad (2-25)$$

where

- i = subscript indicating a boundary cell,
- \vec{q}_i = volume discharge at boundary cell i per unit width (m²/s),
- \hat{e} = unit vector for inflow direction = $(\sin \varphi, \cos \varphi)$,
- φ = inflow direction measured clockwise from North (deg),
- \hat{n} = boundary face unit vector (positive outward),
- Q = specified total volume flux across the boundary (m³/s),
- N = Manning's coefficient (s/m^{1/3}),
- r = empirical constant equal to approximately two-thirds,
- Δl = cell width in the transverse direction normal to flow (m), and
- f_{Ramp} = ramp function (-) (described in Section 7).

The total volume flux is positive into the computational domain. Since it is not always possible to orient all flux boundaries to be normal to the inflow direction, the option is given to specify an inflow direction (φ). The angle is specified in degrees clockwise from true north. If the angle is not

specified, then the inflow angle is assumed to be normal to the boundary. The total volume flux is conserved independently of the inflow direction.

2.3.3 Water Level Boundary

The general formula for the boundary WSE is given by

$$\bar{\eta}_B = (1 - f_{Ramp})\bar{\eta}_0 + f_{Ramp}(\bar{\eta}_E + \Delta\bar{\eta} + \bar{\eta}_G + \bar{\eta}_C), \quad (2-26)$$

where

- $\bar{\eta}_B$ = boundary water surface elevation (m),
- $\bar{\eta}_0$ = initial boundary water surface elevation (m),
- $\bar{\eta}_E$ = specified external boundary water surface elevation (m),
- $\Delta\bar{\eta}$ = water surface elevation offset (m),
- $\bar{\eta}_G$ = water surface elevation component derived from user specified gradients (m),
- $\bar{\eta}_C$ = correction to the boundary water surface elevation based on the wind and wave forcing (m), and
- f_{Ramp} = ramp function (-) (described in Section 7).

The external WSE ($\bar{\eta}_E$) may be specified as a time series, either spatially constant or varying, and calculated from tidal or harmonic constituents as

$$\bar{\eta}_E(t) = \sum f_i A_i \cos(\omega_i t + V_i^0 + \hat{u}_i - \kappa_i), \quad (2-27)$$

where

- i = subscript indicating a tidal constituent,
- A_i = mean amplitude (m),
- f_i = node (nodal) factor (-),
- ω_i = frequency (deg/hr),
- t = elapsed time (hr),
- $V_i^0 + \hat{u}_i$ = equilibrium phase (deg), and
- κ_i = phase lag (deg).

The mean amplitude and phase may be specified by the user or interpolated from a tidal constituent database. The nodal factor is a time-varying correction to the mean amplitude. The equilibrium phase has a uniform component (V_i^0) and a relatively smaller periodic component. The zero superscript of V_i^0 indicates that the constituent phase is at time zero.

Consistent with the tidal database of NOAA, the CMS supports 37 tidal constituents for tidal prediction.

The harmonic boundary condition is provided as an option for simulating idealized or hypothetical cases. If a harmonic boundary condition is applied, the node factors are set to 1, and the equilibrium arguments are set to zero.

The WSE offset $\Delta\bar{\eta}$ can be spatially constant or a temporally varying curve. The former may be used to correct the boundary WSE for vertical datums, and the latter used for the simulation of sea level rise (see Section 6 for the detail description of this topic). Assuming constant in time, regional gradients in the WSE can be represented by the component, $\bar{\eta}_G$, which is only applicable when $\bar{\eta}_E$ is spatially constant. When applying a water level boundary condition to the nearshore, local flow reversals and boundary problems may occur if the wave- and wind-induced setup is not included. This problem can be avoided by adding a correction ($\bar{\eta}_C$) to the local water level to account for the wind and wave setup as

$$\rho g h_B \frac{\partial}{\partial x} (\bar{\eta}_E + \Delta\bar{\eta} + \bar{\eta}_G + \bar{\eta}_C) = \tau_{sx} + \tau_{wx} - \tau_{bx}, \quad (2-28)$$

where h_B is the boundary total water depth and τ_{sx} , τ_{wx} , and τ_{bx} are the wind, wave, and bottom stresses in the boundary direction x .

2.3.4 Cross-Shore Boundary

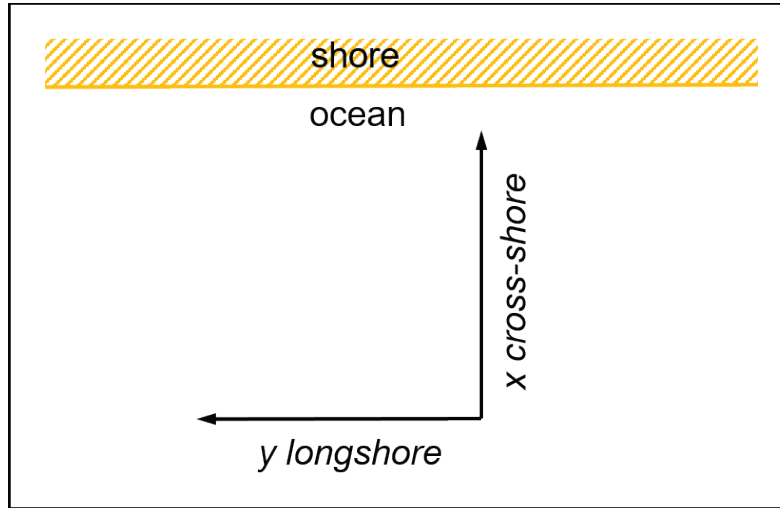
By accommodating the existence of a well-developed longshore current (quasisteady conditions with longshore gradients in advection, diffusion, and zero water levels), a cross-shore boundary condition is applied in the CMS, in which a 1D cross-shore momentum equation (x -direction, Figure 2-1) is solved as

$$\frac{\partial}{\partial x} \left(\rho v_t h \frac{\partial v_y}{\partial x} \right) = \tau_{sy} + \tau_{wy} - \tau_{by}, \quad (2-29)$$

where τ_{sy} , τ_{wy} , and τ_{by} are the surface, wave, and bottom stresses in the longshore direction, respectively. Equation (2-29) is solved iteratively to determine the longshore current velocity, which is applied to the boundary when the flow is directed inwards. When the flow is directed outwards, a zero-gradient boundary condition is applied to the longshore current

velocity. For this type of the boundary condition, the cross-shore component of the velocity is assigned a zero-gradient as well.

Figure 2-1. Cross-shore and longshore coordinate.



The water level due to waves and wind at the cross-shore boundary can be determined by assuming a zero alongshore gradient of flow velocity and negligible cross-shore current velocity. For this case, the cross-shore momentum equation reduces to

$$\rho g h \frac{\partial \bar{\eta}}{\partial x} = \tau_{sx} + \tau_{wx} - \tau_{bx} \quad (2-30)$$

where τ_{sx} , τ_{wx} , and τ_{bx} are the surface, wave, and bottom stresses in the cross-shore direction. The water level boundary condition is applied for the case when the flow is directed inwards. When the flow is directed outwards, a zero-gradient boundary condition is applied to the water level.

3 Wave Transformation

3.1 Governing Equations

CMS-Wave (Lin et al. 2008, 2011) is a 2D spectral wave model formulated from a parabolic, nonlinear equation (Mase et al. 2005a; Lin and Demirbilek 2012) with energy dissipation and diffraction terms. It simulates a steady-state, spectral transformation, and generation of directional waves with ambient currents in the coastal zone. The model is designed for more reliable and realistic representation of wave processes affecting operation and maintenance of coastal inlet, channels, and structures in navigation projects as well as in risk and reliability assessment of shipping in inlets and harbors.

CMS-Wave is a finite-difference, phase-averaged model for propagation of spectral waves over complicated bathymetry and the nearshore where wave refraction, diffraction, reflection, shoaling, and breaking simultaneously act at inlets. Additional features such as wind-wave generation, bottom friction, and spatially varied cell sizes have recently been incorporated into the model to make it suitable for more general use in the coastal region. Recent improvements of CMS-Wave include semiempirical estimates of wave runoff on beach face and overtopping structures, wave energy damping over muddy bed, and theoretically based nonlinear wave-wave interactions. It can operate on nested grids, simulate the full plane wave generation, run in a fast mode, and couple to the hydrodynamic and sediment transport models in the CMS.

The fundamental theoretical basis of CMS-Wave is the wave-action balance equation. This equation represents 2D variation of wave energy in space and considers the effect of the ambient current field on wave behavior. This equation in the Cartesian coordinates (x, y) can be expressed as (Lin and Demirbilek 2012)

$$\begin{aligned} \frac{dN}{dt} &= \frac{\partial N}{\partial t} + \frac{\partial c_{gx}N}{\partial x} + \frac{\partial c_{gy}N}{\partial y} + \frac{\partial c_{g\theta}N}{\partial \theta} \\ &= \kappa \frac{\varepsilon}{\sigma} \left\{ \frac{\partial}{\partial x} \left(c c_g \frac{\partial N}{\partial x} \right) + \frac{\partial}{\partial y} \left(c c_g \frac{\partial N}{\partial y} \right) + c c_g \frac{\partial^2 N}{\partial \theta^2} \right\} + S_{in} + S_{out} , \end{aligned} \quad (3-1)$$

where

- t = time,
 σ = wave frequency,
 $\theta = \theta(x, y)$ = wave travel direction,
 $N = N(\sigma, x, y, \theta) = E(\sigma, x, y, \theta)/\sigma$ = wave action,
 $E(\sigma, x, y, \theta)$ = directional wave energy spectrum,
 $c = \sigma/k$ = wave celerity or wave travel speed (phase speed),
 k = wavelength/ 2π = wave number,
 $c_{gx} = c_g \cos \theta$ = x components of the wave group travel velocity,
 $c_{gy} = c_g \sin \theta$ = y component of the wave group travel velocity,
 $c_g = \frac{\partial \sigma}{\partial k}$ = rate of wave-action transport,
 $c_{g\theta} = \frac{c_g}{k} (\frac{\partial k}{\partial y} \cos \theta - \frac{\partial k}{\partial x} \sin \theta)$ = rate of wave-action transport with respect to direction by wave refraction,
 S_{in} = source function,
 S_{out} = sink function,
 ε = efficiency of diffusion (approximately 10^{-4}),
 κ = intensity parameter for wave diffraction.

The relation between σ and k , according to the linear wave theory, is

$$\sigma^2 = gk \tanh(kh), \quad (3-2)$$

which is known as the first-order dispersion equation, where h is the water depth and g is gravitation constant.

3.2 Wave Characteristics

3.2.1 Wave Diffraction

The first term on the *right side* of Equation (3-1) is the wave diffraction term. In applications, the diffraction intensity parameter κ (great than or equal to 0) normally needs to be calibrated and optimized. The model omits the diffraction effect for $\kappa = 0$ and calculates diffraction for $\kappa > 0$. In practice, values of κ between 0 (no diffraction) and 4 (strong diffraction) were common in comparison to measurements (Lin et al. 2008). For wave diffraction at a semi-infinite long breakwater or at a narrow gap, with the opening equal or less than one wavelength, $\kappa = 4$ is recommended. For a relatively wider gap, with an opening greater than one wavelength, $\kappa = 3$ is recommended. The exact value of κ for modeling is dependent on the structure geometry and adjacent bathymetry and should therefore be verified with measurements.

3.2.2 Wave-Current Interaction

For waves with the ambient current field, \vec{U} , which has the current velocity components (U, V) in the x and y directions. The characteristic velocities in Equation (3-1) need to be modified as

$$c_{gx} = C_g \cos\theta + U, \quad (3-3)$$

$$c_{gy} = C_g \sin\theta + V, \quad (3-4)$$

$$c_{g\theta} = \frac{\sigma}{\sinh 2kh} \left(\sin\theta \frac{\partial h}{\partial x} - \cos\theta \frac{\partial h}{\partial y} \right) + \cos\theta \sin\theta \frac{\partial U}{\partial x} - \cos^2\theta \frac{\partial U}{\partial y} + \sin^2\theta \frac{\partial V}{\partial x} - \sin\theta \cos\theta \frac{\partial V}{\partial y}. \quad (3-5)$$

The dispersion relationship becomes (Jonsson 1990)

$$(\sigma - \vec{k} \cdot \vec{U})^2 = gk \tanh(kh), \quad (3-6)$$

where $\vec{k} \cdot \vec{U}$ is the Doppler-shifting term. Note that the current speed $|\vec{U}| = \sqrt{U^2 + V^2}$.

3.2.3 Wave-Breaking Formulas

The simulation of depth-limited wave breaking is essential in nearshore wave models. A simple wave breaking criterion that is commonly used in shallow water, especially in the surf zone, is a linear function of the ratio of wave height to depth. For random waves, the criterion is

$$\frac{H_b}{h} \leq 0.64, \quad (3-7)$$

where H_b denotes the limit of the significant wave height H_s due to wave breaking. Note the significant wave height H_s is defined as the average of highest one-third waves in a wave record. In the spectral wave model, H_s is calculated as $4\sqrt{E_{total}}$, where E_{total} is the total spectral energy density (Lin et al. 2008).

A more comprehensive criterion is based on the limiting steepness by Miche (1951) for random waves as

$$\frac{H_b}{h} \leq \frac{0.64}{k_p} \tanh(k_p h), \quad (3-8)$$

where k_p is the wave number corresponding to the spectral peak. In the shallow-water condition ($k_p h < 1$), Equation (3-8) reduces asymptotically to Equation (3-7). Iwagaki et al. (1980) verified that Miche's breaker criterion could replicate laboratory measurements over a sloping beach with a current present provided that the wavelength was calculated with the current included in the dispersion equation.

In CMS-Wave, the depth-limited spectral energy dissipation was selected from four different formulas:

- Extended Goda formulation (Sakai et al. 1989)
- Extended Miche (Battjes 1972; Mase et al. 2005b)
- Battjes and Janssen (1978)
- Chawla and Kirby (2002)

These formulas, considered wave breaking on a current, can be divided into two generic categories (Zheng et al. 2008). The first class of formulations attempt to simulate the energy dissipation due to wave breaking by truncating the tail of the Rayleigh distribution of wave height on the basis of some breaker criterion. The Extended Goda and Extended Miche formulas belong to this class. The second category of wave breaking formulations uses a bore model analogy (Battjes and Janssen 1978) to estimate the total energy dissipation. The Battjes and Janssen formula and Chawla and Kirby formula are in this class. The spectral energy dissipation is calculated based on one of these four wave-breaking formulas, and the computed wave height is overall limited by both Equations (3-7) and (3-8).

3.2.4 Bottom Friction Loss

The bottom friction loss (sink) S_{ds} is calculated by a drag law model (Collins 1972)

$$S_{ds} = -c_f \frac{\sigma^2}{g} \frac{\langle u_b \rangle}{\sinh^2 kh} N, \quad (3-9)$$

with

$$\langle u_b \rangle = \frac{1}{2} \sqrt{\frac{g}{h}} E_{total}, \quad (3-10)$$

where $\langle u_b \rangle$ presents the ensemble mean of horizontal wave orbital velocity at the seabed, E_{total} is the total energy density at a grid cell and c_f is the Darcy-Weisbach type friction coefficient. The relationship between c_f and the Darcy-Weisbach friction factor f_{DW} is

$$c_f = f_{DW}/8. \quad (3-11)$$

Typical values of c_f for sandy bottom range from 0.004 to 0.007 based on the Joint North Sea Wave Project (JONSWAP) experiment and North Sea measurements (Hasselmann et al. 1973; Bouws and Komen 1983). Values of c_f applied for coral reefs range from 0.05 to 0.40 (Hardy 1993; Hearn 1999; Lowe et al. 2005). The default value in CMS-Wave is $c_f = 0.005$.

If the Manning friction coefficient n is used instead of the Darcy-Weisbach type coefficient, the relationship between the two drag coefficients is (in SI)

$$c_f = \frac{gn^2}{h^{1/3}}. \quad (3-12)$$

3.2.5 Wave Runup

Wave runup is the maximum shoreward wave swash on the beach face for engineering structures such as jetties and breakwaters by wave breaking at the shore. Wave runup is significant for beach erosion as well as wave overtopping of coastal structures. The total wave runup consists of two components: (1) rise of the mean water level by wave breaking at the shore known as the wave setup and (2) swash of incident waves. In CMS-Wave, the wave setup is computed based on the horizontal momentum equations, neglecting current, surface wind drag, and bottom stresses.

$$\frac{\partial \eta}{\partial x} = -\frac{1}{\rho gh} \left(\frac{\partial S_{xx}}{\partial x} + \frac{\partial S_{xy}}{\partial y} \right), \quad (3-13)$$

$$\frac{\partial \eta}{\partial y} = -\frac{1}{\rho gh} \left(\frac{\partial S_{xy}}{\partial x} + \frac{\partial S_{yy}}{\partial y} \right), \quad (3-14)$$

where S_{xx} , S_{xy} , and S_{yy} are the radiation components from the excess momentum flux due to waves. By using the linear wave theory (Dean and Dalrymple 1984), S_{xx} , S_{xy} , and S_{yy} can be expressed as

$$S_{xx} = E(\sigma, \theta) \int \left[n_k (\cos^2 \theta + 1) - \frac{1}{2} \right] d\theta, \quad (3-15)$$

$$S_{xy} = E(\sigma, \theta) \int \left[n_k (\sin^2 \theta + 1) - \frac{1}{2} \right] d\theta, \quad (3-16)$$

$$S_{yy} = \frac{E(\sigma, \theta)}{2} n_k \sin 2\theta, \quad (3-17)$$

where $n_k = \frac{1}{2} + \frac{kh}{\sinh 2kh}$. Equations (3-13) and (3-14) also calculate the water level depression from the SWL, known as wave setdown, due to waves outside the breaker zone. Equation (3-13) primarily controls wave setup and setdown calculations whereas Equation (3-14) predominantly acts to smooth the water level alongshore.

The swash oscillation of incident waves on the beach face is a random process. The most landward swash excursion corresponds to the maximum wave runup. In the engineering application, a 2% exceedance of all vertical levels, denoted as $R_{2\%}$, from the swash is usually estimated for the wave runup (Komar 1998). This quantity is approximately equal to the local wave setup on the beach or at structures such as seawalls and jetties, or the total wave runup is estimated as

$$R_{2\%} = 2|\eta|. \quad (3-18)$$

In CMS-Wave, $R_{2\%}$ is calculated at the land-water interface and averaged with the local depth to determine if the water can flood the preceding dry cell. If the wave runup level is higher than the adjacent land cell elevation, CMS-Wave can flood the dry cells and simulate wave overtopping and overwash at them. The feature is useful in coupling CMS-Wave to CMS-Flow (Buttolph et al. 2006) for calculating beach erosion or breaching. Calculated quantities of $\partial S_{xx}/\partial x$, $\partial S_{xy}/\partial x$, $\partial S_{xy}/\partial y$, and $\partial S_{yy}/\partial y$ are saved as input to CMS-Flow. CMS-Wave reports the calculated fields of wave setup and maximum water level defined as

$$\text{Maximum water level} = \text{Max} (R_{2\%}, \eta + H_s/2). \quad (3-19)$$

3.2.6 Wave Transmission and Overtopping at Structures

CMS-Wave applies a simple analytical formula to compute the wave transmission coefficient K_t of a rigidly moored rectangular breakwater of width B_c and draft D_c (Macagno 1953):

$$K_t = \left[1 + \left(\frac{k B_c \sinh \frac{k h}{2\pi}}{2 \cosh k(h - D_c)} \right)^2 \right]^{-\frac{1}{2}}. \quad (3-20)$$

The wave transmission over a structure or breakwater is primarily caused by the fall of the overtopping water mass. Therefore, the ratio of the structure crest elevation to the incident wave height is used as the prime parameter governing the wave transmission. CMS-Wave calculates the rate of overtopping of a vertical breakwater based on the simple expression (Goda 1985)

$$K_t = 0.3 \left(1.5 - \frac{h_c}{H_i} \right), \text{ for } 0 \leq \frac{h_c}{H_i} \leq 1.25, \quad (3-21)$$

where h_c is the crest elevation of the breakwater above the SWL and H_i is the incident wave height. Equation (3-21) is modified for a composite breakwater, protected by a mound of armor units at its front, as

$$K_t = 0.3 \left(1.1 - \frac{h_c}{H_i} \right), \text{ for } 0 \leq \frac{h_c}{H_i} \leq 0.75. \quad (3-22)$$

For rubble-mound breakwaters, the calculation of wave transmission is more complicated because the overtopping rate also depends on specific design of the breakwater (e. g., toe apron protection, front slope, armor unit shape and size, thickness of armor layers). In practice, Equation (3-22) still can be applied using a finer spatial resolution with the proper bathymetry and adequate bottom friction coefficients to represent the breakwater.

For permeable rubble-mound breakwaters, the transmission is calculated from the D'Angremond et al. (1996) formula (Lin et al. 2011):

$$K_t = 0.64 \left(\frac{B}{H_i} \right)^{-0.31} \left[1 - \exp\left(-\frac{\xi}{2}\right) \right] - 0.4 \frac{h_c}{H_i}, \text{ for } B < 10 H_i, \quad (3-23)$$

where B is the crest width and ξ is the Iribarren parameter defined as the foreslope of the breakwater divided by the square root of deep-water incident wave steepness. In practice, Equations (3-21) to (3-23) are applicable to both monochromatic and random waves.

3.3 Wind Forcing

The evolution of waves in the large-scale, open coast is more affected by wind-wave interactions than the nearshore wave-current processes. The

result is a nonlinear wave field that is balanced between wind forcing, whitecapping, and wave growth. The surface wind can feed energy into the existing waves and also generate new waves. Conversely, the energy can dissipate through whitecapping from turbulence-wave interactions and air-water interactions. In CMS-Wave, these wind-forcing and whitecapping processes are modeled as separate sink and source terms (Lin and Lin, “Wave Breaking,” 2004; Lin and Lin, “Wind Input,” 2004).

3.3.1 Wind Input Function

The wind-input source S_{in} is formulated as functions of the ratio of wave celerity C to wind speed W , the ratio of wave group velocity to wind speed, the difference of wind speed and wave celerity, and the difference between wind direction θ_{wind} and wave direction θ (Lin et al. 2006):

$$S_{in} = \frac{a_1 \sigma}{g} F_1(\vec{W} - \vec{C}_g) F_2\left(\frac{C_g}{g}\right) E_{PM}^*(\sigma) \Phi(\theta) + \frac{a_2 \sigma^2}{g} F_1(\vec{W} - \vec{C}_g) F_2\left(\frac{C_g}{W}\right) F_3\left(\frac{C_g}{W}\right), \quad (3-24)$$

where

$$F_1(\vec{W} - \vec{C}_g) = \begin{cases} W \cos(\theta_{wind} - \theta) - C_g, & \text{if } \begin{cases} C_g < W \\ C_g \geq W \end{cases} \\ 0, & \end{cases}$$

$$F_2\left(\frac{C_g}{W}\right) = \begin{cases} \left(\frac{C_g}{W}\right)^{1.15}, & \text{if } \begin{cases} C_g < W \\ C_g \geq W \end{cases} \\ 1, & \end{cases}$$

$$F_3\left(\frac{C_g}{W}\right) = \begin{cases} \log_{10} \left[\left(\frac{C_g}{W}\right)^{-1} \right], & \text{if } \begin{cases} C_g < W \\ C_g \geq W \end{cases} \\ 0, & \end{cases}$$

$E_{PM}^*(\sigma) = \frac{g^2}{\sigma^5} \exp\left(-0.74 \frac{\sigma_0^4}{\sigma^4}\right)$ = functional form of the Pierson-Moskowitz (PM) spectrum, $\sigma_0 = g/W$ = the Phillips constant, and

$$\Phi(\theta) = \frac{8}{3\pi} \cos^4(\theta - \theta_{wind}) = \text{normalized directional spreading}$$

$$\text{for } |\theta - \theta_{wind}| \leq \frac{\pi}{2}.$$

The function F_1 presents the wind stress effect, F_2 designates Phillips' mechanisms (Phillips 1957), and F_3 accounts the wave age effect. For swell

or long waves, the wave-group velocity C_g is generally large, and $F_3 < 1$. For short waves, the phase velocity is generally small, and $F_3 > 1$.

3.3.2 Whitecapping Dissipation Function

The wave energy dissipation (sink) S_{ds} (Lin et al. 2006) for whitecapping including current and turbulent viscous effect is

$$S_{ds} = -c_{ds}(a_e k)^{1.5} \frac{\sigma^2}{g} C_g(\sigma, \theta) F_4(\vec{W}, \vec{U}, \vec{C}_g) F_5(kh) N, \quad (3-25)$$

with

$$\begin{aligned} c_{ds} &= \text{proportionality coefficient,} \\ v &= \text{turbulent viscous dissipation,} \\ a_e &= \sqrt{E(\sigma, \theta) d\sigma d\theta} = \text{wave amplitude,} \\ F_4(\vec{W}, \vec{U}, \vec{C}_g) &= \frac{v+W}{|\vec{W}, \vec{U}, \vec{C}_g|}, \text{ and} \\ F_5(kh) &= \frac{1}{\tanh kh}. \end{aligned}$$

At each grid cell, a_e is calculated. To avoid numerical instability and considering the physical constraint of energy loss for the dissipation, the function F_4 is set to equal to 1 if the computed value is greater than 1.

3.3.3 Wave Generation with Arbitrary Wind Direction

In the case of wind forcing only, with zero wave energy input at the sea boundary, CMS-Wave can assimilate the full-plane wave generation. The model will execute an internal grid rotation based on the given surface wind direction to calculate the wave field and map the result back to the original grid. This feature is convenient for the local wave generation by wind in a lake, bay, or estuary, neglecting swell from the ocean (Lin et al. 2012).

3.4 Model features

3.4.1 Variable-Rectangular-Cell Grid

CMS-Wave can run on a grid with variable rectangular cells. This feature is suited to large-domain applications in which wider spacing cells can be specified in the offshore where wave property variation is small and away from the area of interest to save computational time. A limit on the shore-normal to shore-parallel spacing ratio in a cell is not required as long as the calculated shoreward waves are found to be numerically stable.

3.4.2 Grid Nesting

Grid nesting is applied by saving wave spectra at selected locations from a coarse grid (parent grid) and inputting them along the offshore boundary of the smaller fine grid (child grid). For simple and quick applications, a single-location spectrum saved from the parent grid can be used as the wave forcing for the entire sea boundary of the child grid. If multilocation spectra were saved from the parent grid, they are then interpolated as well as extrapolated for more realistic wave forcing along the sea boundary of the child grid.

Multiple grid nesting (e.g., several coexisting child grids) is supported by CMS-Wave. The parent and child grids can have somewhat different grid orientations but need to reside in the same horizontal coordinate system. The difference between grid orientations between parent and child grids should be kept small (no greater than 30 deg) for passing sufficient wave energy from the parent to child grids.

3.4.3 Nonlinear Wave-Wave Interaction

The nonlinear wave-wave interaction is a conserved energy transfer from higher to lower frequencies. The mechanism can produce transverse waves and energy diffusion in the frequency and direction domains. The effect is more pronounced in the intermediate to shallow water depth (Lin et al. 2010). Directional spreading of the wave spectrum tends to increase as the wavelength decreases.

Mase et al. ("Wave Prediction," 2005) showed that calculated wave fields differ with and without nonlinear energy transfer. CMS-Wave applies a theoretical formula proposed by Jenkins and Phillips (2001) to calculate the nonlinear wave-wave interaction.

In finite water depth, the nonlinear wave-wave interaction function can be expressed as (Lin et al. 2010)

$$S_{nl} = a \frac{\partial F}{\partial \sigma} + b \frac{\partial^2 F}{\partial \theta^2}, \quad (3-26)$$

where

$$a = \frac{1}{2n^2} [1 + (2n - 1)^2 \cosh 2kh] - 1 = \text{function of } kh,$$

$$b = \frac{a}{n\sigma},$$

$$F = k^3 \sigma^5 \frac{n^4}{(2\pi)^2 g} \left[\left(\frac{\sigma_m}{\sigma} \right)^4 E \right]^3.$$

3.4.4 Infragravity Wave Effect at Inlets

Infragravity waves behave as shallow water waves, which tend to conserve energy due to change in water depth and channel depth (Dean and Dalrymple 1984). At inlets with variable depth and width of b ,

$$E_{total} c_g b = \text{constant}. \quad (3-27)$$

In CMS-Wave, Equation (3-27) is approximated by reducing wave refraction along the bank of inlet for the infragravity wave effect.

3.4.5 Wave Dissipation over Muddy Bed

The calculation of the wave dissipation over muddy bed in CMS-Wave assumes that the turbulent eddy viscosity is several orders of magnitude greater than the kinematic viscosity of water. By neglecting the kinematic viscous effect, the wave dissipation over a muddy bed can be expressed as (Lamb 1932; Lin et al., “Recent Capabilities,” 2011)

$$S_{d\ p} = -4\nu_t k^2 E, \quad (3-28)$$

where the turbulent eddy viscosity ν_t is equal to a maximum viscosity $\nu_{t, \max}$ representing the wave breaking condition times the ratio of wave height over depth.

3.4.6 Full-Plane and Wind-Field Input Capabilities

The full-plane capability of CMS-Wave performs two half-plane runs in the same grid and is ideal for calculating waves in a bay or estuary connected to a major water body (Lin et al. 2011). The first run is in the half plane with the principal wave direction toward the shore. The second run is in the seaward half-plane as opposed to the first run. Upon the completion of the second run, two half-plane results are combined to one full-plane solution (Lin et al. 2012). This capability is also essential to simulate storm waves in the open coast or around an island. In the case of strong wind-wave interactions, especially under a hurricane, CMS-Wave can read wind field information for more realistic calculation of wave generation,

dissipation, and growth. Because the run time for the full plane is approximately twice of the regular half plane, users should consider the full-plane mode only if the full-plane features exist, such as wave generation and propagation in a bay or around an island.

3.4.7 Fast-Mode Calculation

CMS-Wave can run in a fast mode for simple and quick applications. The fast mode calculates the half-plane spectral transformation for either five directional bins (each 30 deg angle for a broad-band input spectrum) or seven directional bins (each 5 deg angle for a narrow-band input spectrum or 25 deg angle with wind input) to minimize simulation time. It runs at least five times faster than the standard mode, which operates with the default 35 directional bins. The fast-mode option is recommended for large-domain application and in open-water conditions like open coast or in a large bay system. Fast mode is also suitable for generating rapid results if users are seeking preliminary solutions. The wave direction estimated in the fast mode is expected to be less accurate than the standard mode because the directional calculation is based on fewer bins.

4 Sediment Transport

Sediment transport in the water column is traditionally divided into suspended load and bed load. The sum of the two is the total-load transport. Most coastal sediment transport models assume that bed load or total load is instantaneously in equilibrium (Buttolph et al. 2006). Because of the dynamic nature of currents and waves on the coast, the bed load and especially the suspended load are generally not in an equilibrium state. The assumption of local equilibrium may lead to unrealistic results and instabilities that can mask the bed changes and limit long-term simulations (Johnson and Zyserman 2002).

To reduce the number of differential equations to be solved and the computational cost, the CMS combines the bed load and suspended load, and solves the nonequilibrium transport equations for total load. The nonequilibrium sediment transport model accounts for the temporal and spatial lags between flow and sediment transport and is usually more stable and can more easily handle over- and underloading as well as hard (nonerodable) bottoms (Wu 2004).

4.1 Governing Equations

4.1.1 Nonequilibrium Total-Load Transport Model

4.1.1.1 Total-Load Transport Equation

The CMS supports the transport of nonuniform sediment mixture, which is divided into a suitable number of size classes. In the model, the physical processes governing the sediment transport are currents and waves. The current-related transport includes the stirring effect of waves, and the wave-related transport is primarily associated with nearshore wave processes such as wave asymmetry and undertow, surface roller, and steady contributions by Stokes drift.

To compute the transport of the k^{th} size class of total-load sediment in the multiple-sized nonequilibrium transport model, the 2DH equation for the current-related transport can be written as

$$\frac{\partial}{\partial t} \left(\frac{h C_{tk}}{\beta_{tk}} \right) + \frac{\partial (h U_j C_{tk})}{\partial x_j} = \frac{\partial}{\partial x_j} \left[v_s h \frac{\partial (r_{sk} C_{tk})}{\partial x_j} \right] + \alpha_t \omega_{sk} (C_{tk*} - C_{tk}), \quad (4-1)$$

for $j = 1, 2; k = 1, 2, \dots, N$,

where

- N = is the number of sediment size classes,
- C_{tk} = actual depth-averaged total-load sediment concentration (kg/m³) for size class k defined as $C_{tk} = q_{tk}/(Uh)$ in which q_{tk} is the total-load mass transport,
- C_{tk*} = equilibrium depth-averaged total-load sediment concentration (kg/m³) for size class k (see Section 4.1.2 for detail),
- β_{tk} = total-load correction factor (see Section 4.1.1.4 for detail) (-),
- r_{sk} = fraction of suspended load in total load for size class k (see Section 4.1.1.2 for detail) (-),
- ν_s = horizontal sediment mixing coefficient (see the Section 4.3.6 for detail) (m²/s),
- α_t = total-load adaptation coefficient (see Section 4.1.1.3 for detail) (-), and
- ω_{sk} = sediment fall velocity (see Section 4.3.1 for detail) (m/s).

Note that unlike Equation 2-1, the depth-averaged current velocity (U), instead of the total flux velocity (V), is used in Equation (4-1) because the wave-induced sediment transport is not included. The equation performs a single-sized sediment transport simulation if $N = 1$.

4.1.1.2 Fraction of Suspended Sediment

To solve the system of equations for sediment transport implicitly, the fraction of suspended sediment must be determined explicitly. This is done by

$$r_{sk} = \frac{q_{sk}}{q_{tk}} \cong \frac{q_{sk*}}{q_{tk*}}, \quad (4-2)$$

where q_{sk} and q_{tk} are the actual suspended- and total-load transport rates and q_{sk*} and q_{tk*} are the equilibrium suspended- and total-load transport rates.

4.1.1.3 Adaptation Coefficient

The adaptation coefficient is an important parameter in the sediment transport model. There are many variations of this parameter in the literature (Lin 1984; Armanini and di Silvio 1986). The CMS uses the total-

load adaptation coefficient (α_t), which is related to the total-load adaptation length (L_t) and the total-load adaptation time (T_t) by

$$L_t = \frac{Uh}{\alpha_t \omega_s} = UT_t, \quad (4-3)$$

where

- ω_s = sediment fall velocity (m/s),
- U = depth-averaged current velocity (m/s), and
- h = water depth (m).

The adaptation length or time is a characteristic distance or time for sediment to adjust from nonequilibrium to equilibrium transport. Because the total load is a combination of the bed and suspended loads, the associated adaptation length may be calculated as $L_t = r_s L_s + (1 - r_s) L_b$ or $L_t = \max(L_s, L_b)$, where L_s and L_b are the suspended- and bed-load adaptation lengths. The symbol L_s is defined as

$$L_s = \frac{Uh}{\alpha \omega_s} = UT_s, \quad (4-4)$$

in which α and T_s are the adaptation coefficient and the adaptation time for suspended load, respectively. These two parameters (α and T_s) can be calculated either empirically or based on analytical solutions to the pure vertical convection-diffusion equation of suspended sediment (Lin 1984; Gallappatti 1983; Armanini and di Silvio 1986).

The bed-load adaptation length (L_b) is related to the dimension of bed forms. Large bed forms are generally proportional to the water depth, and therefore the bed load adaptation length can be estimated as $L_b = a_b h$ in which a_b is an empirical coefficient on the order of 5–10. Although limited guidance exists on methods to estimate L_b (Wu 2007), the determination of L_b is still empirical and, generally, in the developmental stage. When applied in a calculation, it is recommended that the adaptation length be calibrated with field data to achieve the most reliable results (Wu 2007).

4.1.1.4 Total-Load Correction Factor

The total-load correction factor (β_{tk}) accounts for the vertical distribution of the suspended sediment concentration and velocity profiles as well as the fact that bed load travels at a slower speed than the depth-averaged

current speed (Wu 2007). By definition, β_{tk} is the ratio of the depth-averaged total-load and current speeds.

In a combined bed load and suspended load model, the correction factor is given by

$$\beta_{tk} = \frac{1}{\frac{r_{sk}}{\beta_{sk}} + (1-r_{sk})\frac{U}{u_{bk}}}, \quad (4-5)$$

where u_{bk} is the bed load speed, and β_{sk} is the suspended load correction factor and is defined as the ratio of the depth-averaged suspended load and flow speeds. Since most sediment is transported near the bed, both the total and suspended load correction factors (β_{tk} and β_{sk}) are usually less than 1 and typically in the range of 0.3 and 0.7, respectively.

By assuming current velocity and suspended sediment concentration profiles, the suspended-load correction factor (β_{sk}) is obtained in the CMS (Sánchez et al., “Report 4,” 2011). The bed-load velocity (u_{bk}) is calculated using the van Rijn (1984a) formula with recalibrated coefficients from Wu et al. (2006).

4.1.1.5 Bed Change Equation

The fractional bed change is calculated as

$$\rho_s(1 - p'_m) \left(\frac{\partial z_b}{\partial t} \right)_k = \alpha_t \omega_{sk} (C_{tk} - C_{tk*}) + \frac{\partial}{\partial x_j} \left(D_s q_{bk} \frac{\partial z_b}{\partial x_j} \right), \quad (4-6)$$

where

- z_b = bed elevation with respect to the vertical datum (m),
- p'_m = bed porosity (-),
- ρ_s = sediment (material) density (approximately 2,650 kg/m³ for quartz sediment),
- D_s = empirical bed-slope coefficient (constant) (-), and
- $q_{bk} = hU C_{tk} (1 - r_{sk})$ = the bed load mass transport rate (kg m⁻¹ s⁻¹).

The first term on the *right-hand side* of Equation (4-6) represents the bed change due to sediment exchange near the bed. The last term accounts for the effect of the bed slope on bed-load transport. The bed-slope coefficient

(D_s) is usually approximately 0.1 to 3.0. The total bed change is calculated as the sum of the bed changes for all size classes (Sánchez and Wu 2011):

$$\frac{\partial z_b}{\partial t} = \sum_k \left(\frac{\partial z_b}{\partial t} \right)_k . \quad (4-7)$$

4.1.2 Equilibrium Concentrations and Transport Rates

To close the system of equations describing the sediment transport, bed change, and bed sorting equations, the fractional equilibrium depth-averaged total-load concentration (C_{tk*}) must be estimated from an empirical formula. The depth-averaged equilibrium concentration is defined as

$$C_{tk*} = \frac{q_{tk*}}{U_h} , \quad (4-8)$$

where q_{tk*} is the total-load transport for the k^{th} sediment size class estimated from one of the five empirical formulas employed in the CMS, which are described below.

4.1.2.1 Lund-Coastal Inlets Research Program (CIRP)

Camenen and Larson (2005, 2007, 2008) developed general sediment transport formulas, referred to as the Lund-CIRP formulas, for bed and suspended loads under combined waves and currents. Assuming waves to be symmetric, the current-related bed- and suspended-load transport with wave stirring can be written as

$$\frac{q_{b*}}{\sqrt{(s-1)gd_{50}^3}} = f_b \rho_s 12 \sqrt{\theta_c} \theta_{cw,m} \exp \left(-4.5 \frac{\theta_{cr}}{\theta_{cw}} \right) , \quad (4-9)$$

$$\frac{q_{s*}}{\sqrt{(s-1)gd_{50}^3}} = f_s \rho_s c_R U \frac{\varepsilon}{\omega_s} \left[1 - \exp \left(-\frac{\omega_s h}{\varepsilon} \right) \right] , \quad (4-10)$$

where

- q_{b*} = equilibrium bed load transport rate ($\text{kg m}^{-1} \text{s}^{-1}$),
- q_{s*} = equilibrium suspended load transport rate ($\text{kg m}^{-1} \text{s}^{-1}$),
- θ_c = Shields parameters due to currents (-),
- $\theta_{cw,m}$ = mean Shields parameters due to waves and currents (-),
- θ_{cw} = maximum Shields parameters due to waves and currents (-),
- θ_{cr} = critical Shields parameter (-),

- ε = vertical sediment diffusivity (m^2/s),
 c_R = reference bed concentration (kg/m^3),
 f_b = bed-load scaling factor (default 1.0) (-), and
 f_s = suspended-load scaling factor (default 1.0) (-).

The Shields parameters due to waves and currents are calculated using equations by Soulsby (1997). Using this method, the current- or wave-related shear stress is calculated with the equations described in Section 2, and the total bed roughness is assumed to be a linear summation of the grain-related roughness, form-drag (ripple) roughness, and sediment-related roughness (Soulsby 1997).

For multiple-sized (nonuniform) sediments, the fractional equilibrium sediment transport rates for the k^{th} sediment size class are calculated as (Wu and Lin 2011)

$$\frac{q_{bk*}}{\sqrt{(s-1)gd_k^3}} = f_b \xi_k^{-1} p_{1k} \rho_s 12 \sqrt{\theta_c} \theta_{cw,m} \exp\left(-4.5 \frac{\theta_{crk}}{\theta_{cw}}\right), \quad (4-11)$$

$$\frac{q_{sk*}}{\sqrt{(s-1)gd_k^3}} = f_s \xi_k^{-1} p_{1k} \rho_s c_{Rk} U \frac{\varepsilon_k}{\omega_{sk}} \left[1 - \exp\left(-\frac{\omega_{sk} h}{\varepsilon_k}\right)\right], \quad (4-12)$$

where

- ξ_k = hiding and exposure function (-),
 r_{sk} = fraction of suspended load for each size class (-), and
 p_{1k} = fraction of the k^{th} sediment size in the first layer (-).

The availability of sediment fractions is included through p_{1k} while hiding and exposure of grain sizes is accounted for by directly multiplying the transport rates (see the Hiding and Exposure Section 4.3.2 for detail).

4.1.2.2 van Rijn

The van Rijn (1984a,b) equations for bed load and suspended load transport are used with the recalibrated coefficients of van Rijn (2007a,b) as given by

$$q_{b*} = f_b \rho_s 0.015 U h \left(\frac{U_e - U_{cr}}{\sqrt{(s-1)gd_{50}}} \right)^{1.5} \left(\frac{d_{50}}{h} \right)^{1.2}, \quad (4-13)$$

$$q_{s*} = f_s \rho_s 0.012 U d_{50} \left(\frac{U_e - U_{cr}}{\sqrt{(s-1)g d_{50}}} \right)^{2.4} d_*^{-0.6}, \quad (4-14)$$

where

U_{cr} = critical depth-averaged velocity for incipient motion (m/s) and

U_e = effective depth averaged velocity (m/s).

Both the critical depth-averaged velocity and the effective depth-averaged velocity are calculated based on the bottom wave orbital velocity.

According to van Rijn (2007a), the bed load transport formula predicts transport rates within a factor of 2 of the measurements for velocities higher than 0.6 m/s but underpredicts transport rates by a factor of 2 to 3 for velocities close to the initiation of motion.

The van Rijn formulae were originally proposed for well-sorted sediments. The sediment availability is included by multiplication of transport rates with the fraction of the sediment size class in the upper bed layer. The CMS accounts for hiding and exposure via a correction factor that is multiplied with the critical velocity. When applied to multiple-sized sediments, the fractional equilibrium transport rates are calculated as

$$q_{bk*} = f_b \rho_s p_{1k} 0.015 U h \left(\frac{U_e - \xi_k^{1/2} U_{crk}}{\sqrt{(s-1)g d_k}} \right)^{1.5} \left(\frac{d_k}{h} \right)^{1.2}, \quad (4-15)$$

$$q_{sk*} = f_s \rho_s p_{1k} 0.012 U h \left(\frac{U_e - \xi_k^{1/2} U_{crk}}{\sqrt{(s-1)g d_k}} \right)^{2.4} \left(\frac{d_k}{h} \right) d_{*k}^{-0.6}. \quad (4-16)$$

The availability of sediment fractions is included through p_{1k} while hiding and exposure of grain sizes is accounted for by multiplying the critical velocity (U_{crk}) by a correction function ($\xi_k^{1/2}$).

4.1.2.3 Soulsby-van Rijn

Soulsby (1997) proposed the following equations for the bed load and suspended load sediment transport rates under action of combined current and waves:

$$q_{b*} = f_b \rho_s 0.005 U h \left(\frac{U_e - U_{crc}}{\sqrt{(s-1)g d_{50}}} \right)^{2.4} \left(\frac{d_{50}}{h} \right)^{1.2}, \quad (4-17)$$

$$q_{s*} = f_s \rho_s 0.012 U h \left(\frac{U_e - U_{crc}}{\sqrt{(s-1)g d_{50}}} \right)^{2.4} \left(\frac{d_{50}}{h} \right) d_*^{-0.6}, \quad (4-18)$$

where

$$U_e = \sqrt{U^2 + \frac{0.018}{c_b} u_{rms}^2} = \text{effective velocity (m/s),}$$

u_{rms} = root-mean-square bottom wave orbital velocity (m/s), and
 U_{crc} = critical depth-averaged velocity for initiation of motion for currents based on van Rijn (1984c) (m/s).

The Soulsby-van Rijn formula is modified for multiple-sized sediments similarly to the van Rijn formula (Section 4.1.2.2) using the equations

$$q_{bk*} = f_b \rho_s p_{1k} 0.005 U h \left(\frac{U_e - \xi_k^{1/2} U_{crk}}{\sqrt{(s-1)g d_k}} \right)^{2.4} \left(\frac{d_k}{h} \right)^{1.2}, \quad (4-19)$$

$$q_{sk*} = f_s \rho_s p_{1k} 0.012 U h \left(\frac{U_e - \xi_k^{1/2} U_{crk}}{\sqrt{(s-1)g d_k}} \right)^{2.4} \left(\frac{d_k}{h} \right) d_{*k}^{-0.6}. \quad (4-20)$$

The Soulsby-van Rijn formulae are very similar to the van Rijn formulae except for the definition of the effective velocity and the recalibration of the bed-load formula coefficients in van Rijn (2007a).

4.1.2.4 Watanabe

The Watanabe (1987) formula calculates the equilibrium total-load sediment transport rate as

$$q_{t*} = [f_s r_s + f_b (1 - r_s)] \rho_s A_{Wat} U \left(\frac{\tau_{cr bmax}}{\rho g} \right), \quad (4-21)$$

where

q_{t*} = potential total-load transport rate ($\text{kg m}^{-1} \text{s}^{-1}$),
 τ_{bmax} = combined wave-current maximum shear stress (Pa),
 τ_{cr} = critical shear stress of incipient motion (Pa), and
 A_{Wat} = empirical coefficient typically ranging from 0.1 to 2.0 (-).

The shear stresses (τ_{bmax} and τ_{cr}) due to waves and currents are calculated as in Soulsby (1997). The fraction of suspended sediment

(r_s) is estimated using the van Rijn (2007a,b) transport equations described above.

The Watanabe formula is extended for multiple-sized sediments as

$$q_{tk*} = [f_s r_{sk} + f_b (1 - r_{sk})] \rho_s p_{1k} A_{Wat} U \left(\frac{\tau_{bmax} - \xi_k \tau_{crk}}{\rho g} \right), \quad (4-22)$$

where the subscript k indicates the sediment size class.

4.1.2.5 Cross-SHORE (CSHORE)

Kobayashi and Johnson (2001) developed the Cross-SHORE (CSHORE) sand transport algorithms. Driven by waves, the bed load sediment transport rates can be expressed as

$$q_b = \frac{b P_b}{g(s-1)} \sigma_T^3, \quad (4-23)$$

where P_b is the probability of bed load transport as detailed in Johnson and Grzegorzewski (2011), b is an empirical factor with the default value 0.001, and σ_T is the standard deviation of the instantaneous wave velocity.

The suspended sediment transport rates are calculated by first obtaining the suspended sediment volume V_s per unit horizontal bottom area,

$$V_s = P_s \frac{e_B D_r + e_f D_f}{\rho g(s-1)w_f} (1 + S_{bx}^2)^{0.5} (1 + S_{by}^2)^{0.5}, \quad (4-24)$$

where

P_s = probability of sediment suspension,

D_r = energy dissipation rate due to wave breaking,

D_f = energy dissipation rate due to bottom friction,

e_B = suspension efficiency for D_r ,

e_f = suspension efficiency for D_f ,

ρ = water density,

g = gravitational acceleration,

s = sediment specific gravity,

S_{bx} = cross-shore bottom slope, and

S_{by} = longshore bottom slope.

Assuming longshore uniformity, the suspended sediment transport rates are obtained by

$$q_{sx} = a_x \bar{U} V_s, \quad (4-25)$$

$$q_{sy} = \bar{V} V_s, \quad (4-26)$$

in the cross-shore (x) and longshore (y) directions,

where

$$a_x = [a + (S_{bx}/\tan\varphi)^{0.5}],$$

a = empirical suspended load parameter,

φ = angle of internal friction of the sediment,

\bar{U} = depth-averaged cross-shore velocity, and

\bar{V} = depth-averaged longshore velocity.

4.2 Bed Material Layering and Sorting

In the CMS, the bed is discretized into multiple layers to account for the heterogeneity of bed material size composition with depth. The size composition (fraction of each grain size class) is then calculated and stored in each layer. The mixing layer is the top layer of the bed, which exchanges directly with the sediment moving in the water column. The sediment in the subsurface layers below the mixing layer does not directly exchange with or contact the moving sediment.

Bed sorting is the process in which the bed material changes size composition. The calculation of sediment sorting involves the mixing or active layer concept (Hirano 1971; Karim and Kennedy 1982; Wu 1991). The temporal variation of the bed-material gradation in the first (mixing or active) layer is calculated as (Wu 2007)

$$\frac{\partial(\delta_1 p_{1k})}{\partial t} = \left(\frac{\partial z_b}{\partial t}\right)_k + p_{1k}^* \left(\frac{\partial \delta_1}{\partial t} - \frac{\partial z_b}{\partial t}\right), \quad (4-27)$$

where

δ_1 = thickness of the first layer (m),

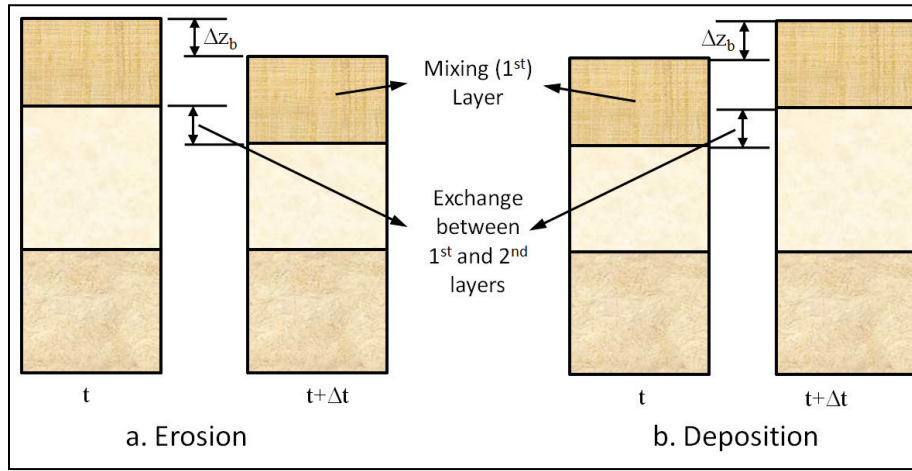
p_{1k} = fraction of the k^{th} sediment size in the first layer (-),

$$p_{1k}^* = \begin{cases} p_{1k} & \text{for } \partial z_b / \partial t - \partial \delta_1 / \partial t \geq 0 \\ p_{2k} & \text{for } \partial z_b / \partial t - \partial \delta_1 / \partial t < 0 \end{cases} \quad (-), \text{ and}$$

$$p_{2k} = \text{fraction of the } k^{th} \text{ sediment size in the second layer } (-).$$

The first term in Equation (4-8) corresponds to the erosion and deposition due to the k^{th} sediment size while the second term corresponds to the sediment exchange between the first and second bed layers (Figure 4-1).

Figure 4-1. Multiple bed layer model of bed material sorting.



At the beginning of each time-step, the mixing or active layer thickness is calculated as

$$\delta_1 = \min[\max(\delta_{min}, 2d_{50}, 0.5H_r), \delta_{max}], \quad (4-28)$$

where H_r is the ripple height and δ_{min} and δ_{max} are the user-specified minimum and maximum layer thicknesses, respectively.

The bed-material sorting in the second layer is calculated as

$$\frac{\partial(\delta_2 p_{2k})}{\partial t} = -p_{1k}^* \left(\frac{\partial \delta_1}{\partial t} - \frac{\partial z_b}{\partial t} \right), \quad (4-29)$$

where δ_2 is the thickness of the second layer. Note that there is no material exchanged between the sediment layers below the second layer.

The sediment-transport, bed-change, and bed-gradation equations are coupled and solved simultaneously, but they are decoupled from the flow calculation at each time-step.

4.3 Sediment Characteristics

4.3.1 Sediment Fall Velocity

The sediment fall velocity may be user specified. In the CMS, the default method is to use the formula by Soulsby (1997):

$$\omega_s = \frac{\nu}{d} \left[(10.36^2 + 1.049d_*^3)^{1/2} - 10.36 \right], \quad (4-30)$$

where

- ν = kinematic viscosity (m²/s),
- d = grain size (m), and
- d_* = dimensionless grain size (-).

The dimensionless grain size is given by

$$d_* = d \left[\frac{(s-1)g}{\nu^2} \right]^{1/3}, \quad (4-31)$$

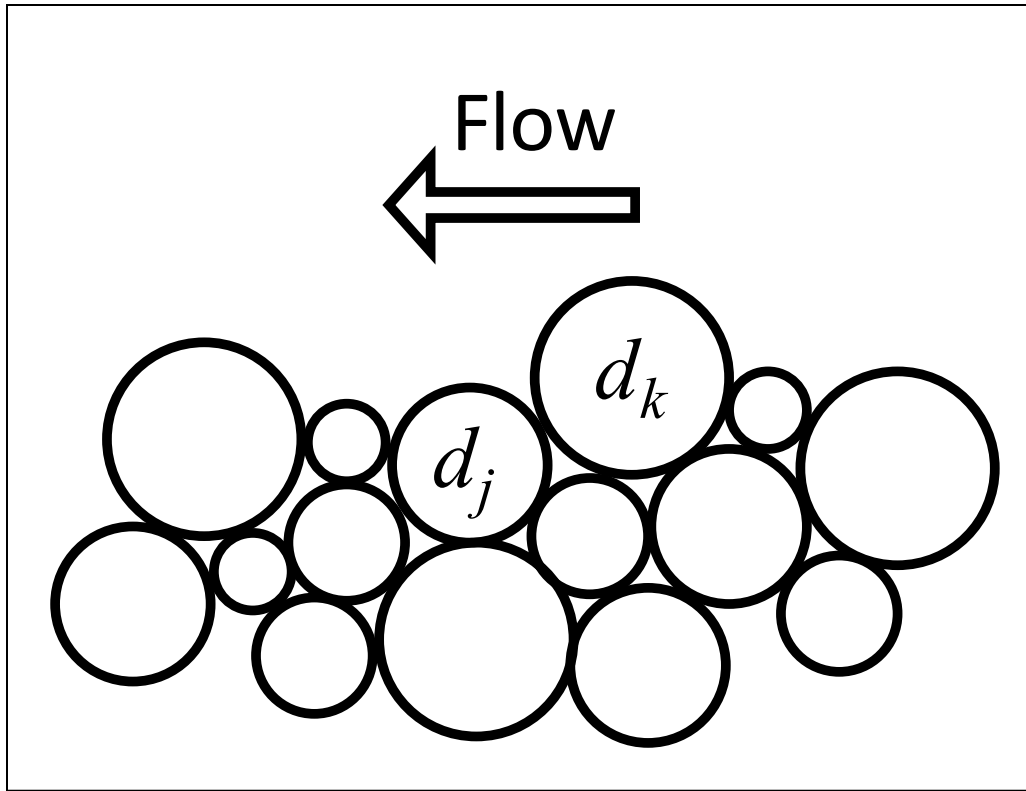
where

- s = sediment specific gravity or relative density (-), and
- g = gravitational constant (9.81 m/s²).

4.3.2 Hiding and Exposure

When the bed material is composed of multiple grain sizes, larger grains have a greater probability of being exposed to the flow while smaller particles have a greater probability of being hidden from the flow. Figure 4-2 shows an example of a sediment grain d_j being hidden by d_k .

Figure 4-2. Schematic of the exposure height of bed sediment grains.



For the transport formulas described above, the hiding and exposure mechanism is considered by correcting the critical shear stress or velocity using a hiding and exposure correction function (ξ_k). Two methods are used to calculate ξ_k depending on whether the sediment transport model is run with a single sediment size or with multiple sediment sizes. For single-sized sediment transport, the correction function for hiding and exposure is calculated following Parker et al. (1982) as

$$\xi_k = \left(\frac{d_k}{d_{50}} \right)^{-m}, \quad (4-32)$$

where m is an empirical coefficient between 0.5 to 1.0. The aforementioned sediment transport equations are implemented by using a single and constant transport grain size (d_k) rather than the bed material (d_{50}). The distribution of d_{50} can be obtained from field measurements and for simplicity is assumed constant during the model simulation time. This method provides a simple conceptual mechanism for parameterizing an important process in the proposed single-sized sediment transport model.

For simulating the transport and sorting of multiple-sized sediments, the hiding and exposure correction for each sediment size class is based on Wu et al. (2000):

$$\xi_k = \left(\frac{P_{ek}}{P_{hk}} \right)^{-m}, \quad (4-33)$$

where P_{hk} and P_{ek} are the hiding and exposure probabilities, respectively, and are calculated by

$$P_{hk} = \sum_{j=1}^N p_{1j} \frac{d_j}{d_k + d_j}, P_{ek} = \sum_{j=1}^N p_{1j} \frac{d_k}{d_k + d_j}, \quad (4-34)$$

where N is the number of grain size classes.

4.3.3 Ripple Dimensions

The bedforms calculated by the CMS are wave- and current-related ripples. The ripple height is used to calculate the mixing layer thickness and is estimated as the maximum of the current- and wave-related ripple heights

$$H_r = \max(H_{rc}, H_{rw}), \quad (4-35)$$

where H_{rc} and H_{rw} are the current- and wave-related ripple heights, respectively.

4.3.4 Scaling Factors

4.3.4.1 Transport Scaling Factors

The bed- and suspended-load transport scaling factors are introduced to calibrate sediment transport rates due to the large uncertainty in the transport formula. In the CMS calculations of sediment transport, these factors are directly applied to multiply the transport capacity or near-bed sediment concentration calculated from the transport formula.

4.3.4.2 Morphologic Acceleration Factor

As a means of speeding up the computational time, the morphologic scaling factor is used to multiply and adjust the calculated bed change at every time-step. This factor is more appropriate for multiple-year (long-

term) simulations and is recommended for periodic boundary conditions or conditions that do not change rapidly over time.

4.3.5 Hard Bottom

By default, the Quadtree grid cells in the CMS are fully erodible. As a morphologic constraint, the hard bottom feature provides the capability to deal with mixed bottom types within a single simulation. This cell-specific feature limits or totally discards the erodibility of the constrained cells down to a specified depth below the water surface. Therefore, two types of hard bottom cells can be specified while setting up a CMS simulation: fully erodible and limited-erodible cells to a specified depth. As an erosion constraint in sediment transport calculations, exposed hard bottom cells may still be covered through deposition and can provide limited sediment for transportation.

4.3.5.1 Bed-Slope

The bed slope coefficient (D_s) in Equation (4-6) accounts for the effect of gravity on sloped beds. Larger bed slope coefficients result in more sediment moving downslope, thereby smoothing the solution.

4.3.5.2 Avalanching

When the bed slope reaches a certain critical angle (i.e., angle of repose), sediment sliding, or avalanching, occurs. In the CMS, avalanching is simulated using a mass conservative relaxation method that limits the bed slope to the critical angle of repose.

4.3.6 Horizontal Sediment Mixing Coefficient

The horizontal sediment mixing coefficient (ν_s) represents the combined effects of turbulent diffusion and dispersion due to nonuniform vertical profiles. In the CMS, the horizontal sediment mixing coefficient is assumed to be proportional to the total eddy viscosity as

$$\nu_s = \frac{\nu_t}{\sigma_s}, \quad (4-36)$$

where σ_s is the Schmidt number and ν_t is the total eddy viscosity. There are many formulas to estimate the Schmidt number (Wu 2007); however, for simplicity, it is assumed to be constant here. The default value for the Schmidt number is equal to 1.0 but may be modified by the user.

4.3.7 Multiple-Sized Sediment Transport

The multiple-sized sediment transport in the CMS is calculated using the multifraction approach in which the total sediment transport is equal to the sum of the transports of discrete sediment size classes. With reference to the single-sized sediment transport, CMS updates for inputting multiple-sized sediment transport are described in the following sections.

4.3.7.1 Sediment Size Classes

In the multiple-sized sediment transport model, the continuous grain sizes are divided into discrete bins or size classes. Each size class, which is defined by the lower and upper limits of the bin, has a characteristic diameter. Because sediment sizes classes are transported from one cell to another, the size classes must be constant over the whole domain. In the CMS there are two options for specifying the grain size information:

- Characteristic diameters
- Size class limits

The characteristic diameters d_k are calculated using the geometric mean of the lower d_{lk} and upper d_{uk} bin limits

$$d_k = \sqrt{d_{lk}d_{uk}} . \quad (4-37)$$

The bin width is given by

$$\Delta d_k = d_{uk} - d_{lk} . \quad (4-38)$$

In a CMS setup, either the characteristic diameters or limits need to be specified; the others can be calculated internally by the model.

4.3.7.2 Fractional Bed Composition

Since the sediment size classes are constant for the whole domain, the bed composition can be specified as the fractional amount of each size class per cell and per bed layer. In the CMS, the following five options are specified for the fractional bed composition.

4.3.7.2.1 D50 Dataset and Geometric Standard Deviation

This option is based on three assumptions: (1) the initial sediment sorting is constant for the whole domain, (2) the initial bed composition is spatially varying around the D50 dataset but vertically constant, and (3) the initial grain size distribution is approximated by a log-normal distribution. Using this option requires the D50 dataset and one parameter, the geometric standard deviation.

The geometric standard deviation σ_g can be defined using the method of moments

$$\sigma_g = \exp \sqrt{\sum p_k (\ln d_k - \ln d_g)^2}, \quad (4-39)$$

where p_k is the fraction, d_k is the size class diameters in millimeters and d_g is the geometric mean in millimeters given by

$$d_g = \exp(\sum p_k \ln d_k). \quad (4-40)$$

4.3.7.2.2 D16, D50, and D84 Datasets

The second option for specifying the initial bed composition requires three datasets: D16, D50, and D84. Similar to the first option, the assumptions include that (1) the initial bed composition is spatially varying around the D16, D50, and D84 datasets but vertically constant, and (2) the initial grain size distribution is approximated by a log-normal distribution.

Using the specified datasets, the bed sorting can be estimated as

$$\sigma_g \approx \left(\frac{d_{84}}{d_{16}} \right)^{1/2}. \quad (4-41)$$

The fractional bed composition is calculated using the log-normal distribution and the above calculated geometric standard deviation.

4.3.7.2.3 D35, D50, and D90 Datasets

Very similar to the previous option, the D35 and D90 datasets are specified and used to estimate the bed sorting for option 3 instead of the more commonly used D16 and D84 datasets. The reason for including this method is that the D35 and D90 datasets are also required for the

Lagrangian PTM, so it reduces the number of datasets that need to be prepared by the user if both models are being run.

For this option, the fractional bed composition is calculated using the log-normal distribution and the following calculation of the geometric standard deviation:

$$\sigma_g \approx \left(\frac{d_{90}}{d_{35}} \right)^{0.61} . \quad (4-42)$$

4.3.7.2.4 Cumulative Grain Size Distribution

This option is used when the bed composition is well known. The percentile diameters that are allowed in the current SMS version are D5, D10, D16, D20, D30, D35, D50, D65, D84, D90, and D95. The cumulative grain size distribution is linearly interpolated from the percentile diameters at the size class bounds and then converted to sediment fractions. The fractional bed compositions are specified for each size class for all cells and all bed layers.

4.3.7.2.5 Size Class Fractions

This option assumes that the initial bed composition is constant at every cell and bed layer for the entire model domain. Therefore, the bed compositions are specified with a constant fraction of each size class for all cells and all bed layers. The fractional bed compositions must sum to 1.0. This option is useful for simulating cases where the bed composition is well known and is constant both in the horizontal and vertical directions.

4.3.7.3 Bed Layer Thickness

For the multiple-sized sediment transport, the initial bed layer thickness needs to be specified. Three types of layer thickness can be predefined in a CMS setup: (1) constant thickness for all cells and bed layers, (2) constant thickness for each bed layer but varying from layer to layer, and (3) varying thickness for each cell and bed layer.

4.3.7.4 Mixing Layer

The mixing layer is the first layer from the surface that is allowed sediment exchange (or mixing) with the sediment in the water column or in the layers below. Using Equation (4-28), the mixing layer thickness can be

calculated based on the median grain size and bedform size. The initial mixing layer thickness can also be assigned a constant value.

4.4 Boundary Conditions

At closed boundaries (interface between land and water), the sediment transport rate normal to the boundary is set to zero. At open boundaries, the CMS implements the equilibrium concentration, which is the concentration reached under steady and horizontally uniform conditions. If the flow is directed into the domain, the sediment concentration is set to the equilibrium concentration. If the flow is directed outward, a zero-gradient boundary condition is used for the sediment concentration.

5 Salinity and Temperature Calculations

Salinity and temperature are important physical properties influencing environmental conditions in aquatic systems. In coastal zones and estuaries, both temporal and spatial variations in salinity and temperature are controlled by oceanic and atmospheric conditions including circulation, tides, waves, air temperature, humidity, precipitation, evaporation, and freshwater inflows. In turn, these controls on salinity and temperature can alter the physical environment and water chemistry, impacting marine organisms and the dynamic behavior of cohesive sediments (Nicholson and O'Connor 1986).

Coastal inlet modifications such as channel deepening, channel widening, jetty rehabilitation, or jetty extension may alter the salinity and temperature distributions within associated embayment. Engineering projects often require simulations of salinity and temperature to ensure compliance with water quality and ecological regulations.

The CMS solves the depth-averaged (2DH) salinity and temperature transport equations and should only be used for cases where the water column is well mixed. If there is flow stratification, a 3D model should be utilized in place of CMS. Note that the CMS holds water density constant; that is, the salinity and temperature calculations are not used to update water density. Thus, any horizontal water density gradients due to varying salinity and temperature are assumed to have negligible influence on the coupled hydrodynamics.

5.1 Governing Equations

5.1.1 Salinity Calculations

The CMS calculates the salinity transport based on the following 2DH salinity conservation equation (Li et al. 2012):

$$\frac{\partial(hS)}{\partial t} + \frac{\partial(hV_j S)}{\partial x_j} = \frac{\partial}{\partial x_j} \left[\nu h \frac{\partial S}{\partial x_j} \right] + S_* , \quad (5-1)$$

where

S = depth-averaged salinity (ppt or psu),
 h = water depth (m),

V_j = total flux velocity (m/s),
 ν = horizontal diffusion coefficient of salt or heat (m²/s), and
 S_* = source/sink term (ppt m/s).

The preceding equation represents the horizontal fluxes of salt, balanced by exchanges of salt via diffusive fluxes. Major processes influencing salinity that are represented by the CMS include seawater exchange at ocean boundaries, freshwater inflows from rivers, precipitation, and evaporation at the water surface. Although groundwater fluxes may also influence salinity (Li et al. 2012), the CMS does not account for the exchange of groundwater and surface water.

5.1.2 Temperature Calculations

The CMS calculates the temperature field based on the following 2DH heat transfer equation (Li and Brown 2017):

$$\frac{\partial(hT)}{\partial t} + \frac{\partial(hV_j T)}{\partial x_j} = \frac{\partial}{\partial x_j} \left[\nu h \frac{\partial T}{\partial x_j} \right] + T_* , \quad (5-2)$$

where

T = depth-averaged temperature (°C),
 $T_* = J_T / \rho c_p$ (°K m/s),
 J_T = net heat flux across water or bed surface (W/m²),
 ρ = water density (kg/m³), and
 c_p = specific heat (J kg⁻¹ °K⁻¹).

Equation (5-2) represents the horizontal heat transfer via advection and diffusion in a water body by treating the heat exchange across the water and bed surfaces as heat sources or sinks. The heat content in the water body is primarily controlled by air-water heat exchange whereas the heat flux due to conduction and convection across the bed surface is assumed to be negligible and is not included in this calculation. In addition, heat inflow from rivers and by tidal currents also affect the temperature of the water body. This can be specified as boundary conditions. Heat flux components across the water surface, J_T , including short-wave solar radiation, long-wave atmospheric radiation, latent heat flux, and sensible heat flux, can be calculated in the CMS using the following meteorological parameters: solar radiation, cloud cover, air temperature, wind speed, and

surface water temperature. The bulk formulas to evaluate the heat flux components were described by Wu (2007), as outlined in the following:

5.1.2.1 Short-Wave Solar Radiation, J_{SW}

$$J_{SW} = J_{SW,CLR}(1 - 0.65C_{CLD}^2)(1 - R_{SW})(1 - f_{SHD}), \quad (5-3)$$

where $J_{SW,CLR}$ is the short-wave solar radiation received on a water surface during a clear (i.e., cloudless) sky (W m^{-2}); C_{CLD} is the cloud cover fraction (0-1.0); R_{SW} is the surface reflection coefficient; and f_{SHD} is the shading factor of vegetation and landscape near a water body. If the measurements of solar radiation are available, they may be directly applied for J_{SW} , and the calculations of Equation (5-3) may be avoided.

5.1.2.2 Long-Wave Atmospheric Radiation, J_{LW}

$$J_{LW} = \varepsilon_{AIR}\sigma T_{AIR}^4(1 + 0.17C_{CLD}^2)(1 - R_{LW}) - \varepsilon_{WTR}\sigma T_{WTR}^4, \quad (5-4)$$

where ε_{AIR} and ε_{WTR} are the emissivities of air and water, respectively; T_{AIR} and T_{WTR} are the air and water surface temperatures, respectively; R_{LW} is the surface reflection coefficient of long wave radiation; and σ is the Stephan Boltzman constant ($5.670 \times 10^{-8} \text{ W m}^{-2} \text{ K}^{-4}$).

5.1.2.3 Latent Heat Flux, J_E

$$J_E = f(U_{WND})(e_{AIR} - e_s), \quad (5-5)$$

where U_{WND} is a function of wind speed, e_{AIR} is the air vapor pressure in millibars, and e_s is the saturation vapor pressure (millibar) at the water surface. In the CMS, $f(U_{WND})$ is calculated using

$$f(U_{WND}) = 6.9 + 0.345U_{WND,7}^2, \quad (5-6)$$

where $U_{WND,7}$ is the wind speed measured at 7 m level above the water surface (Edinger et al. 1974).

5.1.2.4 Sensible Heat Flux, J , J_S

$$J_S = C_B f(U_{WND})(T_{AIR} - T_{WTR}), \quad (5-7)$$

where C_B is the Bowen coefficient (0.62 mbar K^{-1}).

Therefore, the total heat flux, J_T , in Equation (5-2) can be obtained by

$$J_T = J_{SW} + J_{LW} + J_E + J_S . \quad (5-8)$$

5.2 Initial Condition

The initial condition for salinity and temperature calculations may be specified as a constant. However, due to the large spatial variability of salinity and temperature in a coastal system, spatially varying salinities and temperatures are usually desirable to shorten the spin-up time as those scalar variables are ramped from initially assigned values to present field values. The initial salinity and temperature distributions can be obtained from field measurements or from a simulation by solving a 2DH Laplace equation:

$$\nabla^2 C = 0 , \quad (5-9)$$

where ∇^2 is the Laplace operator and C is either S or T . Equation (5-9) is solved given any number of user-specified initial salinity or temperature values at locations within the model domain.

5.3 Boundary Conditions

At land and water boundaries, a zero-flux boundary condition is applied. At open boundaries, either constant salinity and temperature values or a time series of salinity and temperature can be specified. These boundary conditions are applied when the flow is directed into the modeling domain. If the flow is directed out of the modeling domain, then a zero-gradient boundary condition is applied. For temperature calculations, heat transfer components at the air-water interface (surface boundary) need to be prepared using measured meteorological data and Equations (5-3) to (5-8).

6 Coastal Modeling System (CMS) Features

6.1 Model Hot Start

The term *hot start* refers to starting a simulation with a set of initial conditions for all calculated variables, in contrast to the counterpart *cold start* for starting the simulation with default zero initial values. The hot-start feature allows users to stop an ongoing simulation in the middle and restart the simulation with saved intermediate results as initial conditions. Users could employ the hot-start feature to continue simulations that have been interrupted by, for example, electric outages, hardware malfunctions, or model instabilities. In the case of a model crash, the feature also gives users the opportunity to restart the model by readjusting some parameters, such as solver iterations or time-steps to stabilize the simulation.

6.2 Grid Nesting

The CMS supports automated one-way nesting within a parent CMS or an Advance Circulation (ADCIRC) model. When using this feature, the CMS automatically extracts the information from the parent model solution along the child CMS boundaries. To perform the nesting process, users need to specify only the boundary conditions in the child CMS domain and the location and name of the parent model simulation files. The variables to drive the child CMS can be either water levels or water levels and velocities.

When nesting a CMS simulation within an ADCIRC simulation, different vertical datums may be employed because users are able to carry out vertical datum conversion by specifying a WSE offset as described in Equation (2-26). However, the same horizontal datum should be used for both simulations due the lack of internal datum conversion in the present CMS version. To avoid inconsistent model results, the CMS and ADCIRC model forcing should be kept consistent for both simulations as well.

6.3 Sea Level Change

In the CMS, the general formula for the boundary WSE is Equation (2-26). The WSE offset ($\Delta\bar{\eta}$) represents a water level adjustment that can be a spatially and temporally constant value or a time-varying curve. The constant adjustment may be a vertical datum correction or a sea level

change. Projected long-term sea-level changes may be incorporated into the WSE boundary conditions along the CMS open boundaries via usage of time varying WSE values (Li and Brown 2019).

6.4 Coastal Structures

Coastal engineering structures, breakwaters, jetties, revetments, and groins are constructed to protect harbors, navigation channels, and shoreline. In wetland and estuarine applications, structures such as culverts and tidal gates can be used to control flows, waste, and storm water discharges, optimally distribute fresh water, and manage sediment and salinity transport.

Since structures are a significant component of hydrodynamic and sediment transport controls in the coastal zone, some types of structures are incorporated into the CMS. The implementation of these structures is described in the following sections, which are based on papers by Li et al. (2013a, b, c, d).

6.4.1 Rubble Mound

In coastal modeling, rubble mound structures are often represented as solid structures, impermeable to both flow and sediment transport. However, some designs with larger riprap in the core may have sufficient structure porosity to convey flow and fine sediment. Significant sediment storage may also occur within a high-porosity rubble mound structure.

In the CMS, the Forchheimer equation is used to simulate flow through a permeable rubble mound as

$$I = aU + bU^2, \quad (6-1)$$

where I is the hydraulic gradient, U is the bulk velocity, and a and b are dimensional coefficients. The first and second terms on the *right-hand side* represent the laminar and turbulent components of flow resistance, respectively. Equation (6-1) is incorporated into the CMS governing equations to represent the drag forcing of rubble mound structures. In general, the additional resistance terms are included in momentum equations as follows:

$$R_x = -ghu(a + b\sqrt{u^2 + v^2}), \quad (6-2)$$

$$R_y = -ghv(a + b\sqrt{u^2 + v^2}), \quad (6-3)$$

where g is the acceleration due to gravity, h is the water depth, and u and v are the current velocities in the x - and y -directions.

The adjustable coefficients a and b in the Forchheimer equation have been evaluated in a number of studies. Three sets of formulations, proposed by Ward (1964), Kadlec and Knight (1996), and Sidiropoulou et al. (2007), are included in the CMS to determine the two coefficients. The choice of formulation is made by the user when defining the structure and other parameters. The formulas by Ward (1964) are written as

$$a = \frac{360v}{gD^2} \text{ and } b = \frac{10.44}{gD}. \quad (6-4)$$

The formulas of Kadlec and Knight (1998) are

$$a = \frac{255v(1-n)}{gn^{3.7}D^2} \text{ and } b = \frac{2(1-n)}{gn^3D}, \quad (6-5)$$

and the formulas of Sidiropoulou et al. (2007) read as

$$a = 0.0033D^{-1.5}n^{0.06} \text{ and } b = 0.194D^{-1.265}n^{-1.14}. \quad (6-6)$$

In the preceding calculations, ν is the water kinematic viscosity, D is the rock or riprap diameter, and n is the porosity of rubble mound structure.

To account for the rubble mound void space and to simulate the effects of permeability, the porosity of rubble mound structures, n , is introduced into the continuity equation and the equation of bed change for flow and multiple-sized sediment transport (Reed and Sánchez 2011):

$$n \frac{\partial h}{\partial t} + \frac{\partial(hu)}{\partial x} + \frac{\partial(hv)}{\partial y} = 0, \quad (6-7)$$

$$n(1 - p'_m) \frac{\partial z_{bk}}{\partial t} = \alpha \omega_{fk}(C_k - C_{*k}), \quad (6-8)$$

where p'_m is the porosity of bed material, $\partial z_{bk}/\partial t$ is the rate of bed change corresponding to the k th size class of sediment, α is the total-load adaptation coefficient, ω_{fk} is the sediment fall velocity, C_k is the depth-averaged total-load concentration of the k th size class, and C_{*k} is the depth-averaged total-load concentration at the equilibrium state.

6.4.2 Weir

Two approaches are developed to implement weir structures in the CMS. In the first approach, the standard weir equation for a rectangular cross-section is introduced into the model as follows (HEC 2010):

$$Q = C_{df} C_w L_w h^{1.5}. \quad (6-9)$$

where Q is the flow rate over the weir crest, C_w is the weir coefficient, L_w is the weir crest length, h is the upstream water depth above the crest, and C_{df} is the submergence correction factor (also referred to as the drowned flow reduction factor).

To obtain a nondimensional weir coefficient, Equation (6-9) can be rewritten as (Reed and Sánchez 2011)

$$Q = C_{df} C'_w \sqrt{g} L_w h^{1.5}, \quad (6-10)$$

where $C'_w = C_w / \sqrt{g}$. The suggested ranges for C'_w are between 0.55 and 0.58 for a sharp-crested weir and between 0.46 and 0.55 for a broad-crested weir (HEC 2010).

The submergence coefficient (C_{df}) is determined using different methods depending on the weir geometry. For a sharp-crested weir, the Villemonte formula is used:

$$C_{df} = \left[1 - \left(\frac{h_2}{h_1} \right)^{1.5} \right]^{0.385}, \quad (6-11)$$

where h_1 and h_2 are the upstream and downstream water levels above the weir crest elevation, respectively. For a broad-crested weir, C_{df} is calculated as

$$C_{df} = \begin{cases} 1 & h_2/h_1 \leq 0.67 \\ 1 - 27.8(h_2/h_1 - 0.67)^3 & h_2/h_1 > 0.67 \end{cases}. \quad (6-12)$$

For a spillway-type weir, C_{df} is obtained by fitting a curve to data (Reed and Sánchez 2011),

$$C_{df} = 1 - \exp\left(-8.5 \frac{h_d}{h_1}\right). \quad (6-13)$$

Supercritical flow conditions occur when the tail-water elevation is sufficiently low. Under these conditions, the submergence coefficient, C_{df} is equal to 1.0.

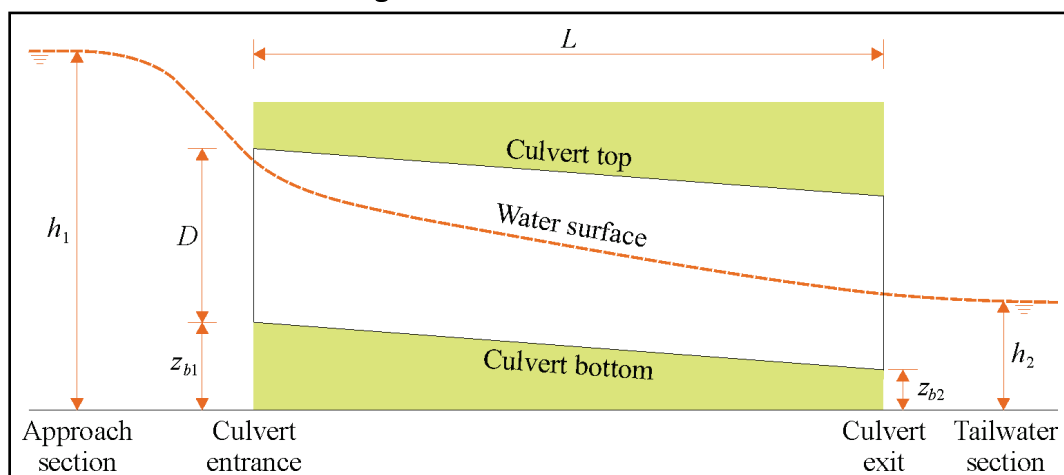
The second approach treats the structure cells as regular internal cells by adding the x - and y -components of the resistance force terms M_x and M_y induced by the weir structures in the depth averaged momentum equations. The resistance forcing is represented by a quadratic drag law, and the Manning's n needs to be specified as the drag coefficient.

6.4.3 Culvert

Circular and rectangular culverts can be represented in the CMS using their cross-sectional area. The flow through culverts is determined using the pipe or open-channel flow equation. The CMS identifies the upstream and downstream cells occupied by the entrance and exit of each culvert and applies the same flow discharge as a source or sink term in the continuity equation. The specially designed implicit scheme for weirs and tide gates is modified for representing the culverts in the Semi-Implicit Method for Pressure Linked Equations Consistent (SIMPLEC) algorithm (W. Wu, personal communication, 13 August 2012).

Bodhaine (1982) described six types of (unidirectional) flow conditions through a culvert that depends on the culvert slope and the upstream and downstream water levels (Figure 6-1). Considering applications in coastal zones, four types of flow conditions are addressed in the CMS and the equations described in the following can be applied for both circular and rectangular culverts.

Figure 6-1. Sketch of culvert flow.



1. The headwater and tail water are higher than the culvert top levels (height, D , plus invert elevations z_b), the culvert inlet and outlet are submerged, and the culvert flow is an orifice flow determined by

$$Q = A \sqrt{\frac{2g(h_1 - h_2)}{K_L}}, \quad (6-14)$$

where K_L is the coefficient of energy loss through the culvert, $K_L = K_i + K_f + K_o$, and K_i is the entrance loss coefficient, K_f is the friction loss coefficient, and K_o is the outlet loss coefficient. The friction loss (K_f) is determined by

$$K_f = \frac{fL}{4R_c}, \quad (6-15)$$

where f is the Darcy-Weisbach friction coefficient, L is the culvert barrel length, and R_c is the hydraulic radius of the culvert barrel. Crowe et al. (2005) and Bodhaine (1982) presented the methods for the determination of f , K_i , and K_o .

2. The culvert inlet or exit unsubmerged case.

(i) The headwater (h_1) is greater than $1.5D + zb_1$ and tailwater (h_2) is lower than $D + zb_2$, and the culvert inlet is submerged but the exit is unsubmerged. In this case, the culvert may be partly or fully occupied by flow (Bodhaine 1982). Here, for simplification, a fully occupied culvert is assumed, and an orifice flow with free outflow is applied as

$$Q = A \sqrt{\frac{2g(h_1 - h_0)}{K'_L + 1.0}}, \quad (6-16)$$

where $K'_L = K_i + K_f$, and h_0 is the tailwater and is assumed to be $D + zb_2$.

(ii) The headwater (h_1) is less than $1.5D + zb_1$, and the tailwater (h_2) is lower than $D + zb_2$, and both the culvert inlet and exit are unsubmerged. This is an open-channel flow case, which can be critical or normal flow depending on the downstream water level and the culvert slope.

3. For the critical flow case, the culvert discharge can be determined by

$$Q = A_c \sqrt{g \frac{A_c}{B_c}}, \quad (6-17)$$

where A_c and B_c are the area and the top width of the flow at the culvert opening, respectively, both being function of the flow depth (h_c) at the opening.

4. For the normal flow case, the culvert discharge is determined by

$$Q = \frac{1}{n} A_c R_c^{2/3} S_c^{1/2}, \quad (6-18)$$

where S_c is the hydraulic gradient. Considering the local head loss, Equation (6-18) can be extended to the following form:

$$Q = A_c \sqrt{\frac{2g(h_1 - h_2)}{K'_i + K'_o + 2gn^2L/R_c^{4/3}}}, \quad (6-19)$$

where K'_i and K'_o are the local head loss coefficients at the culvert entrance and exit, respectively. In this flow case, the local head loss coefficients are assumed to be the same as K_i and K_o in Equation (6-14).

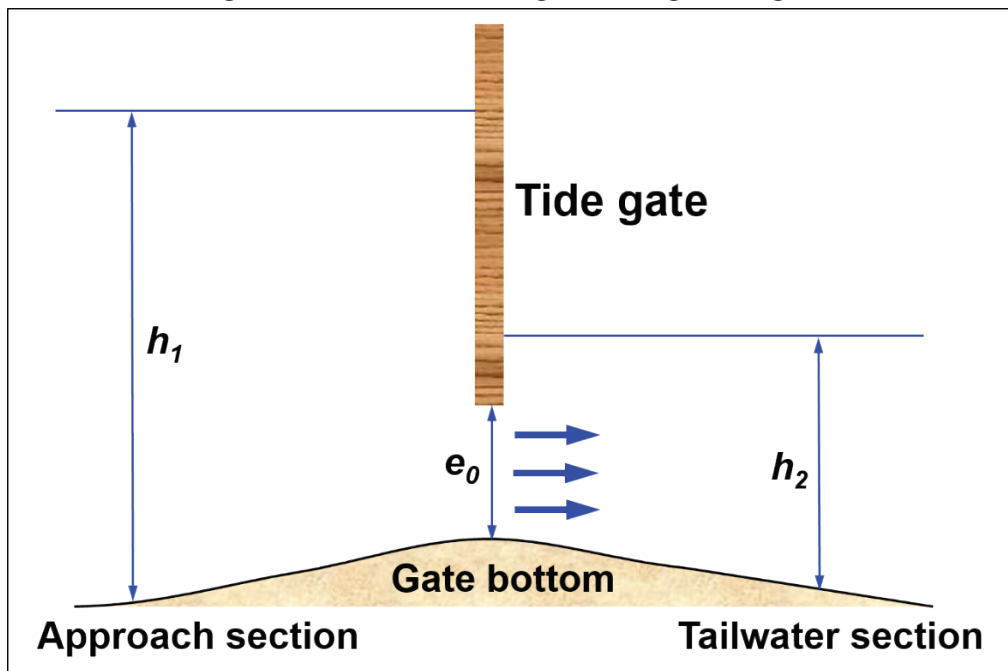
6.4.4 Tide Gate

Similar to the weir implementation, two approaches are developed to implement tide gate structures in the CMS (Li et al. 2013d). In the first approach, the orifice flow equation is used, and the underflow through tide gates is calculated as follows:

$$Q = A_o K_v \sqrt{2g(h_1 - h_2)}, \quad (6-20)$$

where A_o is the opening area, K_v is the gate discharge coefficient, g is the acceleration of gravity, and h_1 and h_2 are the upstream and downstream water levels, respectively. The opening area, A_o , is determined by the opening height of the gate, e_o , and the width of the gate. The discharge coefficient, K_v , is a user-specified parameter that depends on the geometric characteristics of the gate and its opening and the type of flow (submerged or nonsubmerged) (Graf and Altinakar 1998). A definition schematic for the flow and related parameters is provided in Figure 6-2.

Figure 6-2. Schematic showing flow through a tide gate.



The second approach treats the structure cells as other internal cells by adding the x - and y -components of the resistance force terms M_x and M_y induced by tide gates in the depth-averaged momentum equations. The resistance forcing is represented by a quadratic drag law, and the Manning's n coefficient should be specified as the drag coefficient.

Unlike other coastal structures, tide gates are tide regulated, and operation schedules are needed for the opening and closing of a tide gate. Here, four types of schedules are considered in the CMS. The first schedule is to open the gate in a regular time interval—for example, 6 hr from 0800 to 1400 every day. The second schedule is to open the gate in designated time periods—for example, 3 hr from 0800 to 1100 the first day and 7 hr from 1000 to 1700 the second day. The third schedule is to open the gate for ebb tide and close for flood tide, which mimics the function of a flap gate at the seaside. The fourth schedule is for an uncontrolled tide gate that allows the flow to go back and forth with tidal phase changes.

6.5 Dredging Operation

Several hundred million cubic yards of sediment are dredged annually from US ports, harbors, and navigation channels to maintain and improve the nation's navigation system (USACE 2018). Dredging operations can have a significant impact on coastal morphological evolution (Stark 2012).

Hence, a dredging module (DM) has been developed and implemented in the CMS to simulate mid- to long-term coastal morphology change extending over one or multiple dredging cycles.

The DM simulates the dredging and placement operations by simply adjusting the bed elevations of user-defined dredge and placement areas on the CMS-Flow grid. If CMS-Flow is coupled to CMS-Wave, the updated bathymetry is passed to the CMS-Wave grid at each steering interval. The DM is coupled to the hydrodynamics, waves, and sediment transport through the bed elevations. The dredging simulation can also be configured to simulate the construction of islands created through placement of dredged sediment. It is also possible to represent conditions in which the dredged sediment is placed in upland areas or in areas not represented in the CMS grid domain.

A CMS simulation with the DM can be carried out for a uniform or multiple-sized bed composition. For a single grain size application, the options for controlling a dredging or placement event include how the dredging event is triggered, how the material is dredged, and how the material is placed (Reed and Sánchez 2016; Reed and Brown 2019). The DM for a multiple grain size application is an extension of the single grain size approach in which the sediment can be represented by discrete grain size classes, and each size class is eroded, transported, and deposited independently.

The grain size classes interact solely in the bed layers. The top mixing layer exchanges the surficial sediments with deposition from the water column. Below the mixing layer, additional bed layers are defined and are used to track the fraction of each grain size class in the bed, referred to as the bed composition. All bed layers exchange sediment with each other by splitting and merging adjacent layers as their thickness evolves during a simulation due to erosion and deposition.

Dredging simulations are organized into single or multiple dredge operations. Each dredging operation is characterized by a single dredge area and one or more placement areas and can use any of the user-defined dredge and placement areas. All dredge operations use the same dredge update interval at which the dredging and placement occur. The dredging interval is specified only once. The parameter is required for the explicit temporal solution scheme available in the CMS; when the implicit scheme is used, the dredging update interval is automatically set to the

hydrodynamic and sediment transport time-step because this time-step is relatively large. The dredged volume is calculated as the product of the time interval and the dredging rate.

The dredge and placement areas are defined by creating input datasets similar to a bottom-friction or hard-bottom dataset. Cells within the dredge areas are assigned a depth indicating the maximum dredge depth. Cells in the placement areas are assigned a value of 1. Cells outside of the dredge and placement areas are assigned a value of -999, which is the SMS convention for undefined values.

For each dredge area, the following must be defined (Reed and Sánchez 2016):

- Dredging depths dataset (also defines dredging area)
- Criteria for triggering dredging
- Dredging rate
- Method for determining where to dredge first
- Method for placement of dredge material

The four options for triggering dredging for a scenario are

- if any cell in the source area has a bottom elevation above a threshold, as defined by the user;
- if the volume of sediment above the dredged depth is above a threshold, as defined by the user;
- if a certain percentage of the source area's bottom elevation is above a threshold, with both the threshold and the percentage defined by the user;
- specification of a time window during which dredging can occur. Any dredged areas with elevations above the specified depth will be dredged during the specified time period. Multiple time periods can be specified.

The dredging approach defines the order in which cells are dredged to the specified depth. There are two dredging approach options:

- During each dredging interval, the volume dredged initiates from the shallowest point in the source area first.
- A dredging starting point is defined, and the volume dredged during each interval is taken from the cell closest to the starting point first and

then progresses to cells that are farther away from the starting point. The starting point is defined by the user by specifying the cell ID that contains the starting point.

If more than one placement area is specified for a dredging operation, then one of two methods is used to determine how the dredged material is distributed amongst the placement areas. In the first approach, the placement areas are filled in the order that they are defined in the advanced cards. All dredged material is placed in the first placement area until filled and then in the second area and so on. If all placement areas are filled to capacity, then the dredged material is assumed to be placed out of the grid system, and that volume is recorded. In the second scenario, the percentage of dredged material allocated to each placement area is defined during each dredging interval. If any placement area reaches capacity during the simulation, the dredged material is redistributed across the remaining placement areas, based on their relative percentages. If all placement areas fill during a simulation, then the material is placed outside of the grid domain. Note that if no placement area is specified, or the allocation does not sum to 100%, the remaining dredged volume is placed outside of the grid domain.

The following must be defined in each placement area:

- The placement limit, which is the maximum height that dredge material can be placed
- Method for determining where to start the material placement

There are two methods for specifying the placement limit for each placement area:

- Placement is limited to a user-specified thickness above the bed. If the material placed in a cell exceeds the specified thickness, then no more material will be placed in that cell.
- Placement is limited to a minimum water depth above the bed. If the material placed in a cell reduces the cell's water depth to the specified limit, then no more material will be placed in that cell.

Both options can be defined for specifying the placement limit. In that case, the more limiting condition will be used.

There are two options for determining where to start the material placement:

- The volume dredged is placed uniformly across the placement area. Each cell is filled to the specified thickness or the placement water depth limit (also referred to as the placement limit). When a cell reaches its placement limit, no more material is placed in that cell.
- A starting point is defined in the placement area. The volume dredged is placed in the cell closest to the point, and then the placement progresses to cells that are farther away from the starting point. The user defines the starting point by specifying the cell ID. Each cell is filled to the specified thickness or the placement water depth limit.

6.6 Sediment Mapping

As described by Equations (3-1), (3-6), (3-27), the CMS includes the calculation of multiple-sized sediment transport, bed mixing, multiple bed layering, and bed material gradation (Sánchez et al. 2014). Considering the heterogeneity of bed material size composition, the sediment bed can be divided into multiple layers, and the fraction of each size class can be calculated and stored in each layer. The sediment in the active or mixing layer (i.e., the top layer of the bed) directly exchanges or contacts with the sediment moving in the water column and is buried or assigned to deeper layers as a part of the deposition process (Hirano 1971; Wu 1991). The sediment tracer with a certain grain size can be specified as one class of multiple-size sediment. By tagging the sediment tracer and accounting the history of bed composition within each layer, a multiple-size sediment transport simulation can represent the movement of the sediment tracer and perform the tracking of traced volumes of sediments with varying grain sizes across a model domain (Li et al. 2019).

7 Numerical Methods

CMS-Flow provides an implicit numerical discretization scheme for solving the 2D nonlinear shallow water equations (2-24 and 2-2). The implicit solution scheme for CMS-Flow is the SIMPLEC algorithm (van Doornaal and Raithby 1984) on a nonstaggered grid, where water level and velocity components at both x - and y -directions are collocated at the same set of grid nodes. Flow fluxes through cell faces are determined using a Rhie and Chow (1983)-type momentum interpolation method (Wu et al. 2011). CMS-Flow also calculates other variables such as salinity, temperature, sediment concentration, and morphology change, which are also collocated at the same grid nodes as the water level and velocities. The governing equations for the transport of scalar variables have similar forms that can be written as a general transport (advection-diffusion) equation. For the details on implementation of numerical solution schemes, one may refer to Sánchez et al. (2014).

7.1 Computational Grid

CMS-Flow supports generic Cartesian grids, which can be uniform, nonuniform, or telescoping. A guide for generating uniform and nonuniform Cartesian grids can be found in Buttolph et al. (2006). This guide focuses on introducing telescoping Cartesian grids.

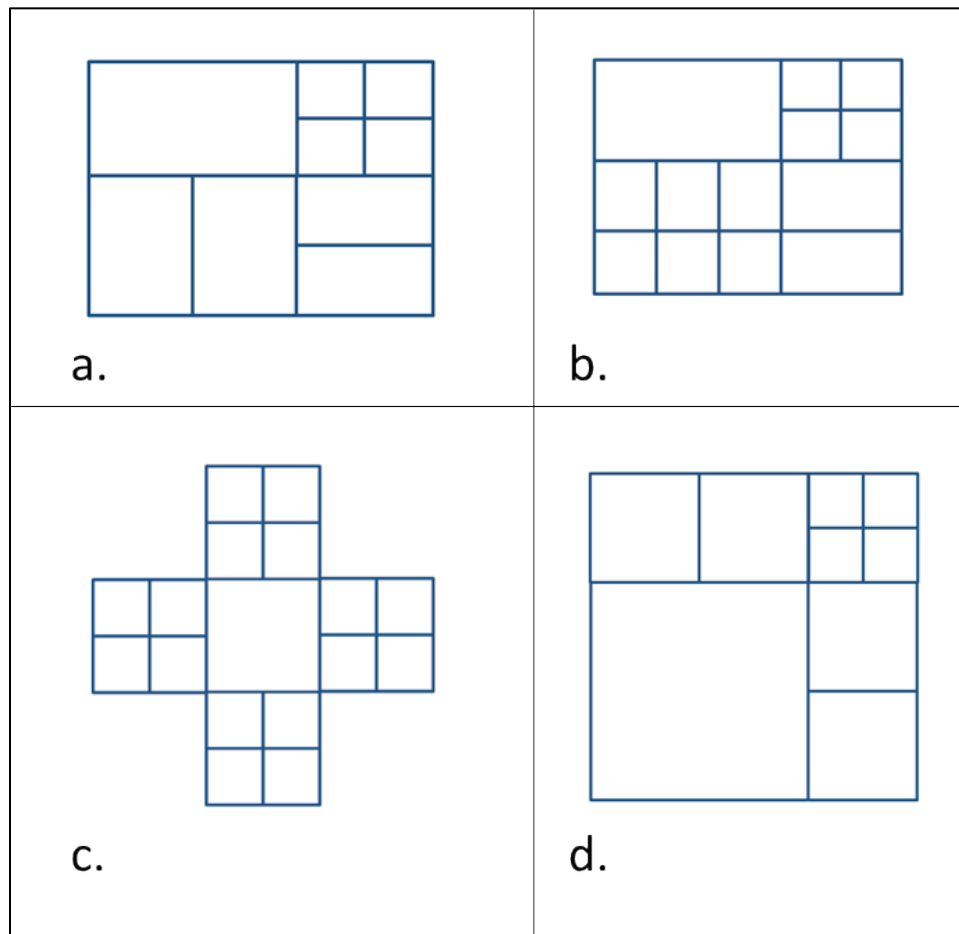
The telescoping locally refines the mesh by splitting a cell into subcells. The only requirement imposed by the numerical methods is that the cells must have a rectangular shape. Additional requirements are imposed by the user interface that limits the variety of types of Cartesian grids to help simplify the grid generation and avoid grid quality issues, which are listed as follows:

- Cells can only be subdivided into four subcells.
- Only two neighboring cells are allowed in the same direction (i.e., north, south, east, and west).
- Cells may have a maximum of six neighbors.
- Refinement levels must be spaced by at least one cell apart (i.e., cells that share the same corner must be one refinement level apart).

Examples of violations of the preceding four requirements are shown in sequential order from Figure 7-1a to Figure 7-1d. Limiting the number of

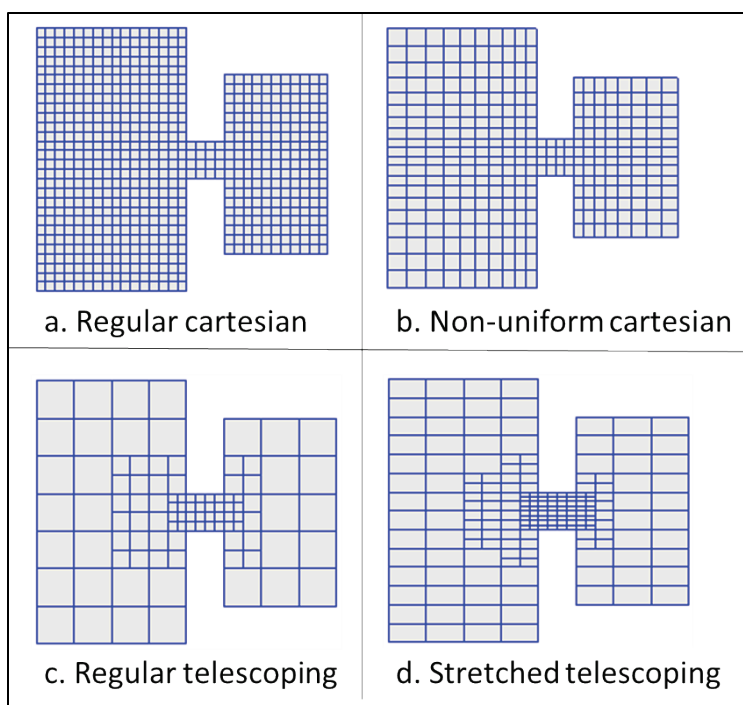
neighboring cells to six avoids excessive cell refinement and limits the band width of the coefficient matrix for the linearized system of equations solved by the implicit solution scheme. The last two requirements avoid having excessive cell refinement which can cause numerical instabilities. The first requirement simplifies the grid generation process but may be relaxed in future versions. The last requirement is enforced for grid quality purposes and a more smoothly varying grid resolution.

Figure 7-1. Examples of invalid Cartesian computational grids.



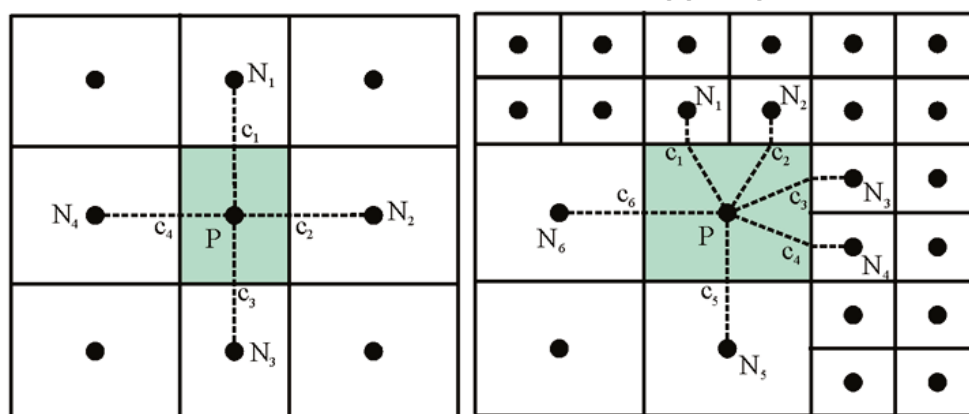
The CMS-Flow grids generated in the SMS interface can be classified as uniform, nonuniform Cartesian grids, regular telescoping, and stretched telescoping grids (Figure 7-2).

Figure 7-2. Types of Cartesian and telescoping grids supported by the Surface-water Modeling System (SMS) interface and CMS-Flow.



On a telescoping Cartesian grid, numerical discretization for solving the governing equations about physical variables such as water levels and velocities was implemented on a nonstaggered grid. To eliminate the checkerboard oscillations in computing flows on a nonstaggered grid, in the CMS-Flow solution scheme, the momentum interpolation technique by Rhie and Chow (1983) was used to ensure spatial stability of velocities. Figure 7-3 shows the location of primary variables on the 5- and 7-point stencils (computational molecule), which often appear in a CMS-Flow mesh.

Figure 7-3. Computational stencils and control volumes for two types of Cartesian grids: nonuniform Cartesian (*left*) and telescoping grid (*right*).



The data structure for a grid can be approached in three ways: (1) block-structured, (2) hierarchical tree, and (3) unstructured. The block-structured approach divides the domain into multiple blocks, and each block is treated as structured. The block-structured approach requires a special treatment between blocks to ensure mass and momentum balance. The hierarchical tree approach is memory intensive and requires parent-child relationships and a tree traverse to determine mesh connectivity. For the unstructured approach, all cells are numbered in a 1D sequence, and tables are used to determine the connectivity of neighboring cells. Among these three approaches, the unstructured approach is the simplest and is therefore applied in CMS-Flow. Computational cells are numbered in an unstructured manner via a 1D index array. Inactive cells (permanently dry) are not included in the 1D index array to save memory and computational time. All active computational cells are numbered sequentially. Note that using an unstructured data approach does not limit the model from using matrix solvers designed for structured grids. For convenience with handling boundary conditions, each boundary cell has a neighboring ghost cell outside of the computational domain.

7.2 Model Discretization

The governing equations of temporal and spatial variations of the CMS-Flow variables such as water levels, velocities, salinity, temperature, and sediment concentration have to be discretized numerically in space and time. In general, spatial discretization was implemented based on a control volume approach which numerically ensures the conservation law of mass and momentum. As mentioned above, CMS-Flow computes flow variables (water levels and velocities) on a telescoping grid, where the variables are collocated at grid nodes. However, the momentum fluxes through an interface of a control volume are calculated by using the momentum interpolation technique by Rhie and Chow (1983). Furthermore, with the variables given at grid nodes and fluxes across control volume interfaces, the nonlinear shallow water equations for water levels and velocities are solved by implementing the SIMPLEC algorithm (van Doornaal and Raithby 1984), which enables users to control the error of continuity in each control volume. For the detailed numerical implementations of the algorithm in a control volume, one may refer to Sánchez et al. (2014).

For temporal discretization of the physical variables in the CMS-Flow governing equations, the second-order implicit temporal scheme is used. Because the scheme requires three time-step levels, the model uses the first-order two-level temporal scheme for the first time-step. In addition, if the time-step is increased or decreased during the simulation, the first-order scheme is triggered as well. Normally, a CMS simulation is set up with a time-step on the order of 5–20 min and is designed for tidal flow and midterm morphology change.

7.3 Solver Options

The numerical spatiotemporal discretization of the CMS governing equations results in a sparse linear system of discretized equations, which contains band matrices. For solving the linear algebraic equations, CMS-Flow provides several iterative solvers for the user to select. There are a total of six iterative solvers as follows:

- The Gauss-Seidel method
- The Gauss-Seidel with Successive-Over-Relaxation
- Strongly Implicit Procedure (SIP) solver (a preconditioned iterative solver)
- Incomplete Cholesky Conjugate Gradient (ICCG) solver (preconditioned conjugate-gradient solver)
- Biconjugate Gradient Stabilized solver (preconditioned conjugate-gradient solver)
- Generalized Minimal Residual (GMRES) solver (an iterative solver based on Krylov subspace with minimal residual of the linear system)

Once a user has selected a solver for a simulation, the same solver is also applied to flow, sediment, salinity, and temperature calculations. The default solver is the GMRES. The SIP and ICCG solvers are available only for nontelegraphing grids (i.e., uniform and nonuniform Cartesian grids). (For instructions on solver selection and number of iterations to solve each governing equation, please refer to Section 8. For the mathematical formulations and the convergence criteria of these solvers, see Sánchez et al. 2014).

7.4 Skewness Correction

When the lines connecting cell centers do not intercept the cell-face centers, the cells are said to be skewed. When interpolating variables to

the cell face or calculating cell-face gradients, a correction is needed for second-order accuracy. There are several ways in which the correction can be conducted but involve some forms of reconstruction of the variables on the cell face or within the neighboring cells. In CMS, a linear cell reconstruction is performed within skewed cells for the correction.

7.5 Advection Schemes

In the implicit solution scheme, the same advection scheme is applied for the flow, sediment, salinity, and temperature equations. Future versions of the CMS will allow the user to select different advection schemes for different governing equations. There are several choices for advection schemes with the implicit model that are listed in Table 7-1. The schemes range from first to third order. The hybrid scheme is fast but is the most diffusive. The exponential scheme is based on the 1D analytical solution to a steady-state advection-diffusion equation and produces very stable results. The Hybrid Linear/Parabolic Approximation (HLPa) scheme is very stable and nondiffusive but requires slightly more computational time. For most applications, the exponential scheme is recommended and is set as the default. The advection scheme may be changed using the advanced card described below.

Table 7-1. Card format for the selection of the advection scheme.

Format	Notes
[cards=ADVECTION_SCHEME] [options=(NONE,UPWIND,HYBRID, POWERLAW,EXPONENTIAL,HLPa, GAMMA,CUBISTA,ALVSMART,HOAB), default=EXPONENTIAL]	Specifies the advection scheme for the implicit solver. The advection scheme is applied to the momentum and sediment and salinity transport equations.

7.6 Wetting and Drying

In CMS, a minimum depth is required for cells to be considered. A cell is classified as wet if the total water depth is larger than this depth. Cell faces are either classified as either open if the two cells neighboring cells are wet or otherwise closed (i.e., cell faces are not classified as wet or dry) to improve stability.

7.7 Parallelization

The CMS-Flow is parallelized for PCs with multicore processors using Open Multiprocessing (OpenMP). The parallelization works by splitting

the computational work into threads among several cores. Some cores are hyper threaded, meaning a single core may support two threads. The number of threads is specified in the CMS-Flow Model Control Window. The number of threads must be equal or greater to 1 and cannot be larger than the number of threads available on the machine. If a number is specified that is larger than the maximum number available on the machine, then the code will default to the maximum number available.

Please note the following:

- The OpenMP parallelization requires that compatibility OpenMP run-time library (libiomp5md.dll file) be in search paths.
- When running multiple simulations at once, the user should keep track of how many threads are being used by each simulation and make sure that the maximum number of threads on the computer is not exceeded. Exceeding the maximum number of threads on the computer will slow down the simulations and also make the computer slow.
- It is always recommended to leave at least one thread unused by model simulations so that the computer is responsive while the simulations are running.

8 CMS-Flow Model Setup

8.1 Overview of Input and Output

CMS-Flow requires several input files, which are described in this section. Some are mandatory, and others depend on what features are needed for the project simulation. By default, a combination of ASCII and binary files are used for both input and output.

Note: All conversion and projection information, model parameter values, and forcing types given in this section are examples and for demonstration only. Every project will be different and will use data and information specific to that project.

8.1.1 Input Files

A minimum of four files are presently required to run CMS-Flow: the parameter file (*.cmcards), the grid definition file (*.tel), a boundary condition file (*_mp.h5), and a grid datasets file (*_datasets.h5). Other files may be used if needed for the project. A full list of the default input files is given in Table 8-1.

Table 8-1. List of CMS-Flow input files.

Input File	Required	Filename	Description
Parameter File (ASCII)	Yes	*.cmcards	Contains most of the setup information for the project including the grid orientation and origin, horizontal projection, information for various processes, and output options
Grid Definition File (ASCII)	Yes	*.tel	Contains information for every cell in the grid including its neighbors, depth, cell ID, and resolution.
Boundary Condition File (Binary)	Yes	*_mp.h5	Contains information for each boundary condition (cell IDs, forcing data)
Grid Datasets File (Binary)	Yes	*_datasets.h5	Contains cell-specific forcing information for the grid (i.e., Manning's n , D50, Hard Bottom, etc.)
Initial Condition File (Binary)	Optional	*.h5	Contains all information about the state of the simulation at the time of writing needed to restart successfully.
Wind Files (ASCII)	Optional	*	Extra files needed to force with a specific wind format (Oceanweather, Navy Fleet, etc.)

8.1.2 Output Files

The output files from CMS come in a variety of types, which are described in Table 8-2. A minimum of two output files are written each time CMS-Flow has been successfully started—an ASCII diagnostic output file and a binary solution file containing water surface information.

Table 8-2. List of CMS-Flow output files.

Output File	Filename	Description
Diagnostic File (ASCII)	CMS_DIAG.txt	Contains most of the output, which is written to the screen during the modeling run. There may be additional diagnostic text written.
Grid Solution File (Binary)	*<type>.h5	Contains solution information for every cell in the grid. <type> can be any of the strings listed in Table 8-3.
Hot Start File (Binary)	AutoHotStart.h5 SingleHotStart.h5	Contains all information about the state of the simulation at the time of writing needed to restart successfully. The user can choose to output either one time (Single) or at a recurring interval (Auto).
Save Point Header File (ASCII)	*.spx	Contains the filenames for each of the type of save point output.
Save Point Data Files (ASCII)	*<type>.sp	Contains the solution information at selected cells only at a user-defined interval. The <type> can be any of “_eta,” “_uv,” “_flux,” or “_totdep.”

Solution files are divided into multiple files depending on the type of data, as shown in Table 8-3.

Table 8-3. Types of grid solution output files.

Type String for Filename	Type Description
“_wse”	Solutions related to WSE
“_vel”	Solutions related to velocity
“_visc”	Solutions related to eddy viscosity
“_sed”, “_sal”, “_temp”	Solutions related to sediment, salinity, or temperature transport
“_morph”	Solutions related to morphology change
“_bedcomp”	Solutions related to bed composition
“_sedfrac”	Solutions related to sediment mixture
“_fric”	Solutions related to bed friction or roughness
“_wave”	Solutions related to wave action
“_met”	Solutions related to meteorology

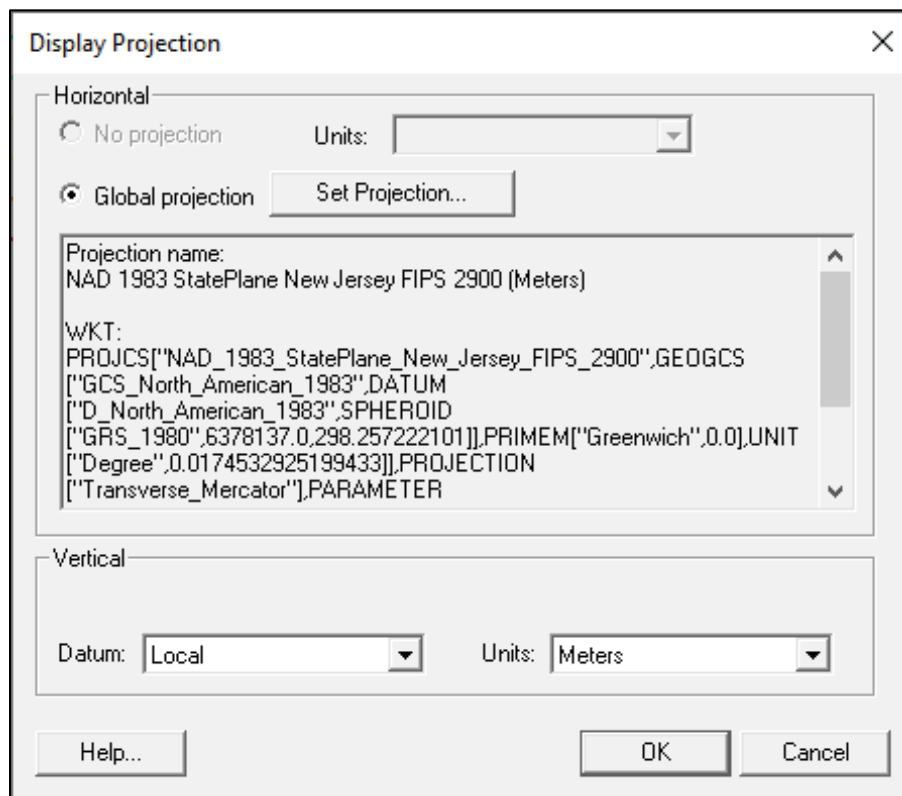
8.2 Display Projections

In the SMS 13.2 interface, multiple data files can be loaded that come from very different sources. Each of these files may have originally been generated using different horizontal projections. For SMS to effectively display each of these files in the correct spot, a Display Projection must be defined. This projection will be the one in which the user wishes the final project to use for all exported modeling files. Changing the projection does not alter the XYZ coordinates of the project data. The CMS models operate in a Cartesian coordinate system such as State Plane or Universal Transverse Mercator and units must always be specified in metric.

The following steps are used to set the Display Projection.

- Choose Display | Display Projection . . . from the pull-down menu, which is shown in Figure 8-1.

Figure 8-1. Display Projection dialog window.

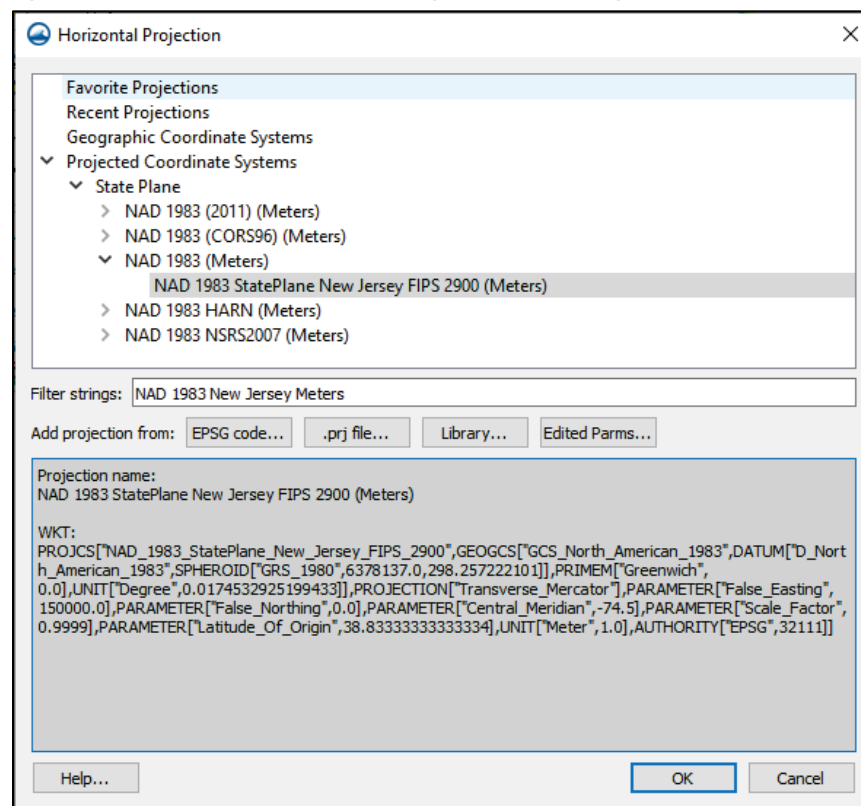


- Click Global Projection and then Set Projection. Find the correct horizontal projection you wish to use. For the examples in this

document, we will be using State Plane New Jersey, North American Datum of 1983, (meters), as shown in Figure 8-2.

- The easiest way to search through all the entries is to type some characters into the Filter Strings box to show matching projections in the top selection box.
- Once you find the right horizontal projection, select it by left-clicking the option in the list. The *bottom (gray)* box will update with the information specific to that projection. Click OK.
- As you add projections in the use of SMS, each new projection is added to Recent Projection for future use.
- From the Display Projection dialog, set the vertical datum to Local projection and units in Meters (Figure 8-1).
- Click OK to exit back to the interface.

Figure 8-2. Horizontal Projection dialog window. Setting the Display Projection.



8.3 Load Bathymetric Information for Project

As mentioned in the previous section, users may import one or more files containing bathymetric information. Bathymetry information can come from different sources such as text files or Geographic Information System (GIS) layers. This section will cover loading bathymetry data from ASCII

text files, which are in a columnar data format. SMS will attempt to open each file according to the extension (such as .xyz or .pts for columnar data).

- During the import process, there are several screens that appear for each dataset (Figure 8-3). On Step 1, click the box next to Space so that spaces are used as delimiters. Once complete, press Next to move to the next step.
- The page for Step 2 (Figure 8-4) allows the user to assign the appropriate type of information to each column. Find the columns which pertain to the coordinates for the point. The column with Easting information should be assigned the type of X. Similarly, the column with Northing information will be given the type of Y, and the column containing depth (bathymetry) information will be given the type of Z. Press Finish to complete the file import.
 - Additional columns may exist in the file and should be defined as type Not Mapped for this step.
- For each imported dataset, SMS will ask you to define the projection for the imported data. Click OK and assign the appropriate projection as indicated from the metadata or report (in the same manner as for setting the Display Projection), making sure the horizontal and vertical projection and units match the information for that survey.

Figure 8-3. File Import Wizard dialog window—Step 1 of 2.

The screenshot shows the 'File Import Wizard - Step 1 of 2' dialog box. It has a title bar with a close button. The main area is divided into sections. The 'File import options' section has two radio buttons: 'Delimited' (selected) and 'Fixed Width'. Below these are checkboxes for 'Set the column delimiters: Space' (checked), 'Tab' (checked), 'Semicolon' (unchecked), 'Comma' (unchecked), and 'Other' (with an empty text box). There are also checkboxes for 'Treat consecutive delimiters as one' (checked) and 'Skip Leading Delimiters' (checked). A 'Text qualifier' dropdown menu is set to '"'. Below this is a 'Start import at row:' field with a spinner set to '1' and a 'Heading row' checkbox (checked). The 'File preview' section shows a table with 5 rows and 3 columns labeled X, Y, and Z. The data is as follows:

	X	Y	Z
1			
2	624756.130	492536.596	-14.000
3	624748.690	492530.646	-15.300
4	624741.220	492524.916	-15.300
5	624733.680	492519.276	-16.500

At the bottom of the dialog are three buttons: 'Help', '< Back', and 'Next >', and a 'Cancel' button.

Figure 8-4. File Import Wizard dialog window—Step 2 of 2.

File Import Wizard - Step 2 of 2

SMS data type: **Scatter Set** Filter Options

☐ No data flag: 999.0

Name: 3364_0409_ft_MLW

Mapping options:
☒ Triangulate data ☐ Delete long triangles
 Maximum edge length: 100000.0
 Merge duplicate points within tolerance: 0.0000100

File preview

Type	X	Y	Z
Options			
Header	X	Y	Z
	624756.130	492536.596	-14.000
	624748.690	492530.646	-15.300
	624741.220	492524.916	-15.300
	624733.680	492519.276	-16.500

First 20 lines displayed.

Help < Back Finish Cancel

- Repeat this process for any additional survey information to be imported with separate files.

8.4 Combining Multiple Datasets for Final Bathymetry

Even though SMS allows multiple files to be imported, only one source of bathymetry is allowed to be specified as the grid bathymetry. It is necessary to prepare each of the imported datasets so they may be merged into one final dataset for assignment to the grid bathymetry.

In preparing the vertical reference for the survey datasets, one must consider the various datum references and the sign and units of the data values. The CMS suite of models (CMS-Flow and CMS-Wave) requires that all bathymetries be oriented so that the values are positive as the water gets deeper and that the data are in metric units.



Beginning with SMS 13.1, the interface now depicts all values consistently positive **UP** regardless of the desired model depth orientation. This contradicts how CMS expects the data values.

The issue is addressed when the model files are exported to disk. For users of previous SMS versions, this attention to this change is critical for a successful modeling outcome.

The files that are obtained from various sources may display positive depths rather than positive elevations. The information for each survey should accompany the data by means of a metadata file. If there are datasets which have vertical references that are positive depths, these must

be converted from positive to negative, either within SMS or externally using a different application.

8.4.1 Changing Vertical Datums

There are two types of vertical datums. Some are local references (such as mean low water or mean higher-high water), and others are national or regional references (such as the North Atlantic Vertical Datum). NOAA maintains a list of datums and offers a benchmark sheet that explains the relationship between the available datums for a given location on their NOAA Tides and Currents website (NOAA, “Tides and Currents,” n.d.). Not all references are available at each location. A sample benchmark sheet for Long Branch Fishing Pier, New Jersey, (NOAA station 8531991) is shown in Figure 8-5. These datum relationships are needed to convert from one to another. For example, for NOAA station 8531991, the value for mean lower-low water (MLLW) is 0.00 m and the value for mean sea level (MSL) is 0.744 m.

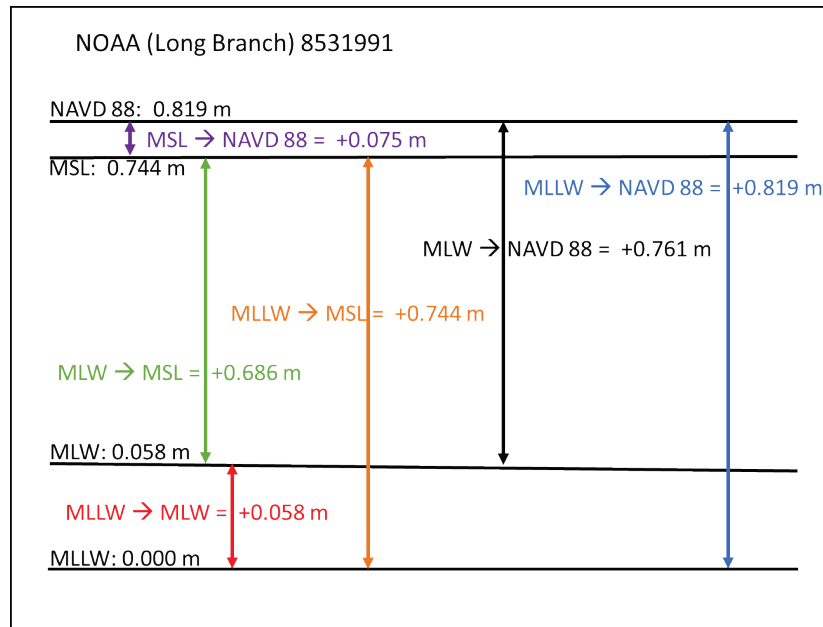
To convert from MLLW to MSL, the user must subtract the desired vertical datum from the individual datum. To convert MLLW to MSL, the following expression must be evaluated: $MSL - MLLW = 0.744 - 0.00 = 0.744$ m. This is generally easy to determine for local datums. Be aware that regional or national datums in some locations may be higher than MSL and in other locations may be lower than MSL.

Figure 8-5. NOAA benchmark sheet for Long Branch Fishing Pier, New Jersey. (Image reproduced from NOAA, “Tides and Currents,” n.d. Public domain.)

Tidal datums at LONG BRANCH, FISHING PIER based on:		
LENGTH OF SERIES:	8 Years	
TIME PERIOD:	January 1979 - December 1986	
TIDAL EPOCH:	1983-2001	
CONTROL TIDE STATION:	8531680 SANDY HOOK	
Elevations of tidal datums referred to Mean Lower Low Water (MLLW), in METERS:		
HIGHEST OBSERVED WATER LEVEL (01/02/1987)		= 2.479
MEAN HIGHER HIGH WATER	MHHW	= 1.504
MEAN HIGH WATER	MHW	= 1.399
North American Vertical Datum	NAVD88	= 0.819
MEAN SEA LEVEL	MSL	= 0.744
MEAN TIDE LEVEL	MTL	= 0.729
MEAN LOW WATER	MLW	= 0.058
MEAN LOWER LOW WATER	MLLW	= 0.000
LOWEST OBSERVED WATER LEVEL (01/10/1978)		= -1.401

Also, there may be additional benchmark information from the survey source that gives relationships for datums in the area. The user may benefit from drawing these relationships of the datums on a graph. One such diagram is shown in Figure 8-6.

Figure 8-6. Graphical representation of datum relationships from benchmark sheet (Figure 8-5). (Image adapted from NOAA, “Tides and Currents,” n.d. Public domain.).



To use elevation datasets with CMS, all datasets must have both units and datums converted. Optimally, MSL is closest to the ambient mean water level along a coastline. Initialization of a new hydrodynamic simulation may require near-MSL water levels for stability. Therefore, MSL in meters is the preferred datum for bathymetry and forcing files in CMS. The following process is used to switch from one datum (and unit) to another.

8.4.1.1 Datum Conversion

Obtain necessary information about the data.

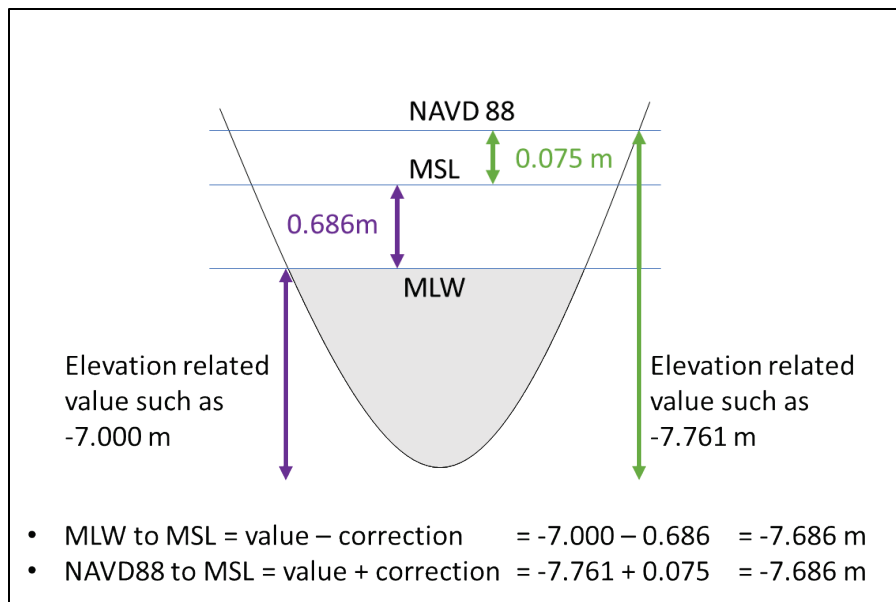
- Known projection information has been gathered and has been created to assist in converting datums. The datum for this file is mean low water (MLW) in feet.
- Using a graph similar to Figure 8-6, derive the necessary conversion to MSL.

- From the NOAA benchmark (in *green*), the distance from MLW to MSL is 2.25 ft (0.686 m).
- Make sure to get the conversion value for the appropriate units (feet or meters) to change the datum reference. The next section covers changing the units from feet to meters, where necessary.



Working with datums can be confusing. Moving from a lower to higher datum (MLW to MSL) will result in a larger depth. Moving from a higher to lower datum (North American Vertical Datum of 1988 to MSL) will result in a smaller depth. The expression used will entirely depend on whether the datasets should be Depths (positive down) or Elevations (negative down). It is strongly advised that users draw a diagram to ensure accurate conversions. See an example of this in Figure 8-7.

Figure 8-7. Diagram of datum changes.



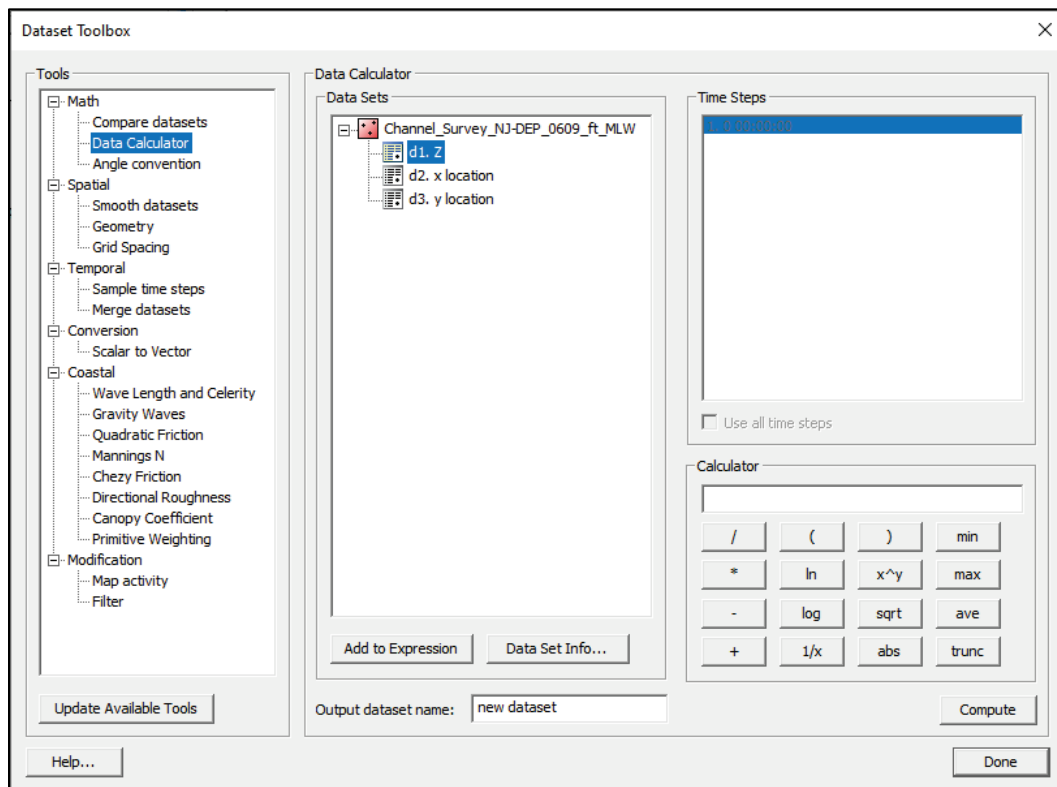
To do the actual conversions and apply them to the datasets, it is good to use a feature in the SMS called the Data Calculator, which is one of many tools in the Dataset Toolbox.

- Select the appropriate survey in the data tree and then click Data | Dataset Toolbox from the SMS pull-down menu shown in Figure 8-8.
- Select Data Calculator and not the item assignment for the Z dataset. It may be different on your computer than in the figure. For this

example, the item is assigned *d1*. Select the *Z* dataset and choose Add to expression.

Remember, the SMS 13.1 and later uses Elevations (negative down).

Figure 8-8. Dataset Toolbox dialog window.



- For the expression in the Calculator blank, add the conversion information computed above. The expression should read $d1 - 2.25$.
- Give a new dataset name (bottom of middle pane) such as MSL, ft, and click the Compute button. Do not hit Enter because we want to stay in this dialog for the next step.

8.4.1.2 Unit Conversion

- From the dataset toolbox, there should be a new entry listed, and its assigned number is *d4*. Next, we want to convert this new dataset from feet to meters.
- Select the new dataset and then hit Add to Expression.
- Enter the conversion from feet to meters in the calculator expression blank so that it reads $d4 * 0.3048$.

- Enter a new name for the converted units, such as MSL, m, and hit Compute.

8.4.1.3 Sign Change

If any of the survey datasets are using a positive value as they go deeper, then a sign change is needed. This is a simple calculation to perform with the data calculator.

- Select the last created dataset value from the data calculator (most likely MSL, m) and multiply that by -1 . Alternatively, place a minus sign in front of the dataset designator (i.e., d5.), give it a new name, and hit Calculate.

Repeat sections 8.4.1.1 through 8.4.1.3 where appropriate for the remaining datasets imported into the SMS.

8.4.2 Merging Data from Surveys

When generating a CMS-Flow grid, one bathymetry set is needed to provide depth values for each cell. If your project only has one imported bathymetry dataset, this step is not necessary.

There are two options for merging scatter sets: (1) merge ALL points from all selected scatter sets and (2) merge points from each selected scatter set based on its assigned priority. When merging all points, special care must be taken to ensure correct results because some scatter sets may overlap others. Overlapping areas of scatter sets should either be deleted or use the second method of merging by prioritization covered in section 8.4.2.3.

8.4.2.1 Merge All Scatter Points

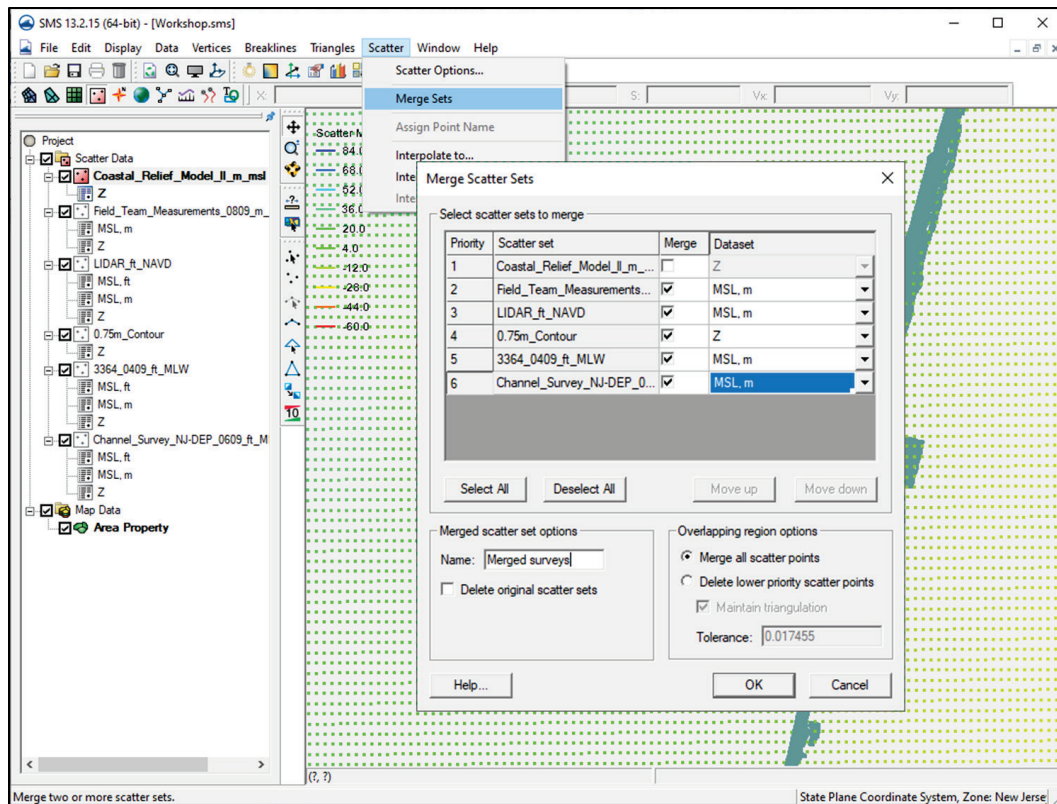
The first option will integrate all points for the selected scatter sets. Figure 8-9 shows the SMS dialog for merging scatter sets. Since the Coastal Relief Model does not have accurate bathymetric data in the nearshore, we will prioritize a more accurate dataset during the merge.

- From the pull-down menu, select Scatter | Merge Sets.
- Select all datasets except the Coastal Relief Model by clicking the Merge check box next to each dataset, or by choosing the Select All button and then deselecting the one we do not want to merge all points.

- For each dataset, select the appropriate dataset value to use for the merge (MSL, m).
- Choose a name for the merged scatterset. The default is Merged.
- Choose Merge all scatter points and click OK.

Once the merge has been completed and you are satisfied with the results, the old datasets can be deleted from the SMS data tree since they are no longer needed. Removing from the data tree will not erase the actual file saved in the folder; it is only deleted from local memory in SMS. When the next Save of the project is made, these datasets will no longer be included in the project file structure.

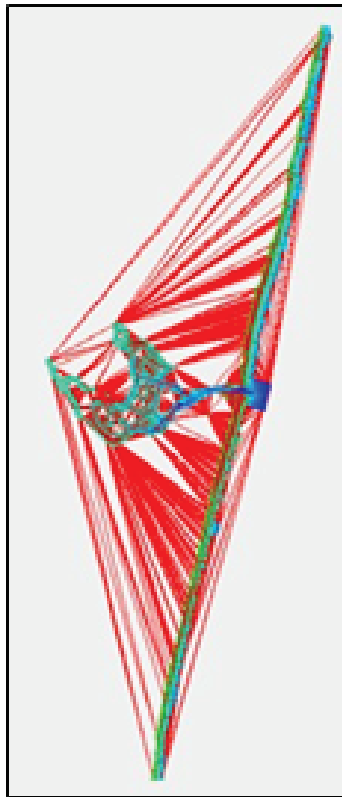
Figure 8-9. Merge Scatter Points dialog window.



At this point, there is only one scatter set that contains all surveys except the data from the Coastal Relief Model. We will use a different method to combine these two datasets so that points from the Coastal Relief Model, which are very coarse with poor nearshore elevation accuracy, are only used in areas where we do not have better data.

This option uses the triangulated area of the scatter sets to decide where to keep given points from a higher priority dataset. In Figure 8-10, we see the merged scatter datasets just created with triangles on (Display Options | Triangles [checked]), and we can see the total triangulated area. If this scatter set is used as a higher priority than another, no points from a lower priority dataset will be kept in the merged set of points where any of the triangles exist. The user may use or remove triangles as needed for prioritizing merged datasets as is discussed in the next section.

Figure 8-10. Triangulated elements for merged scatter set.



8.4.2.2 Removing Triangulated Elements


Due to the nature of triangulation, there can be large areas where no points exist that lie inside of a triangulated area. If needed, there is a tool in the SMS that can assist in finding these empty areas.

- To set a threshold of the maximum edge length of a triangle, click Scatter | Scatter Options, then set a value. Note: the units of the value

are determined by the horizontal projection units (degrees, feet, meters, etc.).

- Enter a value of 500. This will allow SMS to select triangles that have edges 500 m or longer.
- Click the box to Select Long Triangles. This will allow the user to see what will be deleted first.
- To select the affected triangles, click Triangles | Select Long Triangles. All triangles that exceed the given threshold will be selected and can be deleted, if desired.

Another way to remove triangles is to manually select them with the mouse.

- Click the Select triangle tool, .
- Click and hold down the Ctrl key and then use the mouse to left click and drag a line.
 - An arrow will appear as the user drags the mouse.
 - Any triangle that is touching the arrow when the user lifts from a left click will be selected.
 - If multiple selections are desired, add the Shift after the Ctrl is depressed, and each new clicked triangle will be added to the previously selected triangles.
- After selection, the Delete key can be used to delete the cells.
- Repeat as needed to remove additional triangular elements.

8.4.2.3 Merge Scatter Sets with Priority

- In the merged scatter set dialog (Scatter | Merge Sets from pull-down menu), change the selection in the Overlapping region options from Merge all scatter points to Delete lower priority scatter points.
- This will enable the list of scatter sets to be reordered using the Move up and Move down buttons.
- Select and reorder the scatter sets that are to be merged together.
- In our case this is the Merged and Coastal Relief Model... scatter sets.
- Make sure that the Merged scatter set is a higher priority than the other.
- The resulting list of scatter sets is shown in Figure 8-11.
- Make sure the dataset values to be merged are the one containing the desired datum and units (i.e., m, MSL).
- Provide a new name for the resulting dataset, such as Merged all.

- Click OK.

When the resulting scatterset is viewed with points and contours visible, the Merged all scatterset should look like a zoomed inlet area shown in Figure 8-12.

Figure 8-11. Merge Scatter Sets window. Reordered list of scatter sets to be merged with priority.

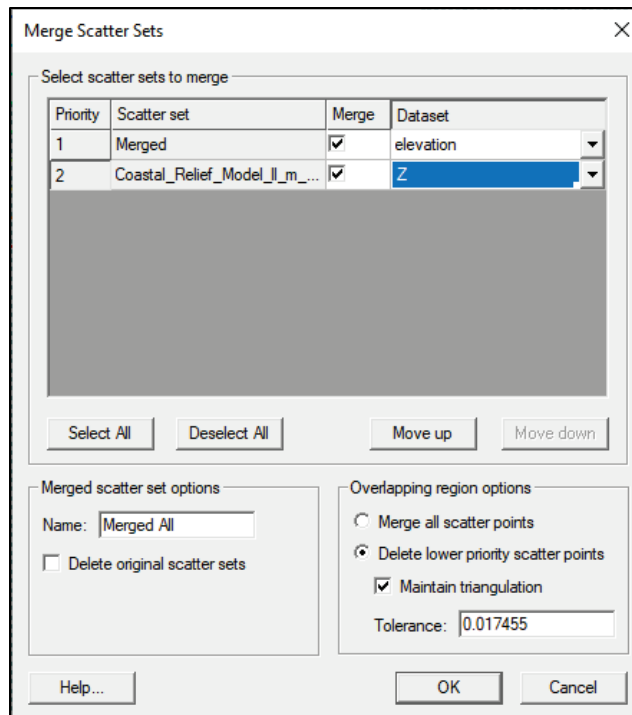
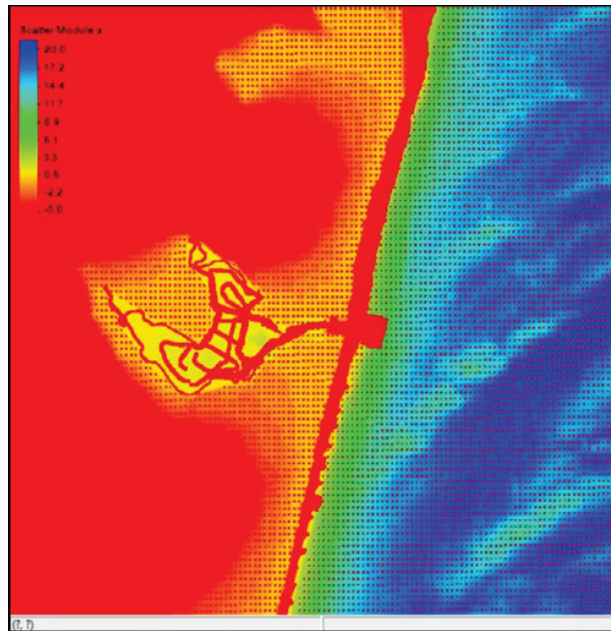



Figure 8-12. Scatter points and contours for the final merged scatter set.



8.5 Using Dynamic Images

- Click the Add Online Maps tool, , that should be on the same line as the lighting tool.
- Select the World Imagery option and click OK.
- SMS will create an image for the world space that is presently in the viewing window.
- Add any rectified aerial photographs you may have, if desired.
 - After loading, right-click on the image name and set the horizontal projection to the appropriate choice for the image and press OK.

The resulting dynamic image will appear in the Data Tree in the GIS Data section. Dynamic images will self-adjust as the user pans or zooms. This can take a few seconds depending on the size spatial extent.

8.6 Building a Conceptual Model for Project

When starting a new project within the SMS 13.2 interface, the user must build a conceptual model of the project using the Map module with a few different types of coverages. These coverages define specific pieces of information that SMS will need to generate and export the correct information for each CMS-Flow simulation. This section shows how to build the conceptual model with a quadtree (also called telescoping) grid.

The user should have a good understanding of the project area so proper care can be taken to generate a good grid. For the example case of Shark River, New Jersey, the main inlet channel is the primary area of focus for capturing the correct current velocity with finer resolution and should have 8–12 cells across it, limiting the cell size down to at least 10 m in the entrance channel. The two main back channels splitting off the entrance, the north and south channel, also have large velocities (the north channel has the strongest current) and should be represented by at least several cells in width (minimum of 5 m in the narrow north channel).

8.6.1 Create the Necessary Coverages

- Right-click Map Data and choose to create new coverages.
 - Expand Models, if needed, and select the CMS-Flow | Boundary Conditions coverage (Figure 8-13). Give a new name if desired and then press OK.
 - Repeat the process to create additional coverages for the Generic | Activity Classification and Generic | Quadtree Generator.
- The resulting data tree will show the new coverages (Figure 8-14).

Figure 8-13. New Coverage dialog window for Coastal Modeling System-Flow (CMS-Flow) boundary conditions.

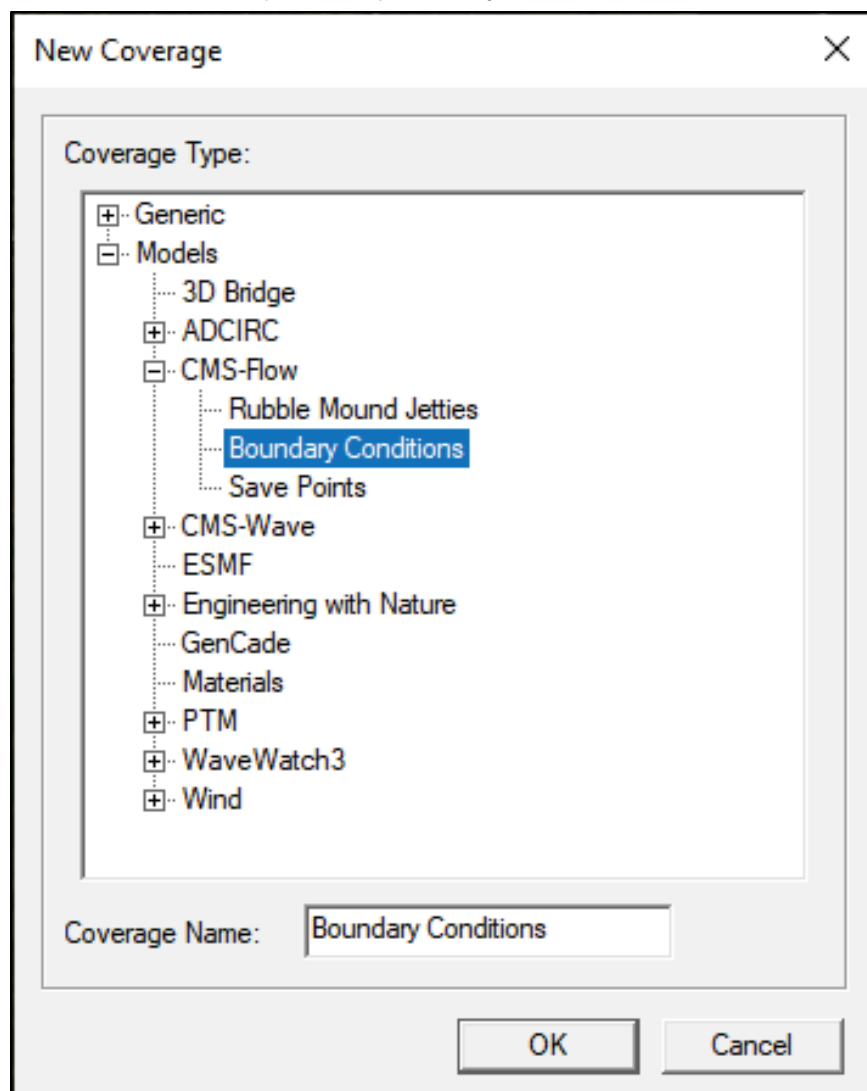
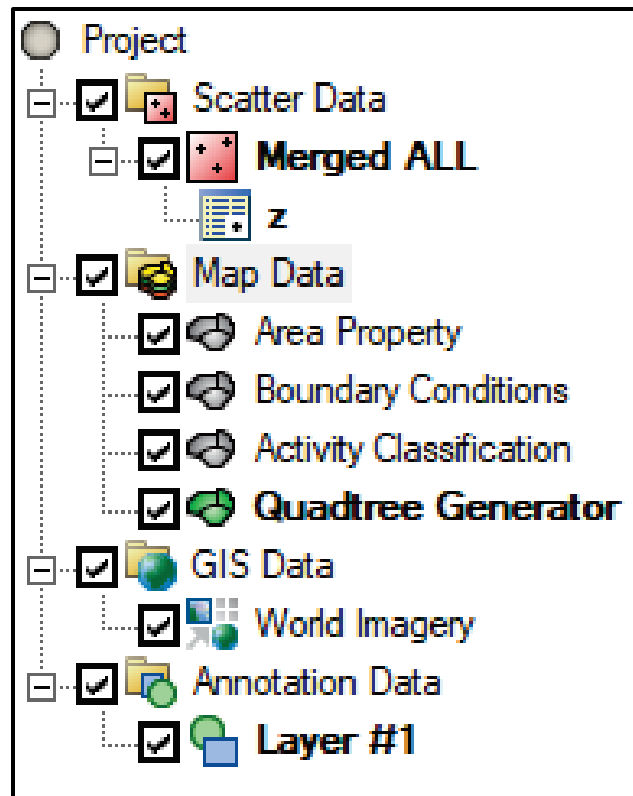



Figure 8-14. Updated coverages in Surface-water Modeling System (SMS) data tree.



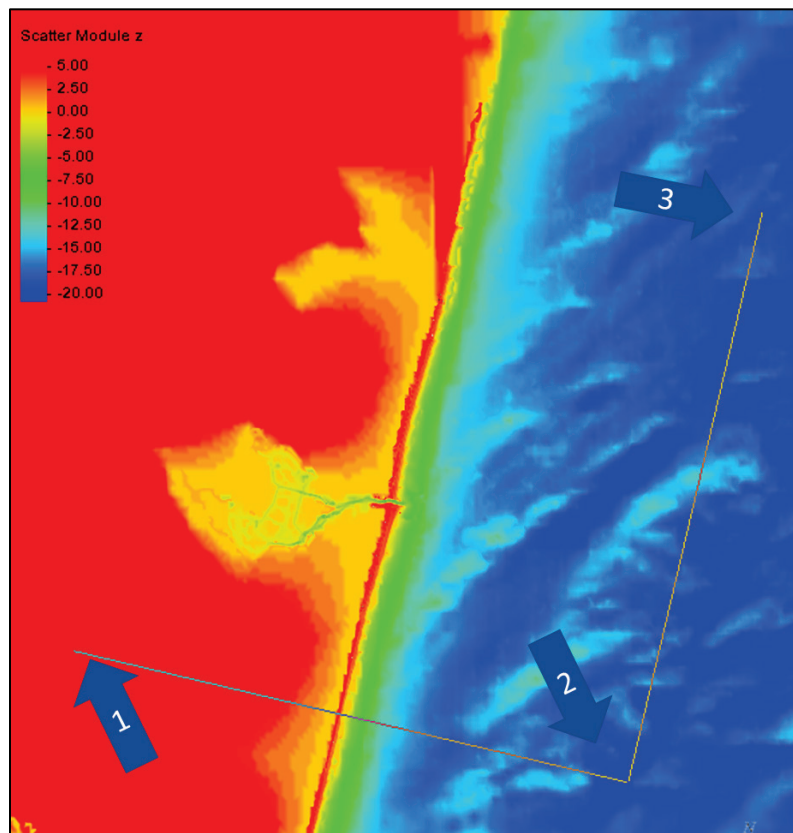
8.6.2 Create Quadtree Project Domain

To define the extents of the project domain, SMS needs the size of the intended simulation area. These choices can be modified later, and an updated grid can always be recreated later, so there is no need to be extremely precise at first.

- From the data tree, left-click the Quadtree Generator coverage (or the name that was chosen when the coverage was created). This will enable an additional tool in the toolbox to define the domain extents.
- Click the Create 2D Grid Frame button, .
- Draw two legs of the rectangular boundary for the model domain by clicking the *lower-left* landward boundary corner point, then the *lower-right* ocean boundary corner, and then the *upper-right* landward boundary corner to close the box as shown in Figure 8-15.
 - Note: for creating the CMS-Flow domain, the three points can come in any order. (This not the case for creating the CMS-Wave domain, which will be covered later in this manual.)

- Also, the grid frame is generated but may be partially hidden from view by filled display contours. Making contours semitransparent can help.
- In a later section, this coverage will be used to assign zones of resolution.

Figure 8-15. Point locations to define the extents of the grid frame.





- Use the Select 2D Grid Frame button  to select the center point of the purple outlined grid domain, adjust the edges by dragging the center point of each edge, and change the orientation by selecting the  at the corner of the grid. Note that the IJ triad should be in the lower-left corner.
- Right-click the highlighted center button and click Properties to further modify the dimensions of the grid boundary as needed. An example for this case is shown in Figure 8-16.

Figure 8-16. Grid Frame Properties dialog window.

The dialog window is titled "Grid Frame Properties" and contains the following fields and options:

- Origin, Orientation and Dimensions:**
 - Origin X: 186200.000000
 - Angle: 347.000000
 - I size: 7630.000000 m
 - Origin Y: 145780.000000
 - J size: 11100.000000 m
- I Cell Options:**
 - ☒ Define cell sizes
 - ☒ Cell size: 10.000000 m
 - ☐ Number of cells: 763
 - ☐ Use refine points
 - Maximum cell size: 10.000000 m
 - Maximum bias: 1.100000
 - ☒ Use inner growth
- J Cell Options:**
 - ☒ Define cell sizes
 - ☒ Cell size: 10.000000 m
 - ☐ Number of cells: 1110
 - ☐ Use refine points
 - Maximum cell size: 10.000000 m
 - Maximum bias: 1.100000
 - ☒ Use inner growth

Buttons at the bottom: Help..., OK, Cancel.

Next, the grid boundary is set square to the general orientation of the coastline, with the computational direction, I and J (or IJ triad), set according to the model type. For the Quadtree Generator coverage, the point of origin will be automatically placed in the lower-left corner of the grid after the grid has been created. This is default for CMS-Flow. This means that for most Atlantic coast (east-facing) projects, the IJ triad will be located over land on the lower-left corner. Do not change the I and J directions because this is specific to CMS-Flow.

8.6.3 Defining the Interface Between Land and Water Interface (Activity Classification)

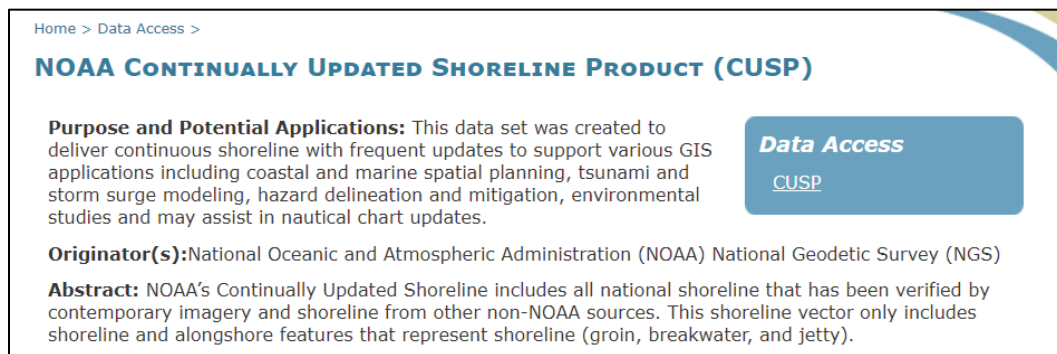
By using polygons with this coverage, the domain will have land (noncomputational) and water (computational) areas. Cells in areas that are defined as land will NEVER be computed, whereas all other cells MAY be computed depending on the water level and wetting and drying criteria during the simulation.

The polygons are defined using feature arcs that are fully enclosed (connected). These polygons can come in from various sources such as ArcGIS, coastline databases, computation from a given bathymetry contour, or even manually defined.

One example of obtaining a shoreline from a coastline database is given here.

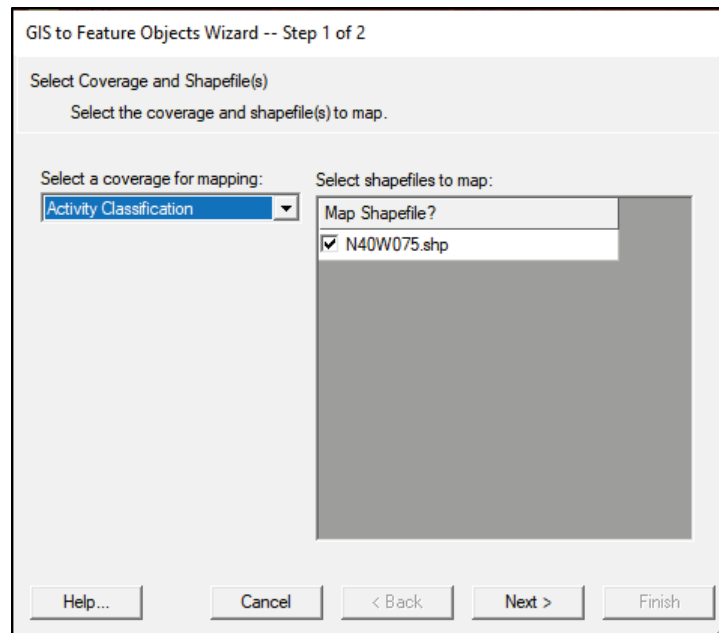
- Using a web browser, go to the NOAA Continually Updated Shoreline Product (CUSP) website located at <https://shoreline.noaa.gov/data/datasheets/cusp.html> (NOAA, “Shoreline Website,” n.d.).
- In the Data Access section (Figure 8-17), click CUSP, then zoom to the area of interest for the project. The available CUSP shoreline for the area will be colored differently than the background (currently green).

Figure 8-17. Data access section of the NOAA website mentioned above. (Image reproduced from NOAA, “Shoreline Website,” n.d. Public domain.)



- Click on the screen near the area of interest and then click Download to get that entire area.
 - A zip file will start to download that contains ArcGIS files with the requested data.
- Extract the files from the zip into a folder; then choose the ArcGIS Shape file with the .shp file extension and drag it into the SMS interface.
- Convert the data from the shape file into feature arcs
 - Right-click the corresponding dataset in the SMS data tree
 - Choose Convert | Shapes → Feature Objects and choose the Activity Classification coverage as shown in Figure 8-18.

Figure 8-18. Geographic Information System (GIS) to Feature Objects Wizard dialog window.



- Click Next. This will bring up a new dialog that allows you to choose which information contains the elevation information, if desired.
- For this case, we are not interested in the actual elevation from that database, only the coastline arc itself, so click Finish to create feature arcs in the Activity Classification coverage for the shoreline.
 - Note that this procedure may take some time as there will be numerous arcs created for the area. In this case, the download file contained a 5×5 degree area, and SMS takes some time to check for duplicates with that many arcs.

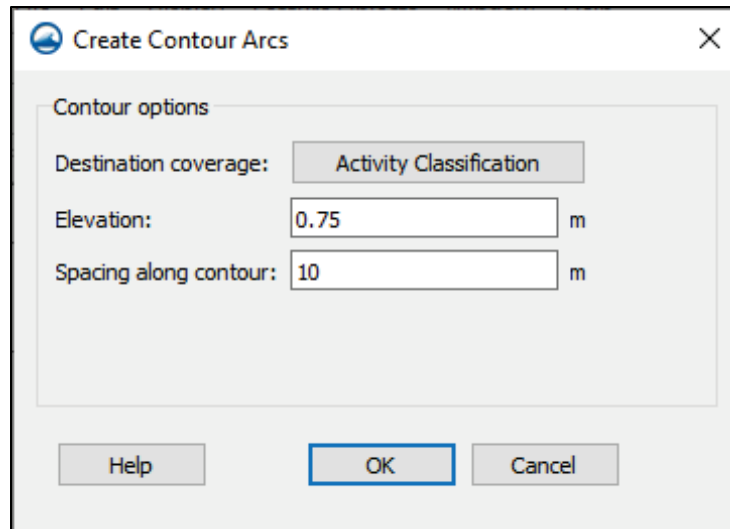


Another method is to create features arcs that follow a certain bathymetric contour. This is normally only used if you have clean bathymetry at a good spacing.

- Select the desired bathymetry scatter set in the data tree for the feature arcs.
- Right-click and choose Convert | Scatter Contours → Map.
- Click next to Destination Coverage and choose the Activity Classification coverage.
- Enter the desired bathymetry contour that will be used for the coastline and spacing for the points (Figure 8-19).

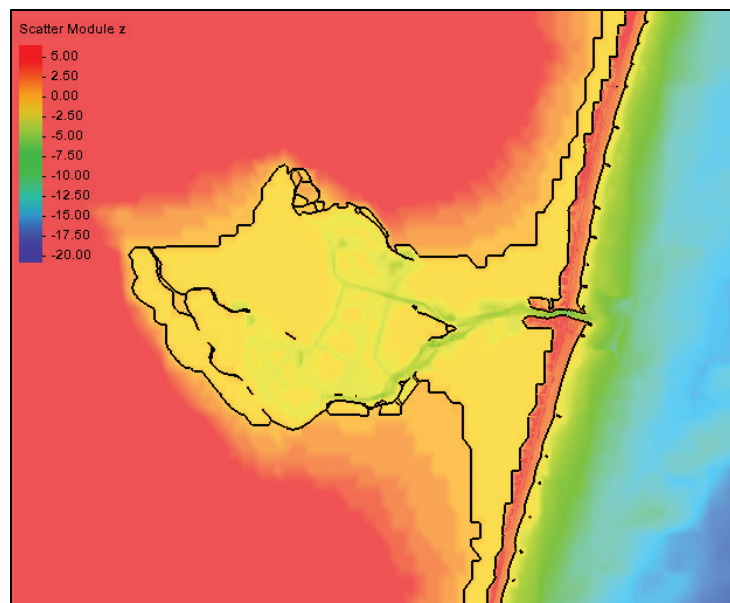
- For this example, the 0.75 m contour will be converted to a feature arc in the Activity Classification coverage.
- Note: with bathymetry contours that are not clean, this method can be time consuming due to the cleanup needed for various feature arcs.

Figure 8-19. Create Contour Arcs dialog window.



As you can see in Figure 8-20, the resulting feature arc can be close to what is needed depending on the correct choice for the elevation chosen (0.75 m in this case), but there are many extraneous arcs that must be removed and the shoreline smoothed a bit.

Figure 8-20. Bathymetry contour converted to feature arc.



The following steps describe how to clean the excess feature arcs.



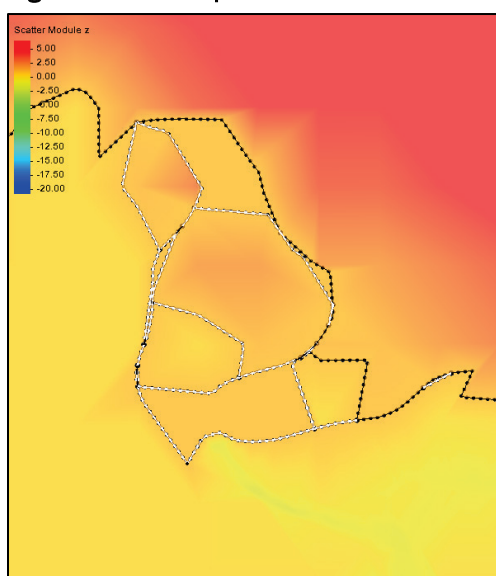

- Click the Feature Arc selection tool, .
- Click the first arc to be removed and then click subsequent arcs while holding the Shift key down to multiselect and press delete.
- Continue for the entire domain area. Example arcs are shown in Figure 8-21.
- A few arcs may need to be connected as well. Click the Create Arc tool, , and start from the end of an existing arc, and then connect to the other arc.

Figure 8-21. Example of extra arcs to delete.



Manual input of feature arcs by clicking points is also allowed.

- Make sure the Activity Classification coverage is active and then choose the Feature Arc Creation tool, .
- Start at any desired location with the understanding that all arcs designating the shoreline should all be connected.


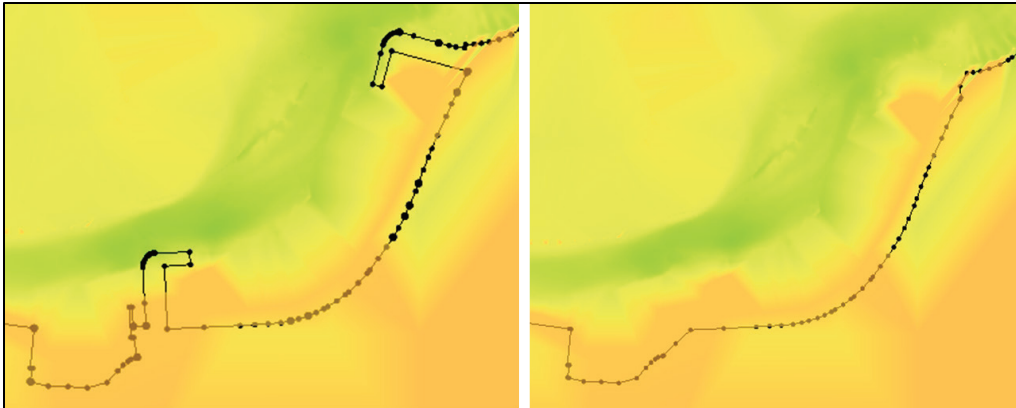
Sometimes there may be too much complexity in the shoreline, and individual vertices must be removed instead of the entire arc. To remove these vertices, choose the Select Vertex tool, , and click the vertices, then delete. Multiselecting vertices can be selected by drawing a rectangle or using Shift to add to the existing selection before hitting Delete. A before-and-after is shown in Figure 8-22.

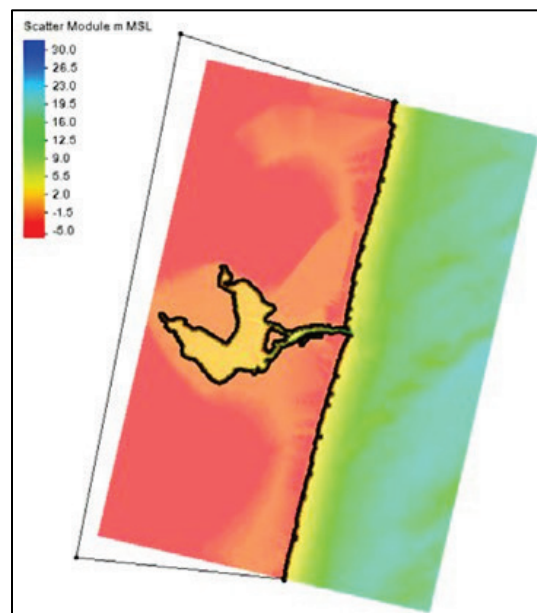
Figure 8-22. Before and after extra resolution is removed from feature arcs.




After the shoreline is adequately defined,

- Use the manual-input method to connect the lateral extents of the shoreline together with another arc that encloses the land area. An example is shown in Figure 8-23. You do not need a closed polygon to depict the ocean area.

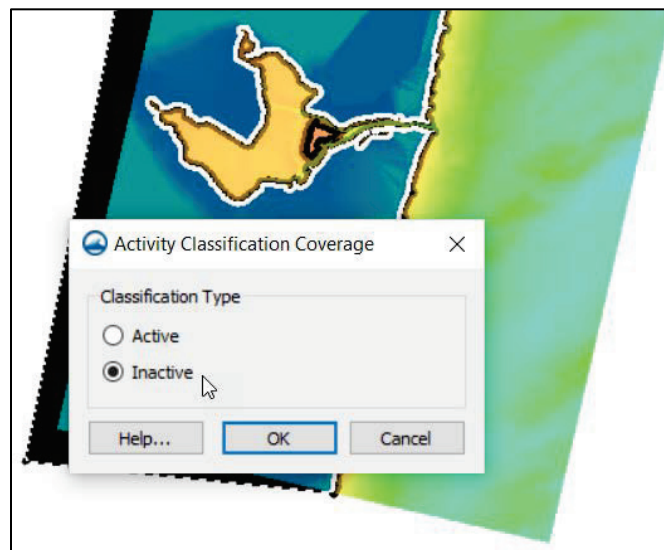
Figure 8-23. Enclosed set of feature arcs for defining land (inactive) area.



- Convert the feature arcs to a feature polygon by choosing Feature Objects | Build Polygons from the pull-down menu.
- Choose the Select Polygon tool, , and then click the land area to select the polygon.

- Choose Feature Objects | Attributes from the pull-down menu and make sure Inactive is selected, and then click OK as shown in Figure 8-24.
- Tips
 - Some iteration of each of these methods is typically needed.
 - Make sure the lateral extent of your shoreline extends to or beyond the edge of your Quadtree grid frame.

Figure 8-24. Activity Classification Coverage dialog window. Activity Classification type selection for polygon.



8.6.4 Defining Grid Resolution

When defining CMS grid resolution for a telescoping grid, the resolution is assigned in zones. These are represented in SMS with feature polygons. In a section above, the Quadtree Generator coverage was created to specify domain extents. There was also some work done in the Activity Classification coverage that specifies the land-water interface.

What would be useful in generating the resolution polygons is to have the same coastline that was just created. However, when coverages are switched from the Activity Classification to the Quadtree Generator coverage, the arcs are not present. It is possible that the arcs from the other coverage will be visible if the display options are set to allow it. To be used, however, those arcs must be copied to the present coverage with the following steps:

- Switch to the Activity Classification coverage.

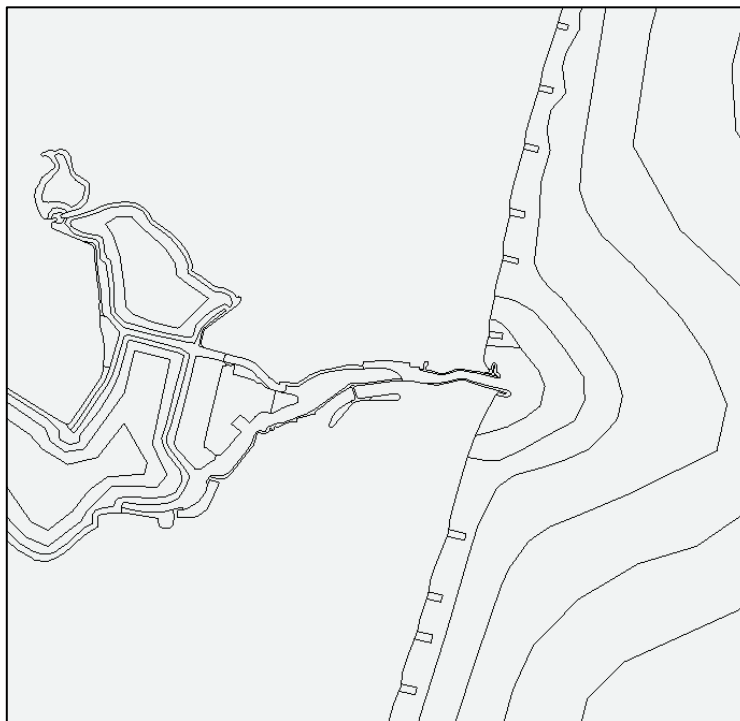
- Select all feature arcs by choosing the Select Feature Arc tool, then press the Control key and the letter A to select all feature arcs. You will see the lines change color a little.
- Next, right-click and choose Copy to Coverage . . .
- Choose the Quadtree Generator coverage and click OK.

When we switch back to the Quadtree Generator coverage, the arcs are now there along with the grid frame that was created earlier.

As mentioned earlier, resolution for CMS telescoping grids is polygon specific. Resolution within each polygon will have a set maximum refinement. The resulting grid may have transition regions within polygons as they interact with neighboring resolutions that differ. An example of a very well-defined resolution map for Shark River is shown in Figure 8-25.

Each polygon can have a different cell size specified. Special attention should be given to areas such as in the inlet throat, jetties, groins, constrictions of flow in the bay, bridge pilings, and others.

Figure 8-25. Example of resolution zones defined for a CMS grid.



Define each polygon with a series of connected feature arcs as previously described.

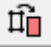
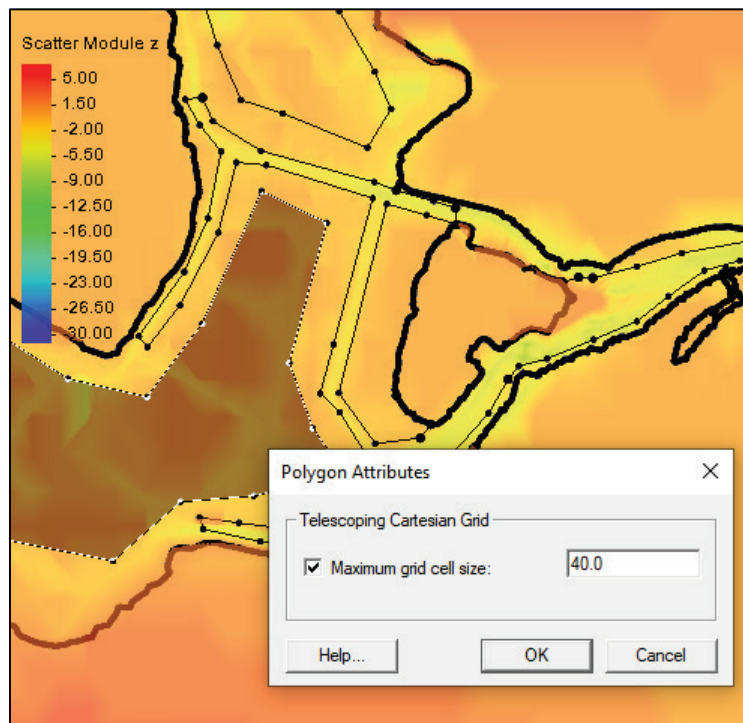
- Using the Create Feature Arc tool, create arcs to delineate the areas for resolution.
 - Each zone must form a polygon with no gaps in arcs around the zone.
- To set the resolution, choose Feature Object | Build Polygons from the pull-down menu, or choose the Build Polygons tool, .
- Then double-click each polygon to assign a maximum cell size as shown in Figure 8-26.
 - Check the box to set the maximum grid cell size and enter a value.
 - If a polygon exists but does not have the box checked, it will use a base cell size as defined later.

Figure 8-26. Polygon Attributes dialog window. Setting a resolution value for a polygon.



8.6.5 Creating the Quadtree Grid

When ready to build the CMS telescoping grid, follow these steps:

- Right-click on the Quadtree Generator coverage and choose Convert | Map -> Quadtree Grid.
 - The resulting dialog is shown in Figure 8-27.
 - The information at the top should be identical to what you entered for the grid frame.
- At the very top, enter a descriptive name for the resulting quadtree grid in the area marked Grid name.
- Enter a maximum (base) cell size for areas where no resolution zones are specified. For this example, a base size of 160 m is chosen.
- Set the source to select the desired bathymetry scatter set, and then click OK and review the quadtree grid.

Figure 8-27. Map → Quadtree UGrid dialog window. Data needed for generating the quadtree grid.

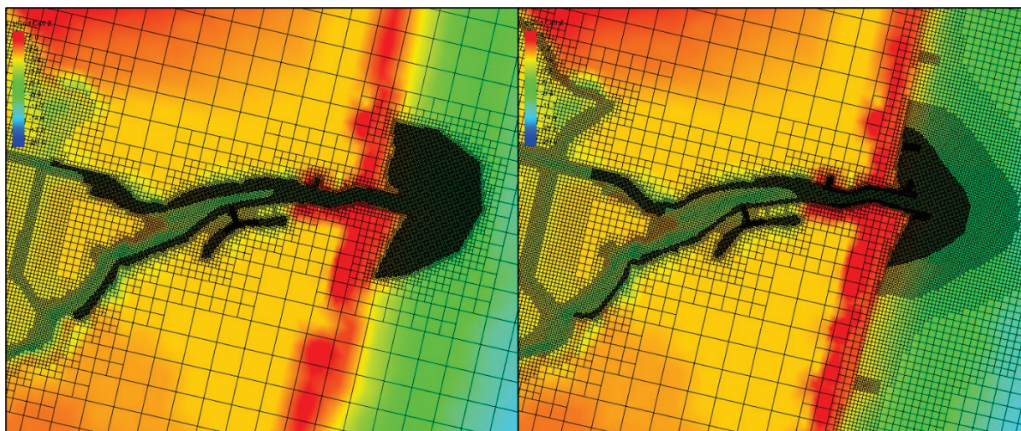
The screenshot shows the 'Map -> Quadtree UGrid' dialog window. The 'Grid name' field is 'Quadtree Generator Grid'. The 'Origin, Orientation and Dimensions' section has 'Origin X: 186200.000000', 'Angle: 347.000000', 'I size: 7680.000000 m', 'Origin Y: 145780.000000', and 'J size: 11100.000000 m'. The 'Target minimum cell size' is '2.500000 m' with an 'Adjust base cell size' button. The 'I Cell Options' section has 'Base cell size: 160.000000 m' and 'Number of cells: 48'. The 'J Cell Options' section has 'Base cell size: 160.000000 m' and 'Number of cells: 70'. The 'Depth Options' section has 'Source: Scatter Set' and a 'Select...' button. The bottom has 'Help...', 'OK', and 'Cancel' buttons.

Repeated attempts of these steps will be needed to form the final quadtree grid for a given project.

- Delete the quadtree grid.
- Make the necessary adjustments in the Quadtree Generator dialog.
- Create a new grid based on the updated information.

A portion of the resulting grid for two variations of map resolution is shown in Figure 8-28. To better see the result in cell resolution, a change can be made in the Display Options | Quadtree pull-down menu.

Figure 8-28. Two resolution variations on a quadtree grid with increasing complexity.



Between SMS versions 11.2 and 13.2, the ability to turn off land cells was lost. This has now returned in SMS version 13.2. To accomplish this, the user must select the cells that they would like to disable. Since this project has an Activity Classification coverage where Land was chosen, the same polygon can be used to turn off the display of those cells.

- Select the Activity Classification coverage, and then select the Land polygon.
- Right-click on the polygon in the graphics window and choose Select Intersecting Objects.
- From this dialog (shown in Figure 8-29), choose the UGrid radio button.
- Make sure Cells is selected in the combo box.
- At the bottom, in the Boundary Treatment area, leave the default selection Ignore boundary, select by point.
- Click the quadtree grid object in the right panel and then click OK. The cells which were inside that polygon are now selected.
- Now right-click and choose Edit Cell Activity, and then choose Off and press OK.

The resulting display after the Land cells are turned off is shown in Figure 8-30.

Note: when cells are turned off in the interface, they cannot be selected unless visibility of Off cells is enabled in the UGrid Display Options.

Figure 8-29. Select Intersecting Objects dialog window. Making the proper selection of cells to turn off.

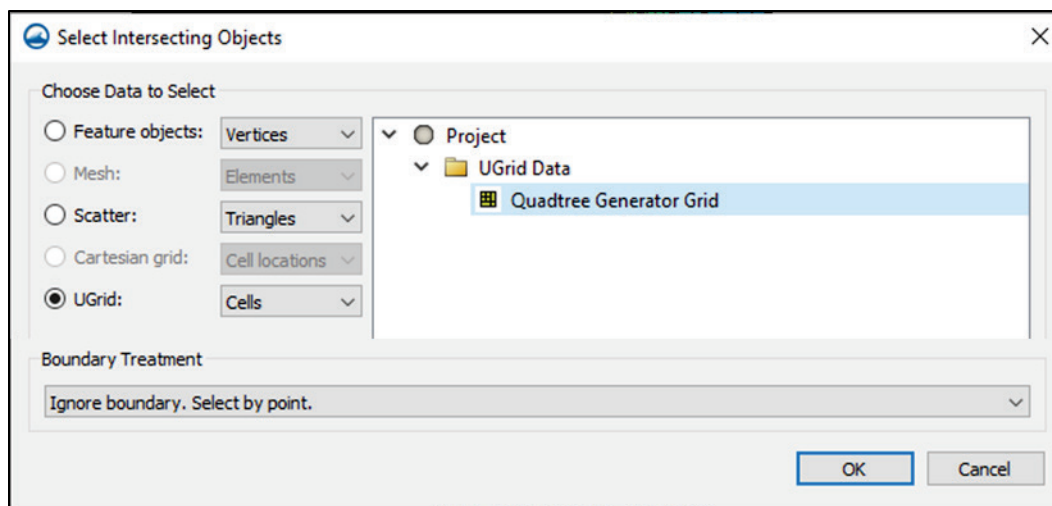
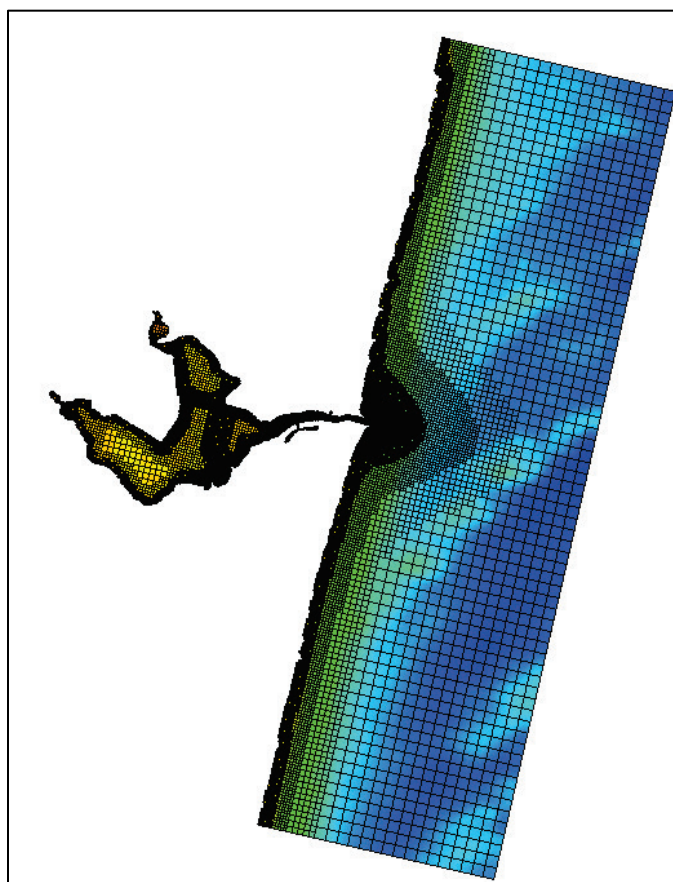


Figure 8-30. Display after selected cells were turned off.



8.6.6 Defining CMS Forcing (Boundary Conditions)

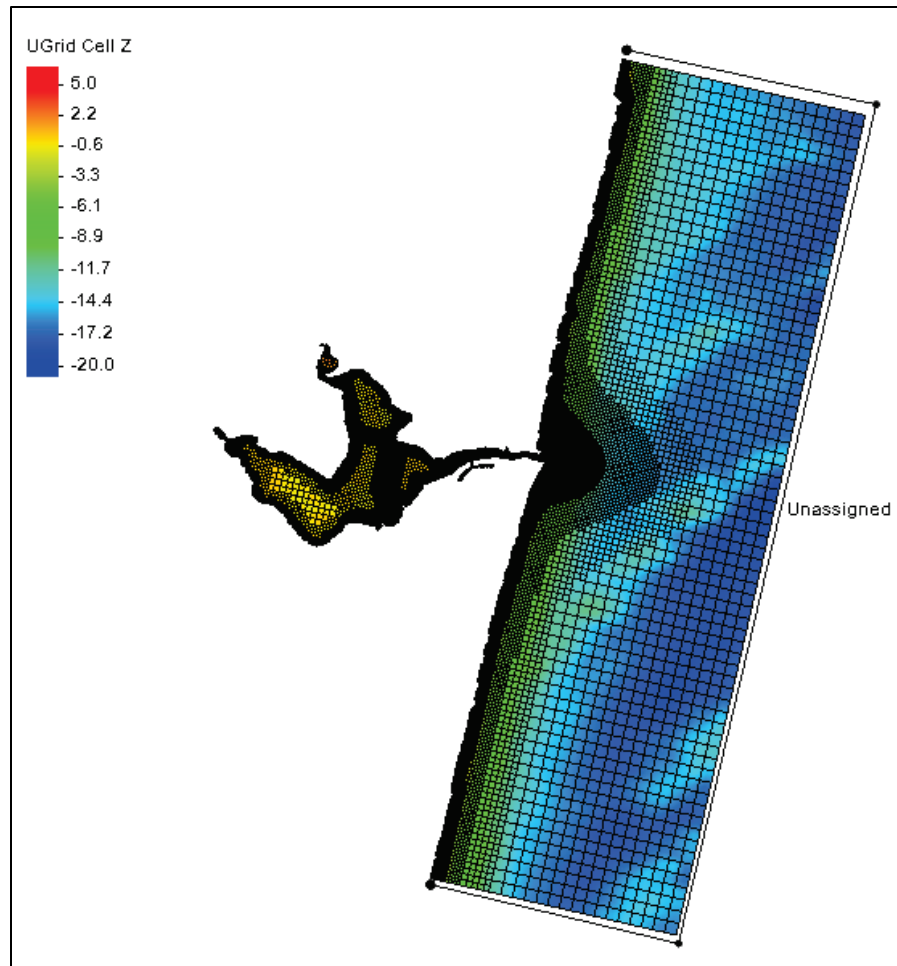
The CMS boundary conditions are set in the Map Module with feature arcs with associated forcing type designations. There are several types of forcing conditions that are used with CMS including water level, river flux, tidal or harmonic constituents, and some that use information from separate hydrodynamic models. For the purposes of this user's manual example, the boundary conditions for water level and river flux will be covered.

8.6.6.1 Water Level Boundary Condition

For the example case of Shark River, New Jersey, there is little appreciable freshwater discharge, so it is not necessary to include the flux in the CMS simulation. The ocean boundary condition will be set to the measured WSEs from a nearby location, Sandy Hook, which is verified with a tide gauge located inside the bay on the marina at the end of the South Channel. Water-level data can come from many sources. One convenient source is from NOAA, by way of its NOAA Tides and Currents website (NOAA, "Tides and Currents," n.d.). In this example, data from the month of August 2009 have been gathered and will be used to apply for this boundary condition.

- Switch to the Boundary Conditions coverage in the data tree.
- As described earlier, create a feature arc to assign as a water level boundary condition for the ocean. The arc should cover the entire offshore edge of the grid and should start and end close to the shoreline. An example is shown in Figure 8-31.

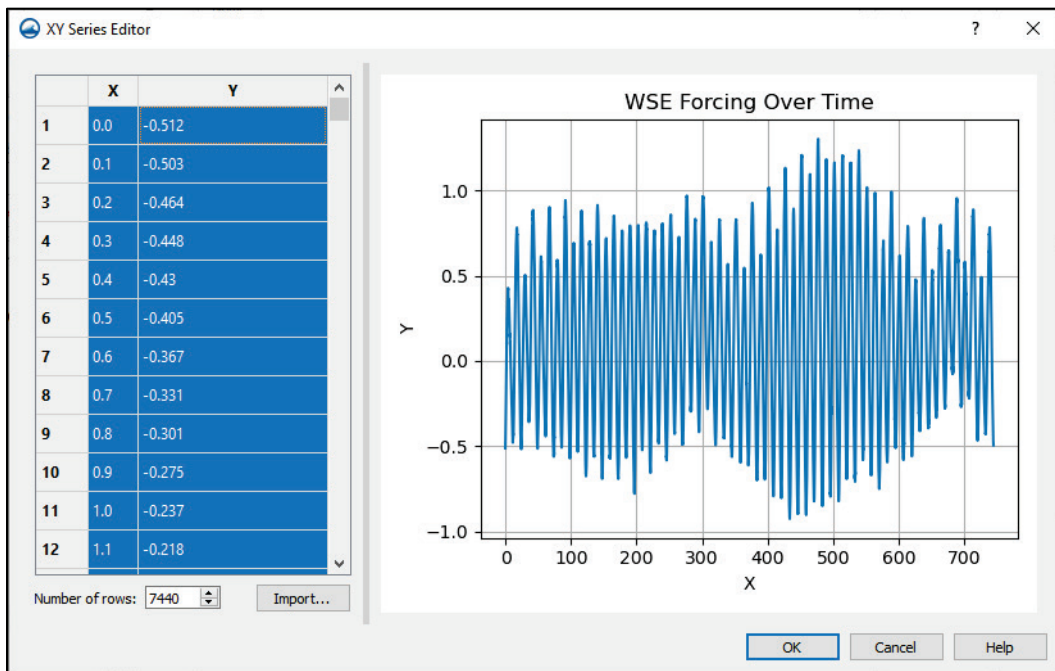
Figure 8-31. Example placement of the water level forcing arc.



- Notice the arc initially appears with the moniker Unassigned. This will change after the forcing information has been applied.
 - Note that the arc does not have to match exactly with the edge of the grid domain. SMS will pull the information and assign to the appropriate cells upon exporting to the CMS files.
- Next, double-click on the arc just created with the selection tool to bring up the Arc Boundary Condition dialog.
- Change the Type to WSE-forcing and the source to Curve.
- Click the button next to the box marked Define curve to enter the water level forcing information.
- Open the water level data obtained from the designated source in some application. Columnar data are best opened with a spreadsheet such as Excel.
 - The X column should contain the time information in units of hours. If the data do not match, perform an expression to create a column with that information in the correct unit.

- Select the entire time series with the time in hours, copy to the clipboard, and then paste it into the XY Series Editor under the *X* column.
 - * Before pasting (Ctrl-V) the data, select either the first cell or the entire row, then paste.
- Select the column for the water level data (ensuring it is in meters), then paste that column under the *Y* column.
- Both columns can be copied and pasted together if they are adjacent in the spreadsheet.
- The resulting curve should now be shown in the XY Series Editor window (Figure 8-32).
- Click OK when done to save the water level curve.
- Enter an offset for this water level curve, if desired.
- Click OK when complete. The boundary condition should change from Unassigned to WSE-forcing.

Figure 8-32. XY Series Editor dialog window. Properly completed XY Series Editor for water level curve.



8.6.6.2 River Flux Boundary Condition

If a river flux boundary condition is necessary, the process to define it is nearly the same as for the water level boundary condition with a few differences.

- The created arc should follow the *I*- or *J*-direction of the model domain. This means that it should attempt to connect to cells all on the same row or column and not a staggered combination of cells from different rows and columns.
- The arc should be located near the land-water interface as specified in the Activity Classification coverage. If hidden, turn on the coverage to better judge where to place the feature arc for this boundary condition.
- The Type should be set to Flow Rate-Forcing, and the flux values provided should represent the total flow for that incoming arc.

By default, the flux forcing for each boundary condition enters the grid perpendicular to the feature arc. If an inflow direction is desired, there is a location in the boundary condition dialog to enable direction, and a value can be entered.



Note: the SMS 13.2 interface presently shows the angle specified should be oriented in a *FROM* direction, which is incorrect and will be corrected in a future SMS release. CMS expects the angle specified to be oriented in a *TO* direction. For example, 0° is to the north, 90° is to the east, etc.

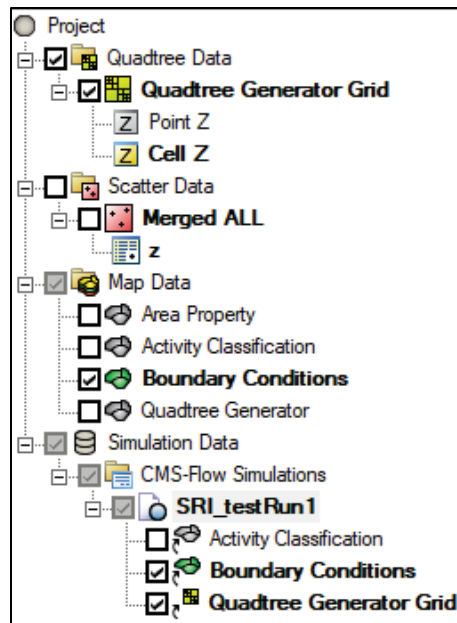
8.7 Running CMS-Flow

SMS does a good job defining CMS-Flow runs. This is with a new feature for Simulations. With this feature, a user can set up multiple runs with different combinations of activity classification coverages, boundary condition coverages, and quadtree grids.

8.7.1 Create a CMS-Flow simulation

- Right-click in the open space at the bottom of the data tree and choose New Simulation | CMS-Flow. This creates an empty simulation named Sim. You may want to rename this to something more meaningful.
 - For the example, the name SRI_testRun1 is used.
- Right-click on the Activity Classification coverage and choose Apply to and select the particular simulation you wish to use this coverage with.
- Repeat this for the Boundary Conditions coverage.
- The simulation does not link to Quadtree Generator coverage; rather, it links to the actual Quadtree Grid. Right-click on Quadtree Grid and Apply to the simulation.
- The resulting data tree can be seen in Figure 8-33.

Figure 8-33. Data tree after adding options to the new simulation.



8.7.2 Defining CMS-Flow Model Control

In previous versions, the CMS-Flow model control was entered by a pull-down menu. With SMS 12.3 and later, the model control dialog is attached to each simulation.

Right-click on the simulation (SRI_testRun1 in this example) and choose Model Control to bring up a dialog containing several pages for different CMS-Flow processes each with its own settings. The pages are General, Flow, Sediment Transport, Salinity/Temperature, Wave, Wind, and Output. Click each tab and set the appropriate information as needed for each project.

8.7.2.1 General Tab

The general page covers a range of topics such as starting date and time, simulation duration, forcing ramp duration, hot start settings, solution scheme choice, and the number of CPU cores or threads to use for the run.

8.7.2.2 Flow Tab

The flow page covers topics related to hydrodynamics, such as time-step selection, wetting and drying depth, Coriolis, bottom and wall friction, bottom roughness, and turbulence parameters.

8.7.2.3 *Sediment Transport Tab*

This page covers topics related to sediment movement and bed load properties with sections for timing, sediment transport type and formula, sediment properties, bed composition, sediment grain size classes, avalanching properties, and definition of hard bottom, if needed.

8.7.2.4 *Salinity/Temperature Tab*

This page covers information needed for simple salinity and temperature transport including water properties, initial conditions for salinity, temperature, and atmospheric parameters.

8.7.2.5 *Wave Tab*

The wave page allows the user to specify if and how the CMS-Wave model will be run in conjunction with the CMS-Flow and lets the user define the wave model file location, steering interval, and extrapolation distances.

8.7.2.6 *Wind Tab*

The wind page allows the user to specify if and how wind is applied for the given simulation. The user can choose from a variety of wind forcing types and other parameter values.

8.7.2.7 *Output Tab*

The output page lets the user define how simulated data are written to solution files for review at a later time.

8.7.3 **Bottom Roughness**

Every simulation should have a bottom roughness dataset associated with it. On the Flow page in the Model Control dialog, there is an option to assign a Bottom Roughness Dataset; however, that dataset must be created first before it can be properly associated.

Different values may be used depending on the type of bottom friction to be applied. These types are Mannings n , Bottom Friction Coefficient, or Roughness Height. In this example, Mannings n is to be selected, and the appropriate default value must be chosen.

- Left-click on the quadtree grid in the data tree to select it.

- Click Data | Dataset Toolbox from the pull-down menu at the top.
- Choose Data Calculator from the list in the leftmost column.
- Enter the appropriate value to be used in this simulation.
- Enter the friction value into the calculator blank. In this case, the value of 0.025 is used.
- Change the Output dataset name to a reasonable value such as Mannings n , then click Compute to create the new dataset.
- When asked, choose to map the values to Cells, then click Done.

There may be times when the user wants to modify the bottom friction coefficients in areas of turbulence, such as near bridge pilings. To modify values from the default,


- Click the Mannings n dataset in the data tree to select it.
- While the dataset selects, the user cannot see any bathymetry values. It may be useful to load a rectified image or to add a dynamic image as previously mentioned. Set the transparency option in the Display Options dialog to a value which allows good view of the image beneath the contour colors.
- Click the Select Cell tool, , and select cells for which to modify the friction value with the methods below. Any of the following methods can be used. Add to an existing selection by holding the shift key.
 - Select a polygon with Edit | Select with Poly.
 - Select a rectangle just by dragging a box.
 - Select individual cells with a left mouse click.
- When all the cells are selected, enter a new value in the *S* box above the display window as shown in Figure 8-34. For this exercise, the value is used 0.03 for a few locations.
- Note: make sure to enter the value in the *S* box and not the *Z* box. Otherwise, the depth values will be modified, which is not the desired outcome.

Figure 8-34. Location of scalar entry point denoted by *S*.

X:	191712.49407678	Y:	150441.94396722	Z:	-10.49609279633	S:	0.03
----	-----------------	----	-----------------	----	-----------------	----	------


8.7.4 Sediment D50 Dataset

Sometimes the median grain size is required for the bed composition and a dataset must be created. This is done in a similar manner as defined for bottom roughness in the last section. The median grain size can be found

from various sources, perhaps from a sediment sample that has been analyzed. Once the information has been obtained, the dataset can be created with the median grain size value to be used for the grid.

- Open the Data Calculator and enter the value for the median grain size into the Calculator box. For this example, the value of 0.26 is used.
- Change the output dataset name to something meaningful, such as D50.
- Click Compute and choose to map the dataset to Cells, then click OK.

Just like the bottom friction dataset, there may be times when the user wants to modify the D50 value for specific areas. One typical location for this is within the main channel where the increased velocity has depleted the finer grain sizes and left more coarse sediment. Using the method discussed for modifying the ManningsN dataset in the previous section, modify the D50 value in the channel.

- Click the D50 dataset in the data tree to select it.
- Right-click on the D50 object and choose to apply dataset specific contours.
 - For a better appearance, the legend can be modified to have a white font with bolded features. Also, a data value range of 0.26 to 0.60 can be selected. Additionally, the colors can be reversed, if desired.
- Click the Select Cell tool, , and click a polygon around the area of the main entrance channel thalweg.
- Change the *S* value from the original default of 0.26 mm (SMS sometimes adds numbers to the small extents of the decimal values, but it is close enough) to 0.4, 0.5, and 0.6 mm or some other values as needed for this area of the project.

8.7.5 Hard Bottom Dataset

The CMS sediment transport and bed equations assume the bed material is available for entrainment. Sometimes one may encounter hard bottoms where bed materials are nonerrodible, such as bare rock, carbonate reefs, and concrete structures.

By default, CMS-Flow cells are fully errodible with no specified hard bottom depth. If the user wishes to use hard bottom to represent areas of nonerrodible cells, they will use a dataset from within SMS. Cells that are to

be fully erodible should have a value of -999.0 . Other values will act as the actual depth that hard bottom exists.




Note: the present version of SMS 13.2 does not flip the sign of this dataset when exporting files as it does for other depth-related datasets. Until this is corrected in a future release, the Hard Bottom dataset should be assigned values related to positive depths and negative elevations.

Open the Data Calculator (Data | Dataset Toolbox | Data Calculator).

- In the Calculator box, enter default value of -999.0 .
- Enter the name HardBottom into the box for output dataset name.
- Click Compute and choose to map the dataset to Cells.
- Then click OK.

It may be desired to define areas where there is a designated hard bottom, which indicates where no additional sediment may be eroded.

- Click the HardBottom dataset in the data tree to select it.
- Right-click on the HardBottom object and choose to apply dataset specific contours.
 - A good transparency value is 35 and can be set. The legend can be modified to have a white font with bolded features for better appearance, and a data value range deselected to get the full range. Also, the colors can be reversed, if desired.
- Click the Select Cell tool, , and click a polygon around the north and south jetties.
- Change the S value to -2 , which indicates that -2 m is the location of the top of the jetties where no additional erosion should be allowed.
- Select cells representing a few groins and change the S value to -1 .
- These values of -1 and -2 are higher than the actual depth values. CMS may give a warning but will use the cells' actual depth as the limit, so there will be no erosion of the structures themselves.
- In a full project, repeat this process as needed for other areas.


8.7.6 Assign Spatially Varying Datasets to Model Control

Return to the simulation Model Control dialog and associate the new datasets just created with their entries for CMS.

To assign bottom friction, perform the following:

- Right-click on SRI_testRun1 and choose Model Control.
- Click the Flow tab.
- Make sure the Bottom Roughness type is set to ManningsN, then click the button for Dataset, and choose the ManningsN dataset from the list.

In the Sediment tab of the Model Control, there are two sections that pertain to sediment grain sizes. These are Size Classes and Bed Composition. Both are used when dealing with multiple sediment grain sizes, but this basic user's manual will be using only one size class and one bed composition layer.

- Click the Sediment Transport tab.
- Scroll down to the Bed composition section.
- There should already be one layer defined, but the D50 dataset needs to be associated. Scroll to the right to find the D50 option, and then click (none selected) and choose the D50 dataset.
- Next scroll down to the Transport grain sizes section.
- Click the icon to add a row, , then change the default value from 0.2 to 0.26.

To assign the Hard Bottom Dataset, perform the following:

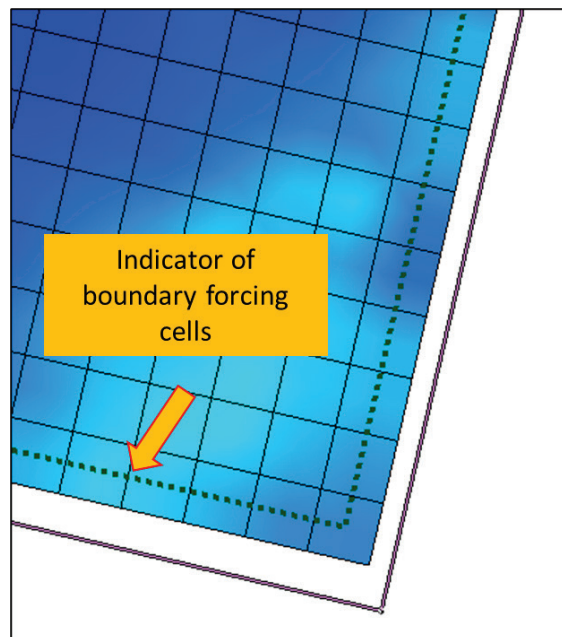
- Scroll to near the bottom of the Sediment Transport tab.
- Check the box for Hardbottom.
- Click the Dataset button and choose the HardBottom dataset.
- Then click OK.
 - There may be an error from SMS, but the values should be stored correctly.
 - If desired, go back into Model Control and verify.

8.7.7 Viewing the Corresponding CMS cells for Boundary Conditions

Since the forcing information is provided through the Map Module (Boundary Condition coverage) and the created telescoping grid is a different entity, it would be beneficial to be able to view the exact cells on which the forcing defined in this section will be applied.

This is possible through a Snap Preview feature in the SMS. Once the Boundary Conditions coverage has been applied to a simulation in the data tree, the feature can be triggered by right-clicking on the CMS-Flow simulation created and choosing Generate Snap Preview. After the tool completes, the user should be able to zoom in to closer proximity to the boundary condition and see a new graphic inside each boundary cell as shown in Figure 8-35.

Figure 8-35. Snapped Preview indicator for boundary cells.



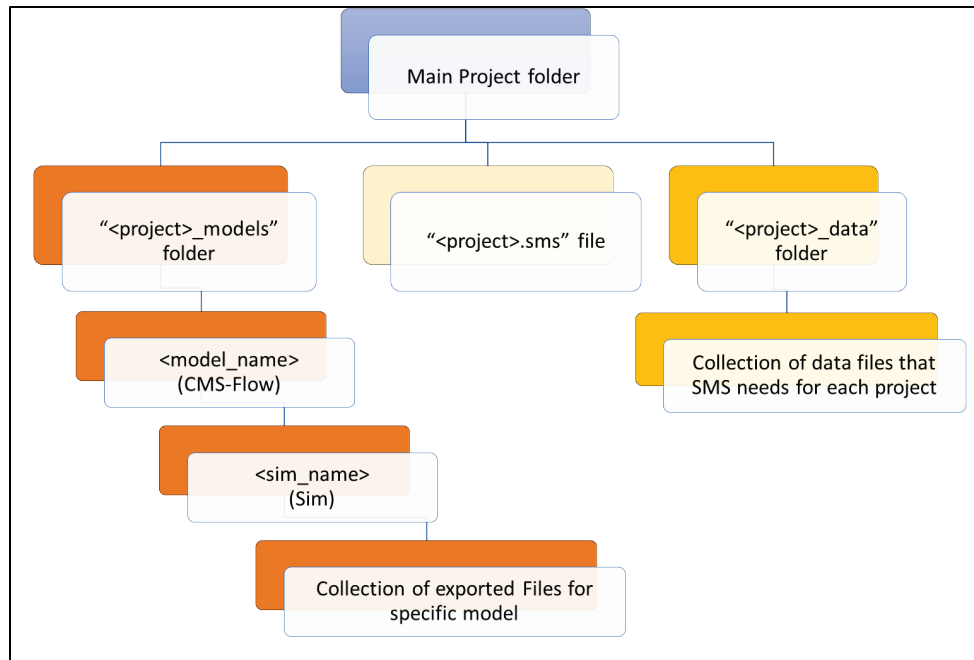
8.7.8 Save Simulation

Before the user can run CMS-Flow, SMS must export the files in the format needed for CMS-Flow. In SMS 13.2, there is an order to the folders saved with each project. This folder structure is shown in Figure 8-36.

- <project> is the saved name of the project.
- <model_name> is the numerical model (i.e., CMS-Flow, ADCIRC, CMS-Wave).
- <sim_name> is the name given for the specific simulation.

Note: there may be more than one model or sim folder depending on the complexity of the project being saved and worked with.

Figure 8-36. Folder structure on disk for each SMS 13.2 project.



8.7.9 Changing Version of Model, If Needed

If needed, users can change the specific version of the model they wish to use.

- Select Edit | Preferences to open the SMS Preferences dialog. Select File Locations and locate CMS-Flow in the Model list under the Model Executables subsection.
 - The corresponding CMS-Flow executable file and path of the file are presented in the Executable list.
 - Users can click the executable file in the list to open Select model executable dialog, where a different executable file can be selected (click Open to make the selection and close the Selection model executable dialog).
 - Once a different executable is selected, it will be used to run the CMS-Flow in the SMS till users change it again.
 - Click OK to close the SMS Preferences dialog.

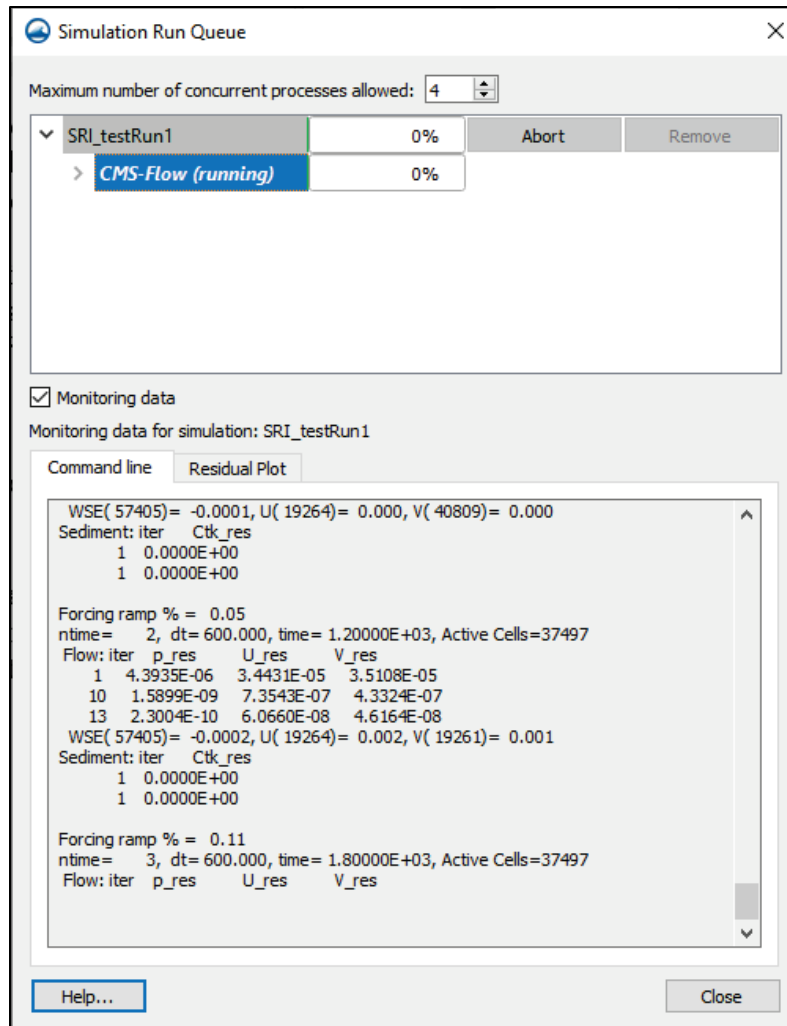
8.7.10 Launch Simulation

Once the simulation has been saved, the user can choose to start a simulation.

- Right-click on the simulation name and choose Run Simulation.

- A new dialog for the Simulation Run Queue will appear that will contain information regarding the CMS-Flow run (Figure 8-37).

Figure 8-37. Simulation Run Queue dialog window for a CMS-Flow simulation.



Users also have the option to combine multiple steps by right-clicking on the simulation name and choosing the option Save Project, Simulation, and Run.

9 CMS-Wave Model Setup

9.1 Overview of Input and Output

The CMS-Wave input and output can be classified as follows (Lin et al. 2008):

- Input
 - Project file (a list of input and output filenames)
 - Control file (model parameters, options, pointers to other files)
 - Geometry (grid and cell features)
 - Boundary conditions (incident waves, wind, and water level forcing)
- Output
 - Transient solution
 - * Global (for the whole domain)
 - * Point (at a single cell)
 - Basic and consequential parameters (wave height, period, wave direction; wave radiation stress gradient, breaking properties, and wave setup elevation)
 - Directional spectrum file

A brief description of the CMS input and output files follows.

9.1.1 Input Files

There are four required input files and nine optional input files to run CMS-Wave. Table 9-1 presents a description of those input files. Users can use the SMS to generate four main input files (*.sim, *.std, *.dep, and *.eng or *.spec) and two optional files (*.txt and *.struct). The optional input files of *.eta and *.cur are normally supplied by CMS-Flow. The wind.dat has the same format as *.cur. The other optional input files including friction.dat, mud.dat, forward.dat, and backward.dat can be created by modifying the *.dep accordingly and saved to the corresponding filename *.dat. The procedure is described in detail in subsequent sections.

Table 9-1 CMS-Wave input files.

Input File	Filename	Description
Project File	*.sim	Specify the grid orientation and origin, and lists input and output filenames
Model Parameters File	*.std	Specify model control parameters and special output cell location(s)
Rectangular Grid File	*.dep	Specify the local grid cell dimensions, and depths for the grid
Incident Wave Spectral File	*.eng or *.spec	Input wave spectral data including timestamp and constant wind and water level forcing
Incident Wave Parameter File ^a	*.txt	Incident wave properties include wave height, period, direction, and timestamp
Structure Cell File ^a	*.struct	Specify structure or land effects on waves at given local cell location(s)
Water Level Field File ^a	*.eta	Spatially varied water level field
Current Field File ^a	*.cur	Spatially varied current component field
Bottom Friction Coefficient Field ^a	friction.dat (default)	Spatially varied friction coefficient field
Forward Reflection Coefficient Field ^a	forward.dat (default)	Spatially varied wave forward reflection field along wet-dry boundary
Backward Reflection Coefficient Field ^a	backward.dat (default)	Spatially varied wave backward reflection field along wet-dry boundary
Muddy Bottom Eddy Coefficient Field ^a	Mud.dat (default)	Spatially varied muddy bed eddy coefficient field
Wind Field File ^a	Wind.dat	Spatially varied surface wind component field

^a Optional input file.

9.1.2 Output Files

Table 9-2 presents a description of the CMS output files. CMS-Wave always writes out a Wave Field File (*.wav), which lists model wave height, period, and direction at all cells in the model domain. There are five optional output files. CMS-Wave writes out optional files named selhts.out (default) and an associated *.obs file if any local output cell location is specified in the model parameter file of *.std. The other three optional output files of *.rad, *.dis, and setup.wav (default) will be saved when they were denoted in the *.std. The output file format is described in detail in subsequent sections.

Table 9-2. CMS-Wave output files.

Output File	Filename	Description
Wave Field File	*.wav	Model wave height, period, and direction at all cells
Local Cell Wave Parameter File ^a	selhts.out	Model wave height, period, and direction at selected cell location(s)
Local Cell Wave Spectral File ^a	*.obs	Model wave spectral data at selected cell location(s)
Wave Radiation Gradient Field File ^a	*.rad	Model wave radiation gradient (component) data at all cells
Wave Breaking Flag or Wave Energy Dissipation Field ^a	*.dis	Model wave breaking flag or wave energy dissipation at all cells
Wave Setup-Setdown Field ^a	setup.dat	Model wave setup-setdown and high-water level mark at all cells

^a Optional output file.

9.2 Grid Generation

9.2.1 Importing the Scatter Set Data File


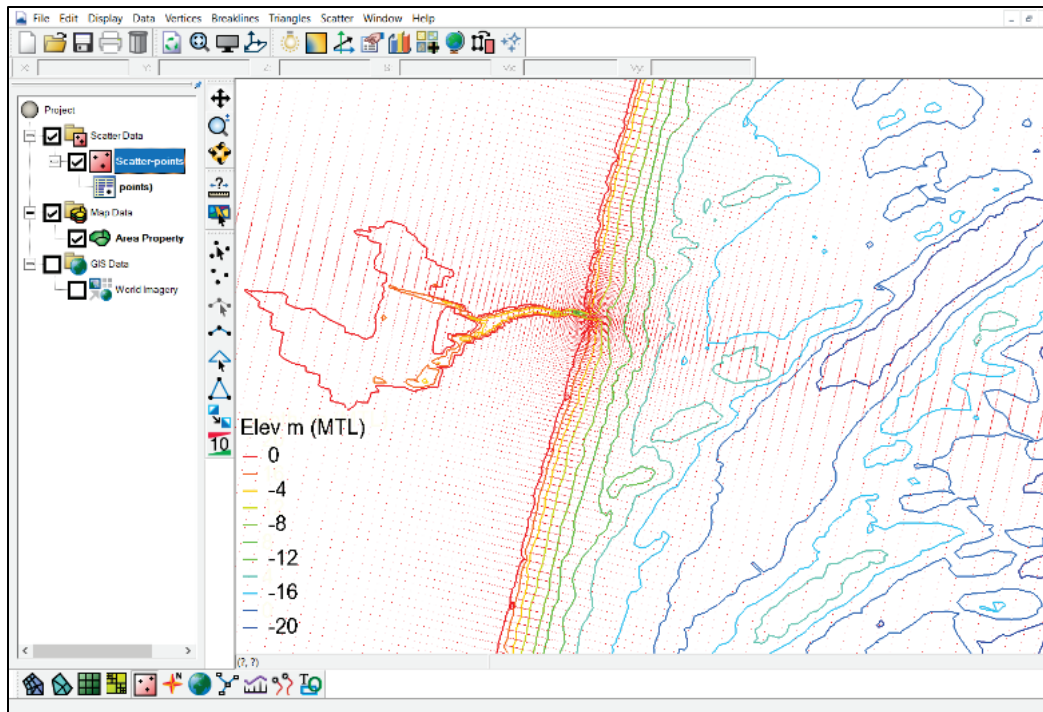
First, upload the scatter data (topography and bathymetry) covering the modeling area of interest to the SMS. Because CMS-Wave, as well as CMS-Flow, requires use of the metric system (in meters) and normally uses the MSL or mean tide level (MTL) for the vertical datum, it is necessary to convert the scatter data accordingly in the SMS if the scatter data are not yet in the metric system or not referenced to the MSL or MTL. In SMS 13.2, scatter data need to be put in the elevation values (positive for land elevation and negative for submerged bed) for the CMS bathymetry grid generation. If multiple datasets are available, users can merge them in the SMS for the grid generation. Figure 9-1 shows an example of the SMS screen with the uploaded scatter dataset in the  Scatter module (Scatter-points in the example under Scatter Data in the Data Tree area).

Figure 9-1. Scatter dataset appearance in the SMS screen.



9.2.2 Setting the Global Projection and Background Maps

It is optional to set the display projection to a Global projection (e.g., State Plane coordinates) or stay in the local system (no projection). To upload any GIS-based image over the scatter set in the SMS, it is necessary to set up the display projection and to ensure that scatter set is projected and aligned to the correct coordinates. Figure 9-2 shows the simple example of using Display to select either Display Projection or Reproject All to set the global projection. Click Library to select State Plane New Jersey (North American Datum of 1983 [NAD83]) with Datum in NAD83 and Units in meters. Click OK to complete and exit the projection selection dialog. Figure 9-3 shows the example of using the Add Online Maps tool to get the online maps and select (click) World Imagery as the background image for the scatter set.

Figure 9-2. Display projection dialogs.

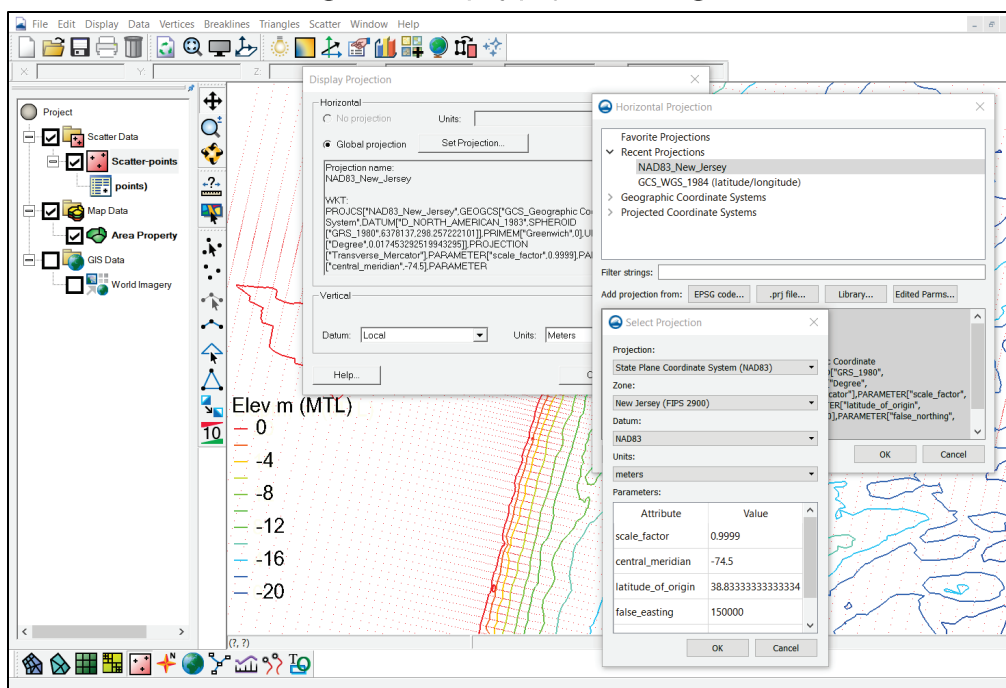
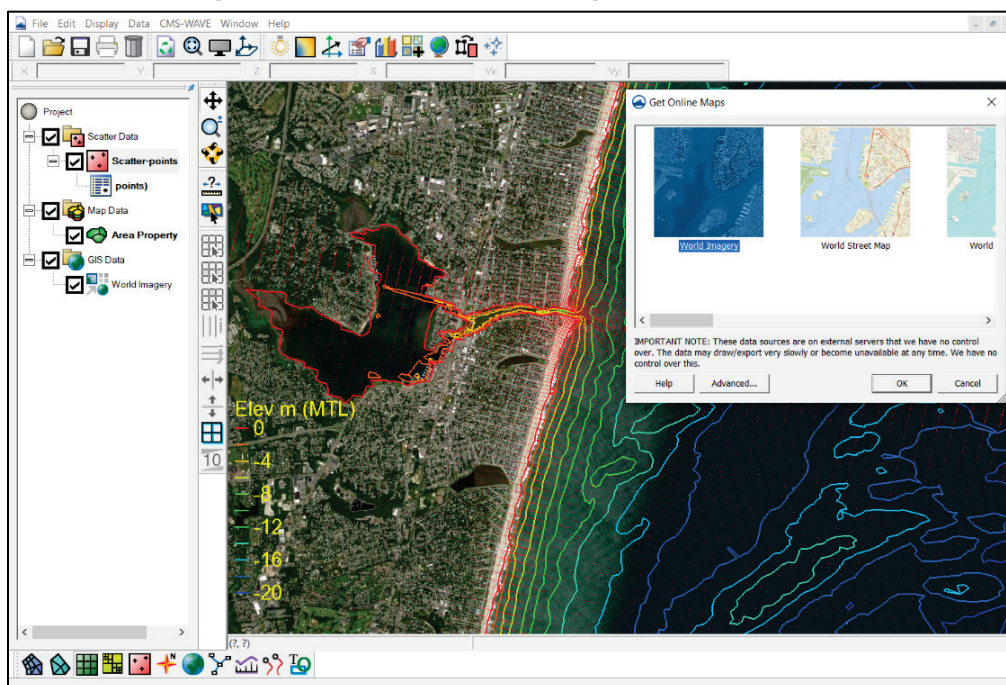



Figure 9-3. Add online dynamic image in the SMS screen.



9.2.3 Creating the Cartesian Grid for CMS-Wave

The Cartesian grid for CMS-Wave can be created by following the steps in the  Map module.






- Switch to the  Map module if not already in the Map module.
- Right-click  Area Properties in the Project Explorer (Data-Tree box), select Type | Models | CMS-Wave.
- Right-click  Area Properties and select Rename.
- Enter CMS-Wave and press Enter to set the CMS-Wave name.
- Using the Create 2D Grid Frame  tool, click out three corners of the grid domain in the order of 1, 2, and 3 shown in Figure 9-4 to create the grid frame. The first point clicked corresponds to the origin of the grid. The first two points clicked define the x-direction (point toward the land), which approximates to the shore-normal direction of incoming waves, and the last two points clicked are placed on the land territory.
- Using the Select 2D Grid Frame  tool, click on the middle point (small black square) of the grid frame to display the Properties tab (Figure 9-5).

Figure 9-4. Creating the Cartesian grid frame.

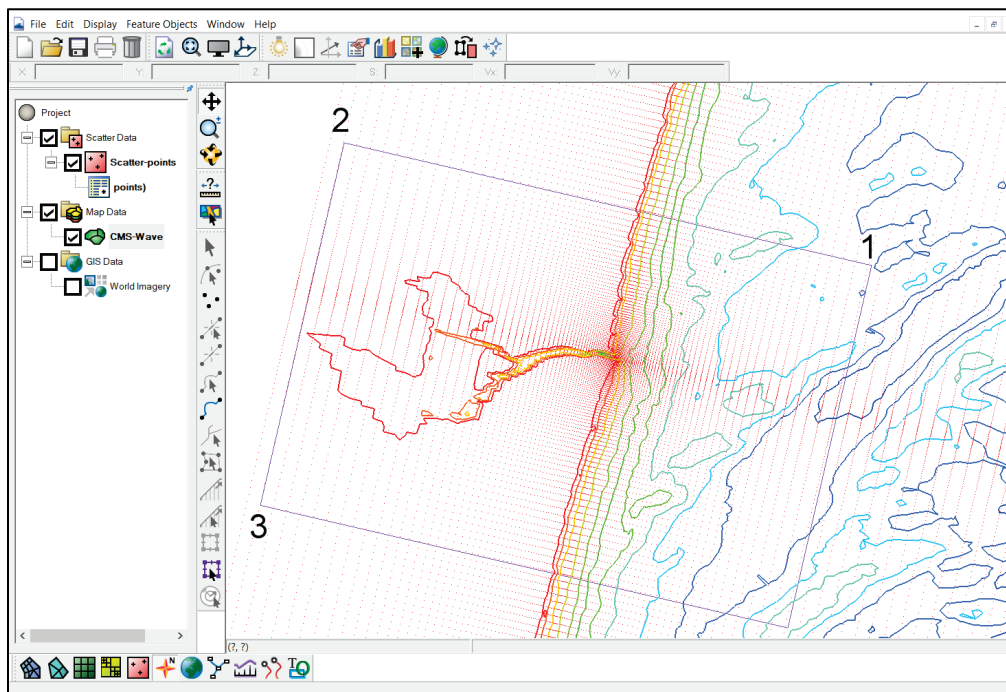
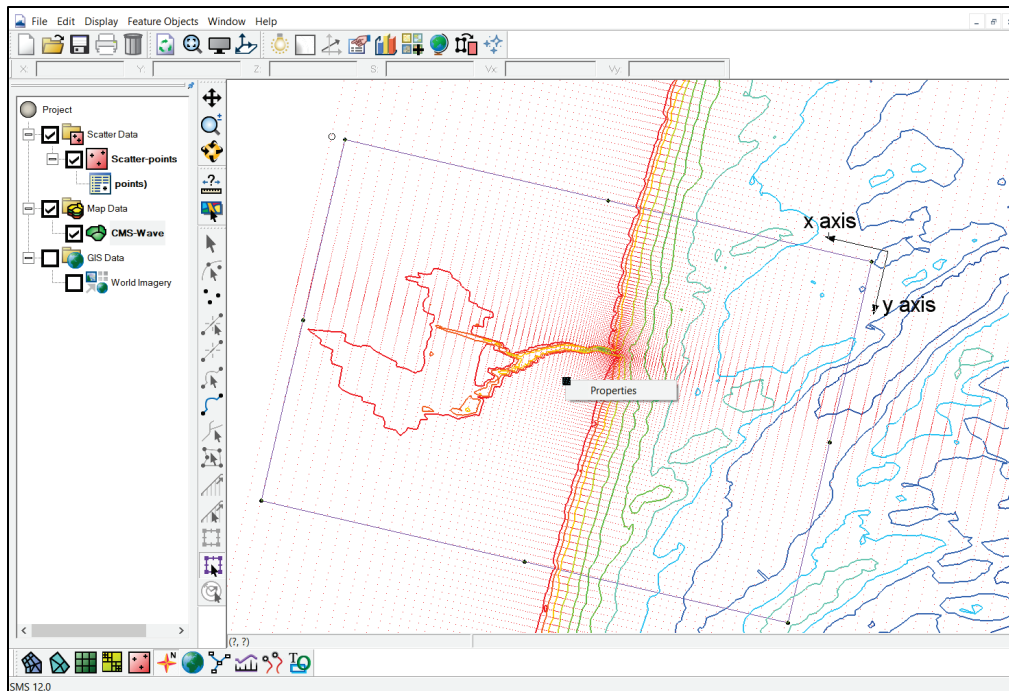


Figure 9-5. The origin is shown at the *upper right corner* of the grid.




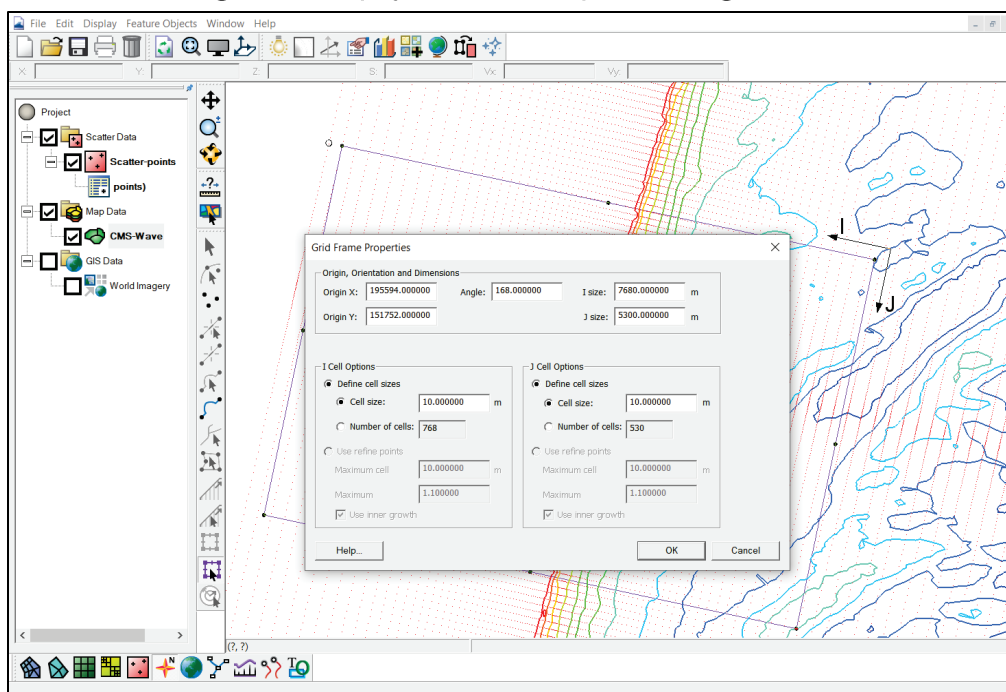
- Resize the grid frame by dragging the edges until the grid frame fits over the desired area. Dragging a corner or side resizes the frame. Dragging the middle point moves the entire frame. Rotate the frame around the origin by dragging the circle handle located at the far end corner of x -axis just outside the grid.
- Right-click the middle point and click Properties tab to bring up the Grid Frame Properties dialog (Figure 9-6). The origin and grid angle can be manually entered in this dialog for greater precision in placement of the grid. In Figure 9-6, the Grid Frame Properties dialog shows a constant cell size of 10 m (default). The grid angle is 168° in the mathematical convention (counterclockwise from the easting direction to the x -axis). There are 768 and 530 cells in the I - (along x -axis) and J (along y -axis)-directions, respectively, with the grid frame. Click OK to close the Grid Frame Properties dialog.
- If variable cell size is preferred (recommended) instead of constant cell size, use Create Feature Point  tool to specify a pair of feature points or multiple pairs of feature points in the grid domain.

Figure 9-6. Display Grid Frame Properties dialog window.




- Use Select Feature Point  tool to select each pair of points and right-click to select the Point Attributes in the drop-down menu (Figure 9-7). This will bring up Refine Point Attributes dialog (Figure 9-8).

Figure 9-7. Display Feature Point properties menu window.

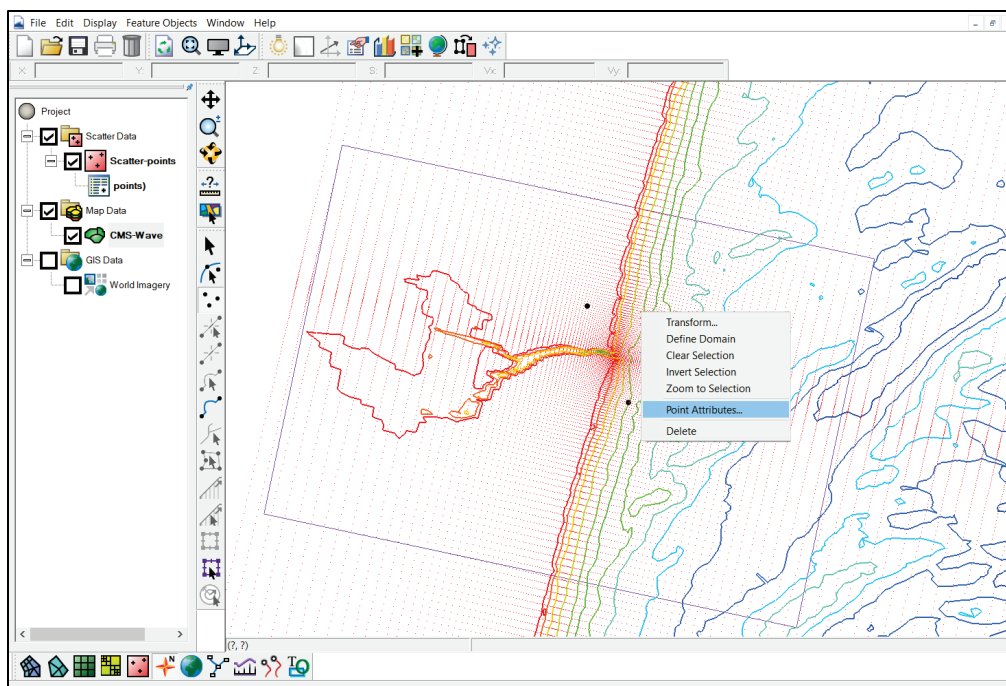
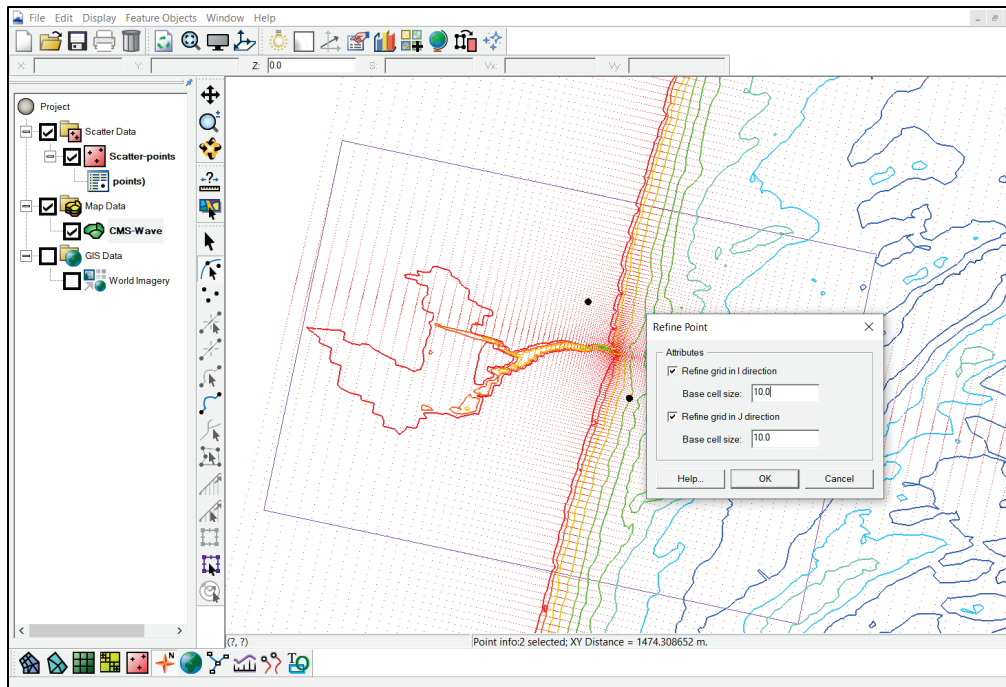


Figure 9-8. Specifying refine base cell size in the Refine Point window.




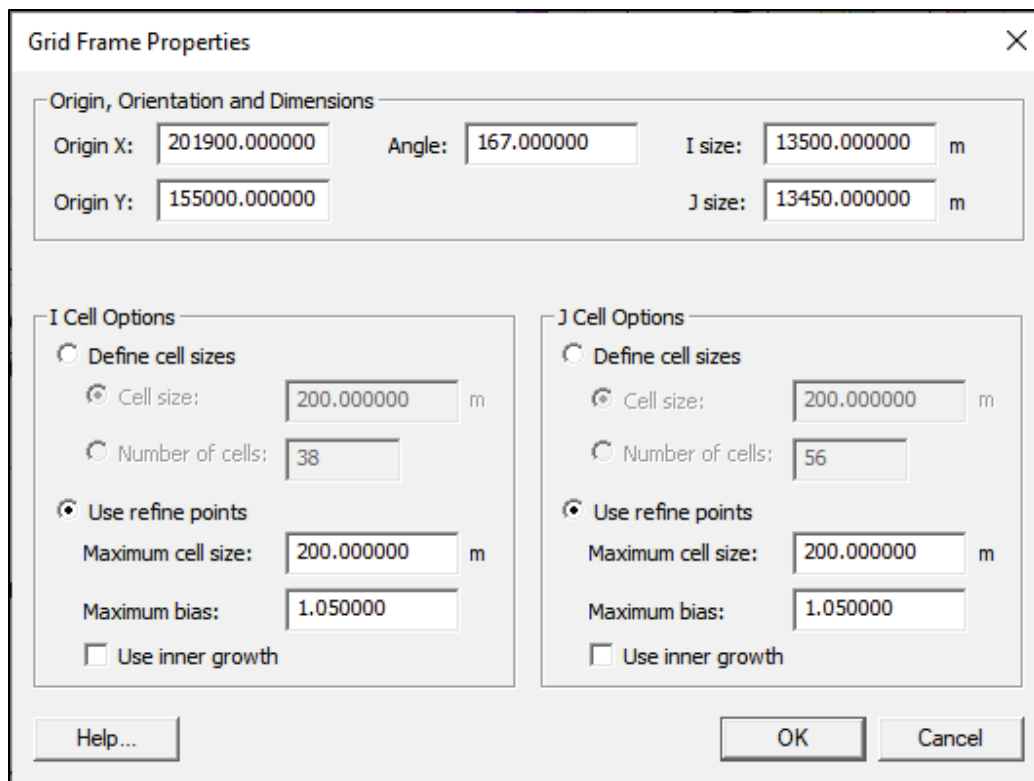
- Select either *I* or *J* or both *I*- and *J*-directions and provide the Base cell size (specifying finer cell size) associated with the selected pair of feature points. Click OK to close the dialog.
- Once the refine feature points with the base cell size(s) were specified (e.g., enter 10 m in each of *I*- and *J*-direction), use Select 2D Grid Frame  tool to return to the Grid Frame Properties dialog. Select Use refine points to provide Maximum cell size and also Maximum (factor) for transition of fine cells (base cell size) to coarse cells (maximum cell size).
- Specify, for example, 200 m for Maximum cell size and 1.05 for Maximum (factor) as shown in Figure 9-9. Users can edit more information in the Grid Frame Properties as desired. In the Use refine points feature, there is also the choice to apply Use inner growth for each pair of refine feature points. This feature is not typically applied for most grid generations.

Figure 9-9. Grid Frame Properties dialog window. Specifying refine point maximum cell size and growth factor.



The image shows the 'Grid Frame Properties' dialog window. It has a title bar with a close button (X). The dialog is divided into several sections. The top section is 'Origin, Orientation and Dimensions' and contains input fields for 'Origin X' (201900.000000), 'Angle' (167.000000), 'I size' (13500.000000 m), 'Origin Y' (155000.000000), and 'J size' (13450.000000 m). Below this are two side-by-side sections for 'I Cell Options' and 'J Cell Options'. Each section has three radio button options: 'Define cell sizes' (unselected), 'Cell size' (selected), and 'Number of cells' (unselected). In the 'Cell size' options, the value is 200.000000 m. In the 'Number of cells' options, the value is 38 for I and 56 for J. Below these are two more radio button options: 'Use refine points' (selected) and 'Use inner growth' (unselected). Under 'Use refine points', there are input fields for 'Maximum cell size' (200.000000 m) and 'Maximum bias' (1.050000). At the bottom of the dialog are three buttons: 'Help...', 'OK', and 'Cancel'.

Section	Field	Value	Unit
Origin, Orientation and Dimensions	Origin X	201900.000000	
	Angle	167.000000	
	I size	13500.000000	m
	Origin Y	155000.000000	
	J size	13450.000000	m
I Cell Options	Define cell sizes	<input type="radio"/>	
	Cell size	200.000000	m
	Number of cells	38	
	Use refine points	<input checked="" type="radio"/>	
	Maximum cell size	200.000000	m
	Maximum bias	1.050000	
J Cell Options	Define cell sizes	<input type="radio"/>	
	Cell size	200.000000	m
	Number of cells	56	
	Use refine points	<input checked="" type="radio"/>	
	Maximum cell size	200.000000	m
	Maximum bias	1.050000	

- Click OK to close the Grid Frame Properties dialog.
- Select Feature Objects | Map → 2D Grid to bring up the Map → 2D Grid dialog (Figure 9-10).
- Verify values in the Origin, Orientation and Dimensions section. In the Depth Options section, select Scatter Set (the default is Constant with Depth: 0.00) from the Source drop-down.
- Click Select to bring up the Interpolation dialog (Figure 9-11).
- In the Scatter Set To Interpolate From section, select (click to highlight) one scatter set from the list of available scatter set data.

Figure 9-10. Display Map → 2D Grid dialog window.

Figure 9-11. Display Interpolation dialog window.

- In the Interpolation Options section, select Linear (the default) from the interpolation drop-down and Inverse Distance Weighted from the Extrapolation drop-down.
- Click OK to exit Interpolation dialog.


- Click OK to exit the Map → 2D Grid dialog and create the CMS-Wave grid (Figure 9-12) with variable cell size in the  Cartesian Grid Module. The higher resolution appears in the area associated with the selected pair of feature points. Figure 9-13 shows the CMS-Wave grid domain with bathymetry contours and GIS data (World Imagery).

Figure 9-12. CMS-Wave grid with variable cell size.

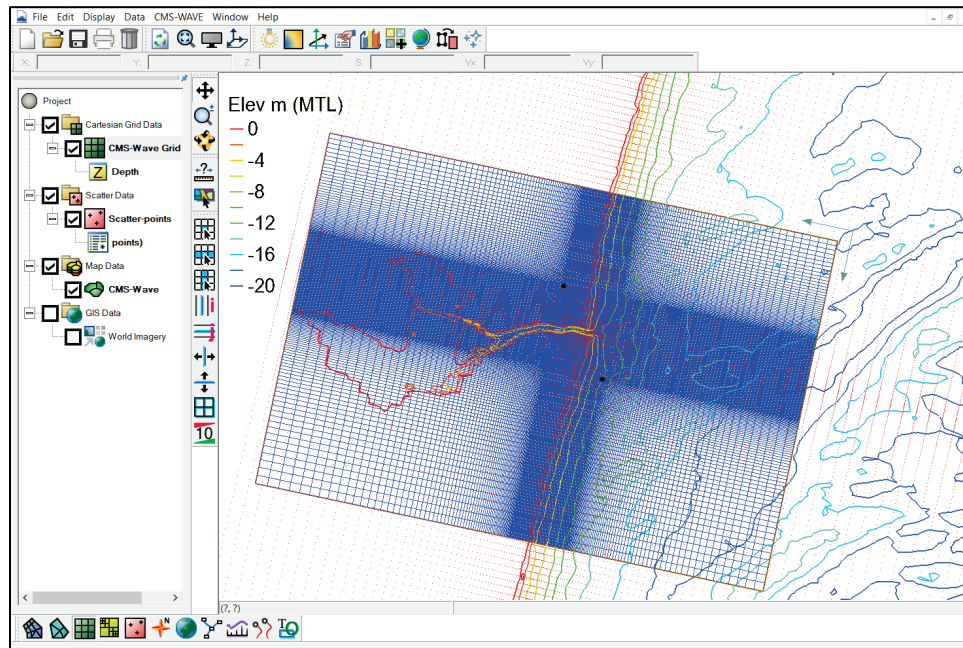
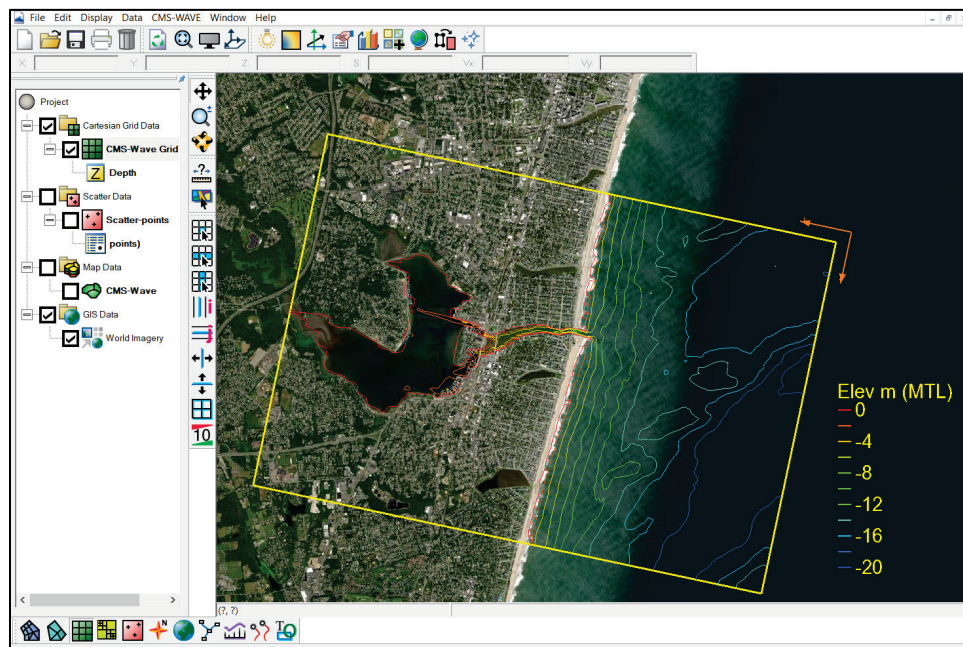


Figure 9-13. CMS-Wave grid with bathymetry contours.




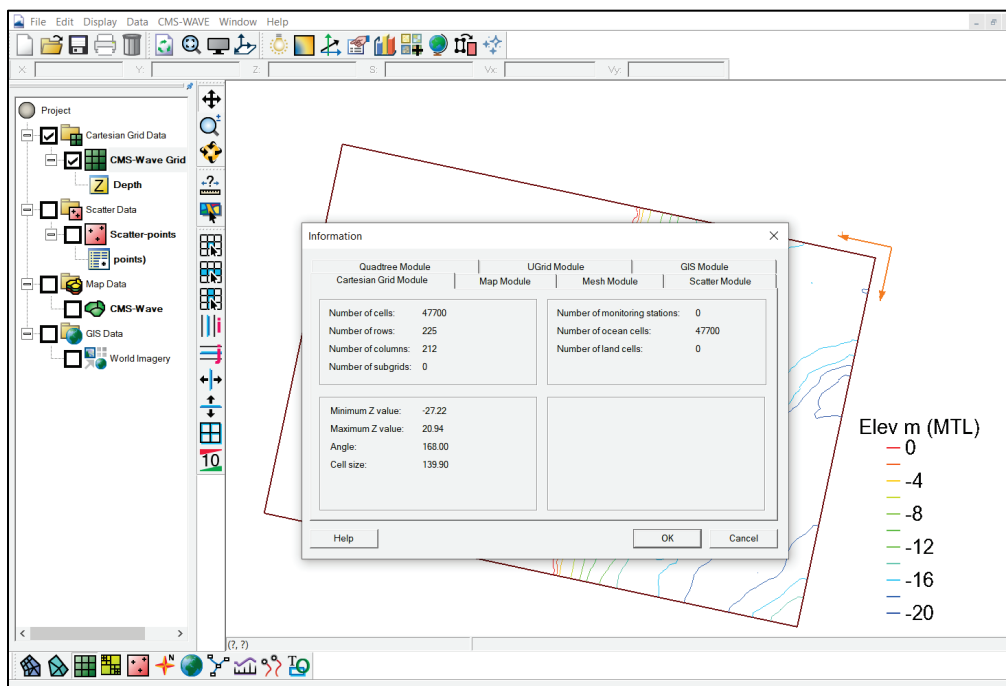
- Select File | Get Info to open the Information dialog which provides the number of rows and columns in the CMS-Wave Grid (Figure 9-14). In the example of CMS-Wave Grid with variable cell size, there are 212 Columns and 225 Rows.
- In the  Cartesian Grid module, select File | Save Project to save the project including the new grid that was created.
- The actual CMS-Wave files will be exported in a step later in this section.

Figure 9-14. Display Information dialog window.



9.3 Generating Wave Spectral Input for CMS-Wave

The basic application of CMS-Wave is typically for a linear coastline where wave input (incoming or incident waves) may be required only along the seaward boundary. Because CMS-Wave is a steady-state model, the simplified wave input in this case would be a constant wave condition specified along the seaward boundary. The essential wave input to CMS-Wave is binned, directional wave spectral data. It can be the hypothetical or design wave condition(s), hindcast wave conditions, or directional wave data collected in the field.

In the SMS, the CMS-Wave spectral input (*.spec) file can be generated by the following steps.

- Load the project containing the CMS-Wave grid, if needed.


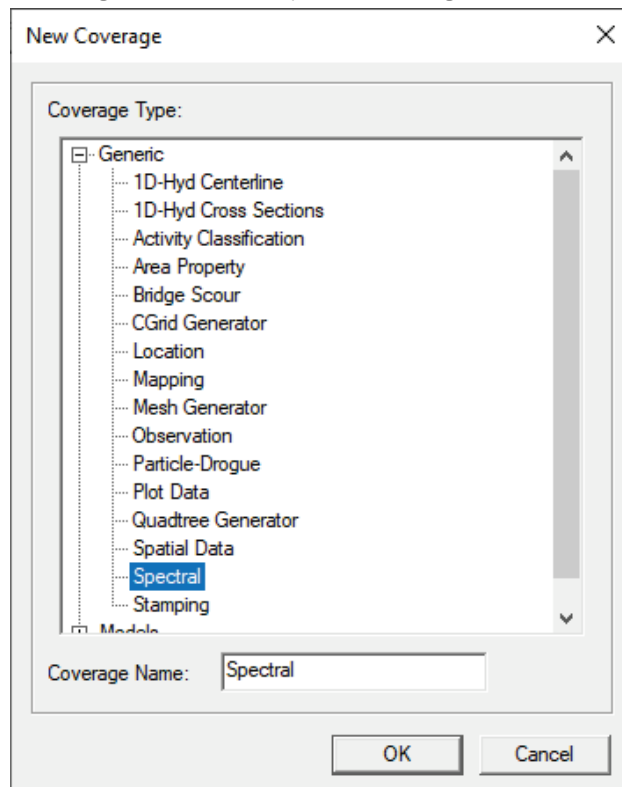
- Right-click  Map Data in the Project Explorer (Data-Tree entry window) and select New Coverage to bring up the New Coverage dialog.
- In the Coverage Type section, select Generic | Spectral (Figure 9-15).

Figure 9-15. Display New Coverage window.






- Click OK to close the New Coverage dialog. A new list for Spectral is now available under  Map Data.
- Use the Create Feature Point  tool to create (click) a node on or near the middle of the grid seaward boundary.
- Use (click) Select Feature Point  tool, double-click on the node to bring up the Spectral Energy dialog (Figure 9-16).
- In the Spectral Manager section, click Create Grid to bring up the Spectral Grid Attributes dialog.
 - The Grid angle (in degrees) is the same as the grid orientation angle specified earlier (in this case it is 168°).
 - The Spectral energy grid plane type can be either Global or Local (default) from the Spectral energy grid plane type drop-down.
- Click OK to close the Spectral Grid Attributes dialog, and it will open the Create Spectral Energy Grid dialog (Figure 9-17).

Figure 9-16. Display Spectral Energy dialog window.

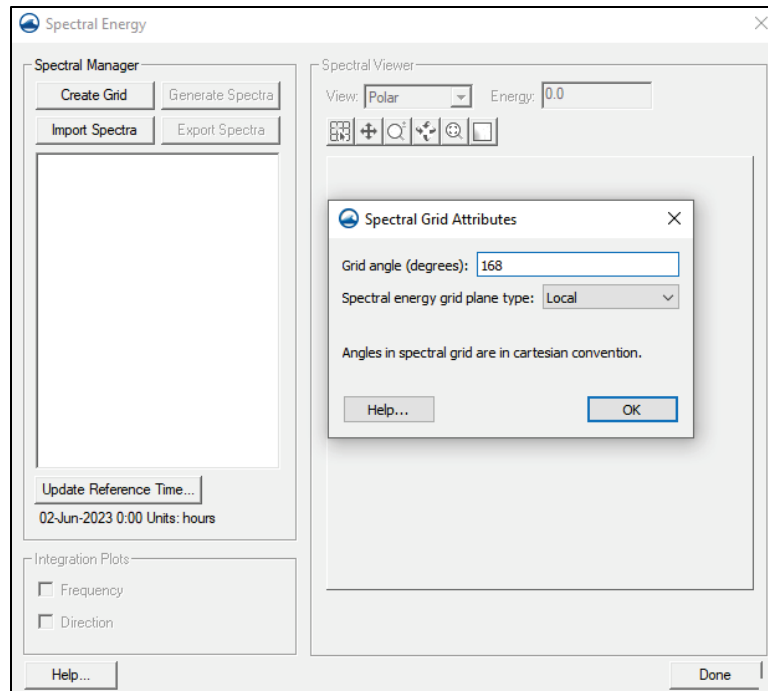
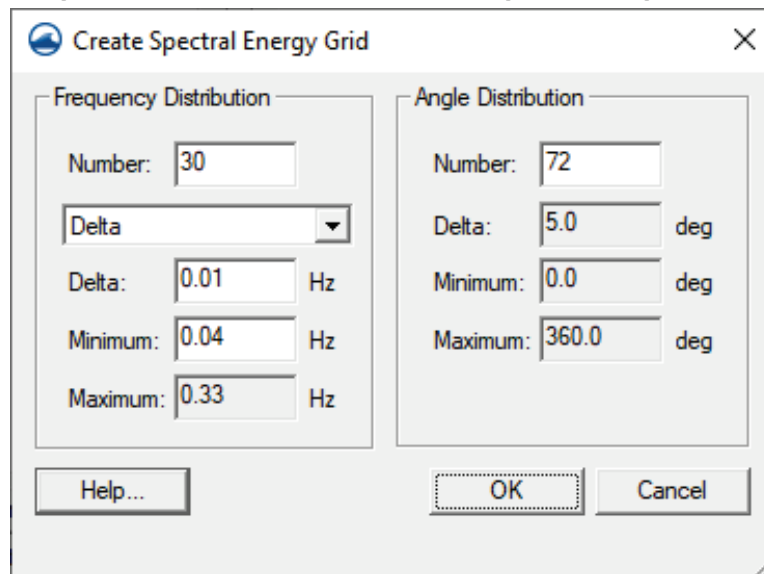


Figure 9-17. Display Create Spectral Energy Grid dialog window.



- In the Frequency Distribution section, enter 30 (default) as the Number. In the Angle Distribution, enter 72 (default) as the Number (cover 360° range).
- Leave the combo box beneath Number set to Delta and use the default values for Delta and Minimum.
 - In this case, the Minimum (smallest frequency bin) is 0.04 Hz and the Maximum (largest) is 0.33 Hz. The corresponding 30 wave

period bins used in CMS-Wave will range from 3 sec (0.33 Hz) to 20 sec (0.04 Hz).

- For coastal applications in the Gulf of Mexico, users may enter 40, 0.01, and 0.06 as the Number, Delta, and Minimum respectively, which correspond to 40 frequency binds covering wave periods ranging from 2.2 sec to 17 sec wave energy.

The sea basin of the Gulf of Mexico is much smaller than the Atlantic and Pacific Oceans. Accordingly, spectral waves in the Gulf of Mexico are skewed more toward higher frequencies than waves in the Atlantic or Pacific Oceans.

- Click OK to close the Create Spectral Energy Grid dialog, and it will open the specified spectral energy grid (cover 360° range).
- Click Generate Spectra to bring up the Generate Spectra dialog.
- In the Spectral Parameters section, select Texel Marsen Arsloe (TMA) (shallow water) spectrum in the Generation Method drop-down_menu. The user can enter parameters (Example values shown in Table 9-3). The H_s and T_p are the significant wave height (in meters) and the spectral peak period (in seconds), respectively. The Gamma is the peak enhancement factor in the TMA or JONSWAP (deep water range) spectrum, and the nn is the power (an even number) of a cosine-type function for distribution of wave energy with respect to the mean wave direction (Lin et al. 2008).
- In the Spectral Settings section, select Specify once for all spectra under the Seaward Boundary Depth and enter the average depth along the offshore row of cells in the box field (it is the average depth along the wave grid seaward boundary). For example, enter 20.1 m for the Seaward Boundary Depth (Figure 9-18).

Table 9-3. Example of incident wave parameters.

Time (hr)/index	Angle (deg)	H_s (m)	T_p (sec)	Gamma	nn
0.0	-20.0	2.0	8.0	3.3	50
3.0	0.0	2.0	8.0	3.3	50
6.0	20.0	2.0	8.0	3.3	50

Figure 9-18. Display Generate Spectra dialog window.

Generate Spectra

Parameter Settings

Generation Method: TMA (Shallow Water)

☒ Replace Old Spectra

Directional Spreading Distribution:

☐ Wrapped Normal

☒ Cosine Power

Seaward Boundary Depth:

☒ Specify once for all spectra

20.1 m

☐ Specify for each spectrum

Angle Settings

Projection: Shore Normal

Spectral Parameters

	Time Offset (hrs)/Index	Angle (deg)	Hs (m)	Tp (s)	Gamma	nn
1	0.0	-20.0	2.0	8.0	3.3	50
2	3.0	0.0	2.0	8.0	3.3	50
3	6.0	20.0	2.0	8.0	3.3	50
4						

Import Import from GenCode Export Spectral Defaults >>

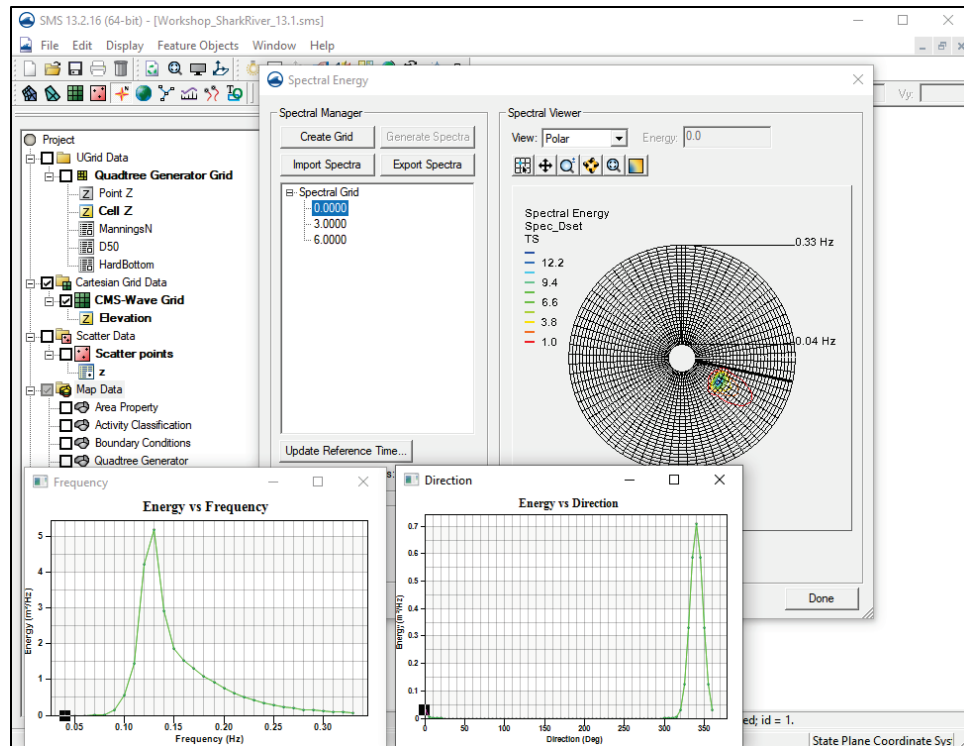
Help... Generate Cancel



Note that the reference of Angle (deg) is given in the Angle Settings section. In this example, select Shore Normal from the Projection drop-down. For Shore Normal (referenced to the local grid), zero (0)° corresponds to positive (+) x -direction (approximately shore-normal direction), -20° angle is oblique to the right, and 20° angle is oblique to the left of the + x -direction.

- Click Generate to generate the spectral wave data, and at the same time it will close the Generate Spectra dialog.

A list of time offsets (or indexes) should appear below the Spectral Grid in the spectral energy tree box. Click any of the time offsets to display corresponding spectral energy contours (directional wave energy distribution) in Spectral Energy section. Note spectral direction in the display is shown as the from direction (Figure 9-19). The bold radial line shown in the spectral energy grid corresponds to 0° on the local plane in the global (meteorological) coordinate system.

Figure 9-19. Display spectral contours in Spectral Energy dialog window.



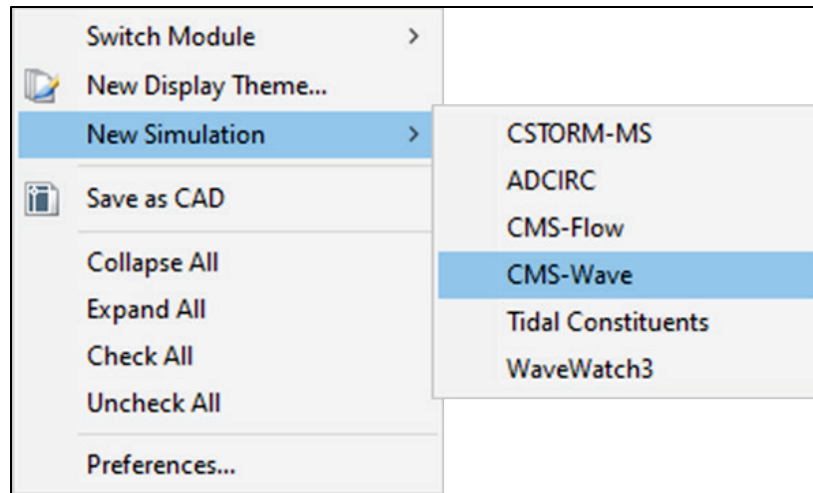
- Users can check Frequency or Direction under Integration Plots section to view corresponding Energy versus Frequency or Energy versus Direction plots, which are also shown in the *lower left* of Figure 9-19. Uncheck the selection to close the plots.
- Click Done to exit the Spectral Energy dialog.
- Switch to the  Cartesian Grid module from the  Map module.
- Save the Project again to ensure the data will be retained.

9.4 Create a New CMS-Wave Simulation

Similar to how the CMS-Flow model needed a simulation in the data tree, CMS-Wave follows the same method.

- Right-click in the open space in the data tree and choose New Simulation | CMS-Wave (Figure 9-20).
- A new set of entries will appear in the data tree. Sim is the default name and can be changed to something descriptive about the simulation.

Figure 9-20. Choices to create a new CMS-Wave simulation.



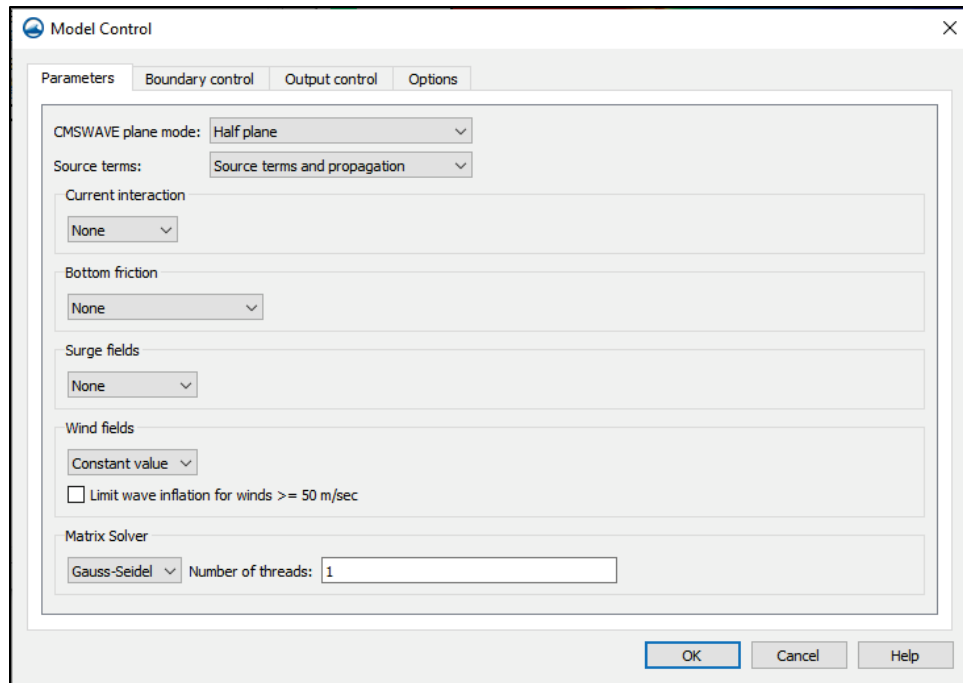
Next, the CMS-Wave grid created earlier must be added to the simulation.

- Right-click on the CMS-Wave grid and choose Apply To, then click choice for the appropriate simulation.
 - The user could also click and drag the grid icon down to the Simulation section.
- A shortcut for the CMS-Wave grid will appear beneath the simulation name.

9.5 Model Control and CMS-Wave Parameters

- To enter CMS-Wave Model Control, right-click on the simulation name (not the CMS-Wave grid) and choose Model Control (Figure 9-21).
- On the Parameters page, the following typical entries can be made:
 - Select Half plane from the CMSWAVE Plane mode drop-down menu for Source terms.
 - Select Source terms and propagation (Note: the Source terms denote the wind input was applied for the wind effect on wave propagation and generation).
 - For Bottom friction, select the Darcy-Weisbach constant with a default value of 0.005.
 - For Wind fields, select Constant value.
 - For the Matrix solver, use the default Gauss-Seidel algorithm.
 - Specify 2 in the Number of threads box (Note: the simple rule in number of threads is equal to total number of grid cells along the x-axis divided by 300).

Figure 9-21. Display CMS-Wave Model Control dialog window.




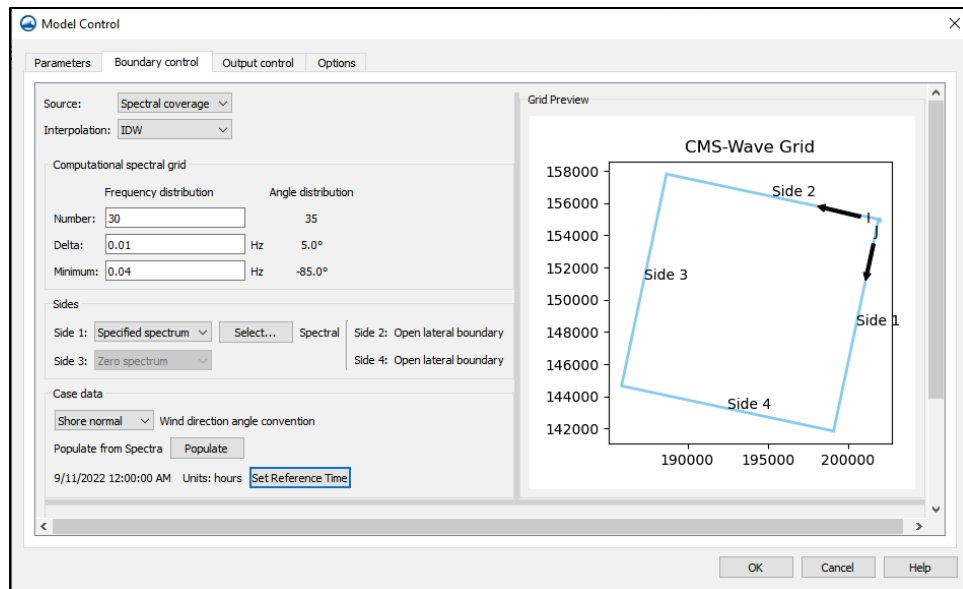
- On the Boundary Control page (Figure 9-22), perform the following:
 - Select Spectral Coverage from the Source combo box.
 - In the Sides section, for Side 1 select Specified spectrum and click Select to open the Select Spectral Coverage dialog. Check  Spectral box from the list (it was created under the Map Data in the Data-Tree window and click OK to close the dialog.
 - In the Case data section,
 - * Select Shore normal for wind direction angle convention.
 - * Click the Populate button to bring in the times from the interval specified when generating spectra earlier in this section.
 - * Click Set Reference Time to open the CMS-Wave Simulation Reference dialog, then click OK and the user will be able to choose to apply the specified reference time from a Yes/No selection box. If No is selected, the spectrum label will be used instead of the reference time.

Figure 9-22. Display Boundary Control page from Model Control dialog window.



- On the Options page (Figure 9-23),
 - Check Allow wetting and drying.
 - Check Diffraction intensity and specify a value of 4.0.
 - Select Constant from the Forward reflection combo box and specify a value of 0.5 for the reflection coefficient.
 - Select Extended Goda from the Wave breaking formula box.
 - Select 12-digits from the Date format combo box to use a timestamp in the YYYYMMDDHHII format. The older 8-digit format of YYMMDDHH is still available, but it is discouraged.

Figure 9-23. Model Control dialog window. Display CMS-Wave simulation Options page.

Model Control

Parameters | Boundary control | Output control | **Options**

- ☒ Allow wetting and drying
- ☐ Infragravity wave effect
- ☒ Diffraction intensity
- ☐ Nonlinear wave effect
- ☐ Run up
- ☐ Fast-mode run
- Roller effects
- Forward reflection
- Backward reflection
- Muddy bed
- Wave breaking formula
- Date format

OK Cancel Help

9.6 Selecting Special Output Stations

CMS-Wave will output a *.wav file containing significant wave heights, peak period, and mean wave direction for all cells in the grid. Special output locations (monitoring stations) can be specified to save directional spectral output data (in *.obs file) and additional wave parameters (swell, local sea, associated current, flow rate, etc.) in the selhts.out (or *.out) file. To specify special output locations in the SMS,

- create a new coverage in the Map module, of type Models | CMS-Wave | Observation Cells,
- use the Create Feature Point tool to create points at the desired locations, and
- once finished, right-click on the Observation Cells coverage and choose to Apply to the correct simulation from the list. These points will be

used as special output locations when the CMS-Wave files are exported.



The model output file selhts.out (or *.out) for the special output stations writes out 17 columns as listed in Table 9-4.

Table 9-4. List of column contents for selhts.out file.

Column	Description of Column Value
1	spectrum label (or timestamp)
2	<i>i</i> index in Cartesian (i,j)
3	<i>j</i> index in Cartesian (i,j)
4	significant wave height (m)
5	spectral peak wave period (sec)
6	mean wave direction (deg, local coordinate system)
7	swell height (m)
8	swell wave period (sec)
9	swell direction (deg)
10	local generated wave height (m)
11	local generated wave period (sec)
12	local generated wave direction (deg)
13	wave breaking index (nonzero for breaking)
14	water level mark (m) if calculated
15	flow rate (m*m/sec) if calculated
16	east west flow velocity component if calculated
17	north south flow velocity component if calculated

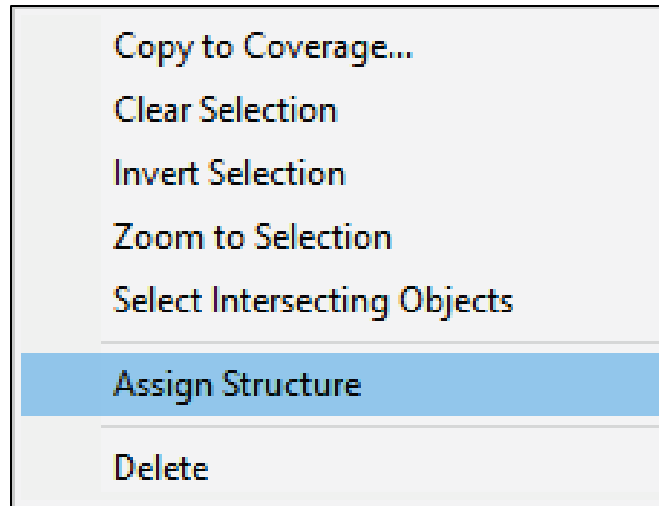
9.7 Specifying Optional Structure Features

Other selected cells can be assigned as structure cells or grid nesting output cells. Use the following steps to specify these types of features for CMS-Wave in the SMS:

- Create a new coverage in the Map module, of type “Models | CMS-Wave | Structure.
- Switch to the  Cartesian Grid module, select the Select Grid Cell  tool.
- Click a grid cell of interest (or group of cells) in the SMS screen to select it. Users can hold Shift key while selecting (clicking) multiple cells.
- Once each cell or collection of cells that designate a particular type of structure or grid nesting output cells have been selected, Right-click

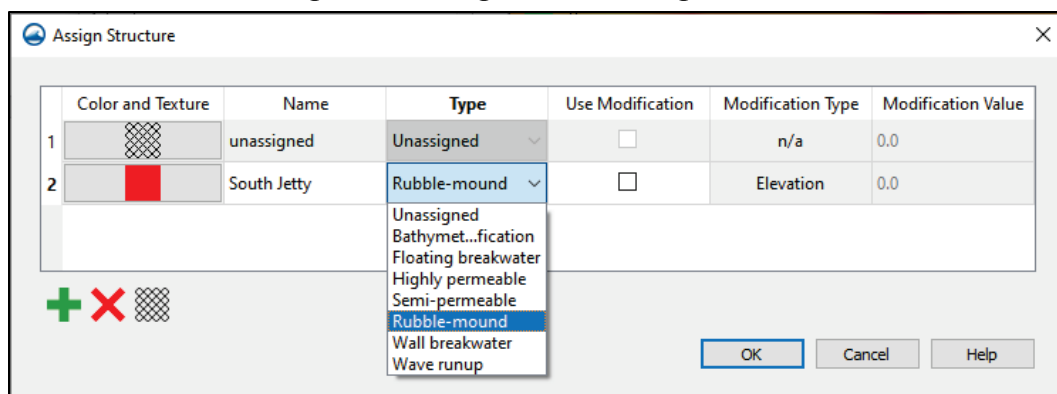
- and select (click) the Cells to Active Coverage option to define polygons for the selected cell(s) in the Structures coverage.
- Switch to the Structures coverage by clicking it in the data tree.
 - Using the Select Polygon tool, select the polygon or multiple polygons, then right-click and choose Assign Structure (Figure 9-24).

Figure 9-24. Assign Structure selection window from the right-click menu.



- From the resulting dialog (Figure 9-25), the user can choose from a variety of colors and textures, assign a structure name, choose a type from list, and choose to apply a modification type and give that modification value.

Figure 9-25. Assign Structure dialog window.



When finished creating structures, the coverage must be connected to the Simulation by right-clicking on the Structures coverage in the data tree and choose Apply to then choosing the simulation from the list.

The structure cell types include

- bathymetry modification,
- floating breakwater,
- highly permeable (for piers or docks)
- semipermeable (for rubble-mound breakwaters),
- rubble-mound (nonpermeable),
- wall breakwater (for caissons), and
- wave runup.

When finished creating structures, the coverage must be connected to the Simulation by right-clicking on the Structures coverage in the data tree and choosing Apply to, then choosing the simulation from the list.

Once the CMS-Wave files are exported, the structure cell information will be stored in the *.struct file.

More details of CMS-Wave structure cells can be found in the CMS-Wave technical report (Lin 2008).

9.8 Running CMS-Wave

CMS-Wave can be run in the SMS or in the Windows Command Prompt (DOS Command Window). To run CMS-Wave in the SMS, users can check and locate the CMS-Wave executable file selected in the SMS as shown in the previous chapter for CMS-Flow.

9.8.1 Export CMS-Wave files

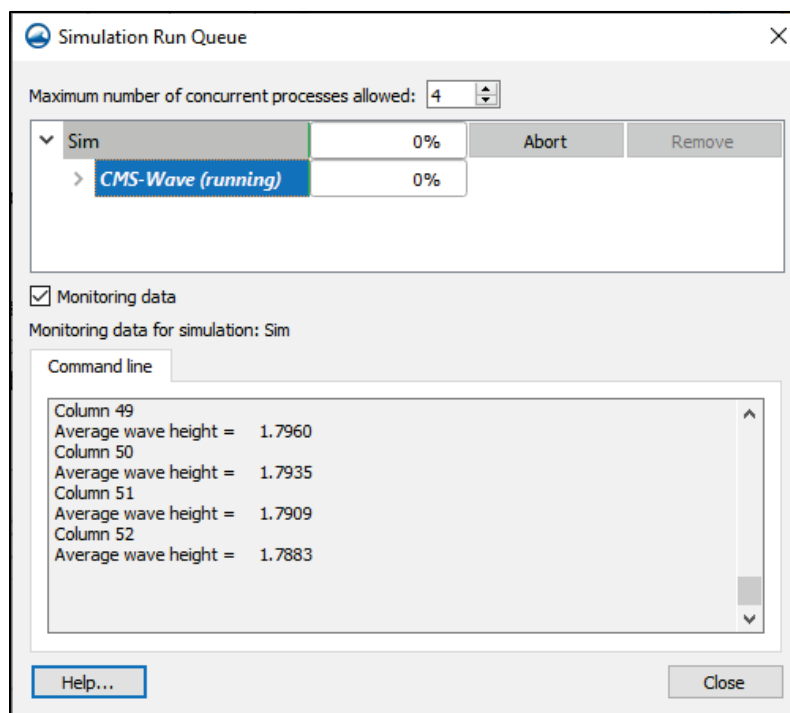
- If changes have recently been made to the project, save the project as previously instructed.
- Right-click the simulation name for the CMS-Wave simulation and choose Save Simulation.
- Exported files will appear beneath the project structure in the <project>_models/<model_name>/<sim_name> folder.
 - For example, for a project named Shark-River-Inlet-NJ-CMS-Wave, a CMS-Wave simulation named Sim would be written to the folder Shark-River-Inlet-NJ-CMS-Wave/CMS-Wave/Sim.

9.8.2 Running from SMS

Once the simulation has been saved, the user can choose to start a simulation.

- Right-click on the simulation name and choose Run Simulation.
- A new dialog for the Simulation Run Queue will appear that will contain information regarding the CMS-Wave run (Figure 9-26).

Figure 9-26. Simulation Run Queue dialog window for a CMS-Wave simulation.



Users also have the option to combine multiple steps by right-clicking on the simulation name and choosing the option Save Project, Simulation, and Run.

9.9 Specifications of Advanced CMS-Wave Features

The most recent CMS code developed is Version 5.3. Several new capabilities and advanced features for CMS-Wave have been added to this version:

- Fast mode versus standard mode
- Full-plane
- Automatic wave run-up calculation

- Infragravity wave
- Nonlinear wave-wave interaction
- Muddy bottom
- Permeable structures
- Spatially varied wind input
- Spatially varied spectral input
- Grid nesting
- Wave surging (roller) in surf zone

Details and theory of CMS-Wave capability and advanced features can be found in Section 3.

9.9.1 Fast Mode Versus Standard Mode

CMS-Wave can run in a fast mode to reduce the runtime (Lin et al. 2008). In the fast mode, CMS-Wave will reduce both frequency and direction bins internally for spectral wave transformation. The runtime will be reduced approximately by a factor of 10 to 15 depending on if wind forcing is included or not in the model run. The fast model is recommended for large-domain application and in more open-water conditions like open coast or in a large bay system. The standard mode is recommended for small model domain, especially in the lee of inlet or coastal structures.

9.9.2 Full-Plane

In this mode, CMS-Wave performs two half-plane runs in the same grid. The first run is in the half-plane with the principal wave direction toward the shore. The second run is in the seaward half-plane as opposed to the first run. Upon the completion of the second run, two half-plane results are combined to one full-plane solution (Lin et al. 2012). Because the run time for the full-plane is approximately twice that of the regular half-plane, users shall consider the full-plane mode only if the full-plane features like wave generation and propagation in a bay or around an island.

9.9.3 Wave Run-Up, Infragravity Wave, Nonlinear Wave-Wave Interaction, Muddy Bed, Spatial Wind Input

To include (trigger) either of wave run-up, infragravity wave, nonlinear wave-wave interaction, binary (xmdf or *.h5) output, multiple processors, muddy bed, and spatial wind field input is just a one-click step in the SMS interface. Additional files are required for the muddy bed and spatial wind field input.

If the muddy bed calculation is required, users shall prepare a mud.dat file or *.mud (in the same format as *.dep) to list the spatial varying maximum kinematic viscosity for the entire grid (recommended maximum kinematic viscosity for mud is 0.04 m²/sec).

If the spatial wind field input is required, users shall prepare a wind.dat file or *.wind (in the same format as *.cur) to provide the *x*- and *y*-component wind data corresponding to the incident wave conditions in the model grid.

9.9.4 Permeable Structures

Users can select and specify permeable structure cells in SMS with the steps identified in Section 9.7.

9.9.5 Grid Nesting

Grid-nesting users can utilize the CMS-Wave Assign Cell Attributes and Nesting Output to specify the wave information output cells for saving spectrum data file (to serve as wave input to a child grid run). The nesting output file is *.nst (Lin et al. 2010, 2012).

9.9.6 Spatially Varied Spectral Wave Input

Spatially varied spectral input is simply the case as in a child grid that spatially varied wave spectra are permitted to assign at user specified locations along or near the seaward boundary of the child grid. To apply spatially varied spectra for wave input without a parent grid, users will need to prepare the wave input file with the format as described in the child grid run.

9.9.7 Wave Roller in Surf Zone

The wave roller parametric formulation is commonly applied in the wave spectral model to modify breaking wave energy dissipation nearshore to mimic better the surf zone dynamics. The wave roller effect used in CMS-Wave is based on the roller model developed by Zhang et al. (2014).

10 CMS Dynamic Coupling (Steering)

Once users have working CMS-Flow and CMS-Wave grids, sometimes the users want to run each model together to produce a simulation with wave-modified currents and current-modified waves. This is possible in CMS by running in in-line steering mode. Within the SMS, there are a few things to make sure of before starting the steering simulation.

- Care should be taken to make sure that the CMS-Wave setup begins on the same day and time as the CMS-Flow setup.
 - This means that the Simulation Reference time is set accordingly so all spectra written out will have the correct date and time.
- Both grids must be loaded into the same instance of SMS and each projection should be identical (Main Display, Flow grid, and Wave grid).
 - The user can take an existing project where one type of grid (flow or wave) has already been defined and a simulation set up, then load the other type of grid into the interface.

Next, a few additional steps must be completed by the user to enable this feature.

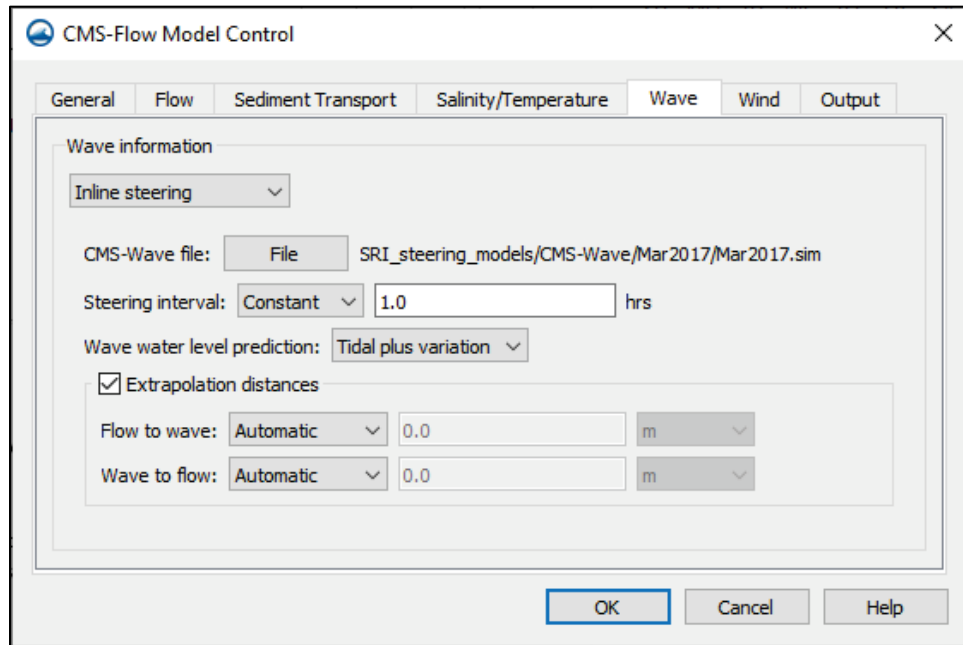
- Save the project with a new name for this simulation that will contain both Flow and Wave grid setups.
- Make sure there is a Flow simulation and Wave simulation defined beneath Simulation Data in the data tree.
- Save the Wave model simulation files.
 - Right-click on the CMS-Wave Simulation and choose Save Simulation.

10.1 Modify Flow Model Control for steering

- Enter the Flow Model Control and assign the Wave Parameters (shown in Figure 10-1)
 - Right-click on the Flow Simulation and choose Model Control.
 - Open the Wave page and switch to Inline steering in the topmost combo box.
 - Click the File button and search for the wave project simulation that was just saved and select the <project>.sim file.
 - Enter the Steering Interval (i.e., Constant–1.0 hr).

- Enable the Extrapolation distances and set the Flow to Wave and Wave to Flow settings to Automatic.
- Click OK.

Figure 10-1. CMS-Flow Model Control dialog window, Wave tab.



- Resave the project with the new link to the wave case.
- Save the CMS-Flow simulation.
 - Right-click on the CMS-Flow simulation and choose Save Simulation.
 - This step will now do two things.
 - * Save the CMS-Flow specific files.
 - * Take the needed CMS-Wave files from the chosen folder and make copies of them in the CMS-Flow folder so all Flow and Wave files exist in the same place.

10.2 Start the Steering Run

The steering process is triggered by running the CMS-Flow model with a link to the CMS-Wave files. The only step remaining is to start the run. A typical example of the SMS 13.2 screen at this point is shown in Figure 10-2.

- Right-click the CMS-Flow simulation and choose Run simulation.

- This should bring up a new dialog for the Simulation Run Queue that will contain information regarding the CMS-Flow and CMS Wave steering run (similar to Figure 10-3).

The Simulation Run Queue dialog will show output from both CMS-Flow and CMS-Wave as they are run in sequence.

Figure 10-2. Example of the SMS interface for CMS-Flow and CMS-Wave steering.

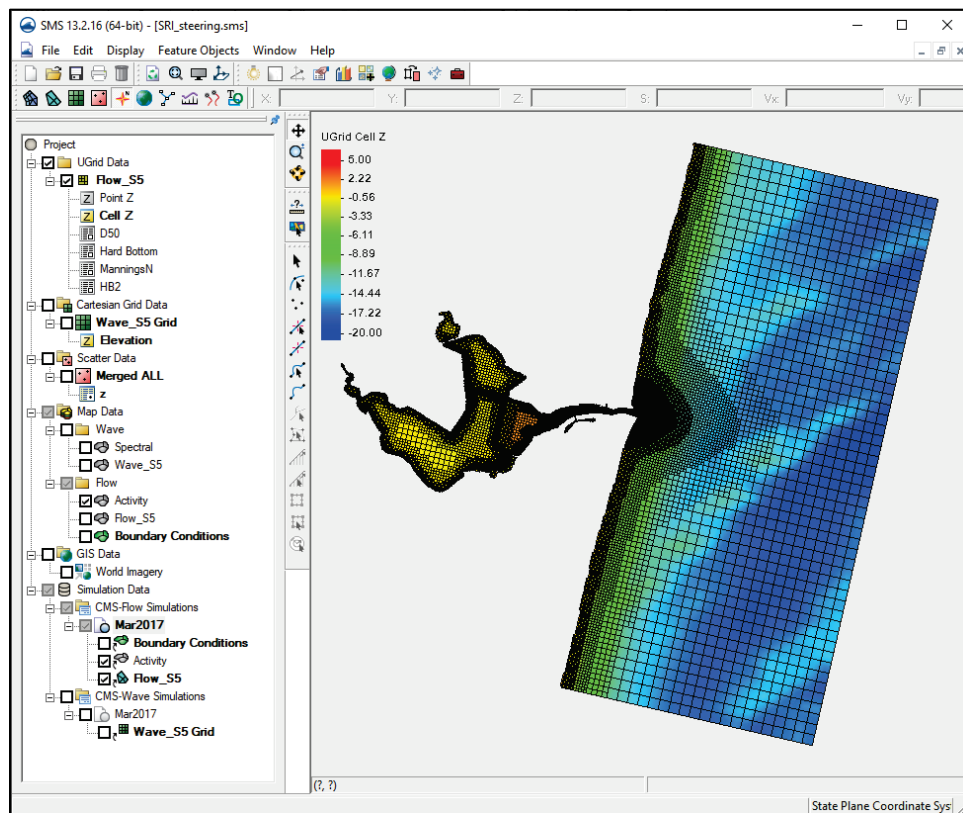
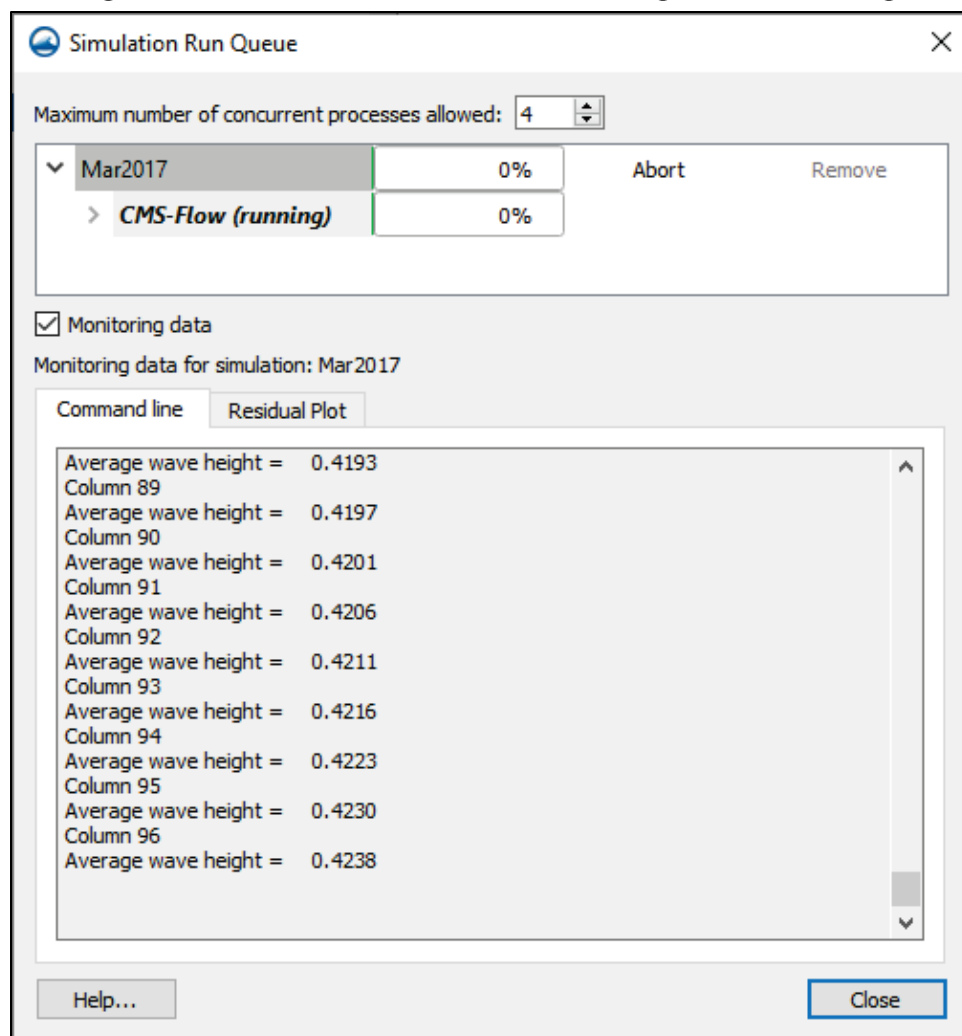


Figure 10-3. CMS-Flow Simulation Run Queue dialog window for steering.



11 Summary

The CMS is an integrated wave, current, sediment transport, and morphology change model available in the SMS. The CMS was developed under CIRP, an Operations and Maintenance Navigation research program at ERDC, Coastal and Hydraulics Laboratory.

The CMS consists of two main components: a spectral wave transformation model named CMS-Wave and a hydrodynamic, salinity and temperature, sediment, and morphology change model named CMS-Flow. Both CMS-Wave and CMS-Flow support regular and nonuniform Cartesian grids while the CMS-Flow also supports regular, nonuniform, telescoping, and stretched telescoping Cartesian grids. The CMS-Wave and CMS-Flow grids may be the same or have different spatial extents and resolutions. The two models are tightly coupled within a single inline code but may be run as stand-alone.

The CMS User Manual serves as a reference guide to the applied theory, numerical methodology, framework, and application of the modeling system. Information presented herein was prepared for use in SMS 13.0 and higher, although many features may exist in earlier versions of SMS. The latest guidance, documentations, and downloads are available at <https://cirp.usace.army.mil/> and from the CIRP wiki at https://cirpwiki.info/wiki/Main_Page.

References

- Andrews, D. G., and M. E. McIntyre. 2006. "An Exact Theory of Nonlinear Waves on a Lagrangian-Mean Flow." *Journal of Fluid Mechanics* 89 (4): 609–46. <https://doi.org/10.1017/s0022112078002773>.
- Aquaveo. 2023. "SMS 13.3—the Complete Surface-Water Solution." <https://www.aquaveo.com/software/sms-surface-water-modeling-system-introduction>.
- Armanini, A., and di Silvio, G. 1986. "A Depth-Averaged Model for Suspended Sediment Transport. Edited by G. Gallappatti and C. B. Vreugdenhil. *Journal of Hydraulic Research* 24 (5): 437–441.
- Batten, Brian K., and Nicholas C. Kraus. 2006. *Evaluation of Downtdrift Shore Erosion, Mattituck Inlet, New York: Section 111 Study*. ERDC/CHL-TR-06-1. Vicksburg, MS: US Army Engineer Research and Development Center, Coastal and Hydraulics Laboratory. <https://hdl.handle.net/11681/7605>.
- Battjes, J. A. 1972. "Set-Up Due to Irregular Waves." In *Proceedings 13th International Conference on Coastal Engineering*, ASCE, 1993–2004. <https://ascelibrary.org/doi/epdf/10.1061/9780872620490.116>.
- Battjes, J. A., and J. Janssen. 1978. "Energy Loss and Set-up due to Breaking of Random Waves." In *Proceedings 16th International Conference Coastal Engineering*, ASCE, 569–587.
- Beck, Tanya M., and Nicholas C. Kraus. 2010. *Shark River Inlet, New Jersey, Entrance Shoaling: Report 2, Analysis with Coastal Modeling System*. ERDC/CHL-TR-10-4. Vicksburg, MS: US Army Engineer Research and Development Center, Coastal and Hydraulics Laboratory. <https://hdl.handle.net/11681/7678>.
- Beck, Tanya M., and Kelly Legault 2012. *St. Augustine Inlet, Florida: Application of the Coastal Modeling System: Report 2* ERDC/CHL-TR-12-14; Rept. 2. Vicksburg, MS: US Army Engineer Research and Development Center, Coastal and Hydraulics Laboratory. <https://apps.dtic.mil/sti/pdfs/ADA571681.pdf>.
- Beck, Tanya M., Honghai Li, Hans R. Moritz, Katharine Groth, Trapier Puckette, and Jon Marsh. 2019. "Sediment Tracer Tracking and Numerical Modeling at Coos Bay Inlet, Oregon." *Journal of Coastal Research* 35 (1): 4–25. <https://doi.org/10.2112/jcoastres-d-17-00218.1>.
- Bodhaine, G. L. 1968. *Measurement of Peak Discharge at Culverts by Indirect Methods*. US Geological Survey, Techniques of Water-Resources Investigations, Book 3, Chapter A3. <https://pubs.usgs.gov/twri/twri3-a3/>.
- Bouws, E., and G. J. Komen. 1983. "On the Balance between Growth and Dissipation in Extreme, Depth Limited Wind-sea in the Southern North Sea." *Journal of Physical Oceanography* 13: 1653–1658.

- Buttolph, Adele M., Christopher W. Reed, Nicholas C. Kraus, Nobuyuki Ono, Magnus Larson, Benoit Camenen, Hans Hanson, Ty Wamsley, and Alan K. Zundel. 2006. *Two-Dimensional Depth-Averaged Circulation Model CMS-M2D: Version 3.0, Report 2, Sediment Transport and Morphology Change*. ERDC/CHL TR-06-9. Vicksburg, MS: US Army Engineer Research and Development Center, Coastal and Hydraulics Laboratory. <https://erdc-library.erdcdren.mil/jspui/bitstream/11681/7613/1/CHL-TR-06-9.pdf>.
- Bye, John A. T. 1985. "Chapter 6 Large-Scale Momentum Exchange in the Coupled Atmosphere-Ocean." In *Coupled Ocean-Atmosphere Models*, 51–61. Elsevier Oceanography Series. [https://doi.org/10.1016/s0422-9894\(08\)70702-5](https://doi.org/10.1016/s0422-9894(08)70702-5).
- Byrnes, Mark Richard, Sarah F. Griffee, and Mark S. Osler. 2010. *Channel Dredging and Geomorphic Response at and Adjacent to Mobile Pass, Alabama*. ERDC/CHL TR-10-8. Vicksburg, MS: US Army Engineer Research and Development Center, Coastal and Hydraulics Laboratory. <https://hdl.handle.net/11681/7722>.
- Camenen, B., and M. Larson. 2005. "A General Formula for Non-Cohesive Bed Load Sediment Transport." *Estuarine, Coastal and Shelf Science* 63: 249–260.
- Camenen, B., and M. Larson. 2007. *A Unified Sediment Transport Formulation for Coastal Inlet Application*. ERDC/CHL CR-07-1. Vicksburg, MS: US Army Engineer Research and Development Center, Coastal and Hydraulics Laboratory.
- Camenen, B., and M. Larson. 2008. "A General Formula for Noncohesive Suspended Sediment Transport." *Journal of Coastal Research* 24 (3): 615–627.
- Chawla A., and J. T. Kirby. 2002. "Monochromatic and Random Wave Breaking at Blocking Points." *Journal of Geophysical Research* 107 (C7): 10.1029/2001JC001042.
- Crowe, C. T., D. F. Elger, and J. A. Roberson. 2005. *Engineering Fluid Mechanics*. Hoboken, NJ: John Wiley & Sons, Inc.
- Dabees, Mohamed A., Brett D. Moore, and Kenneth K. Humiston. 2011. "Evaluation of Tidal Inlets Channel Migration and Management Practices in Southwest Florida." In *Proceedings of the Coastal Sediments 2011*, 484–96. https://doi.org/10.1142/9789814355537_0037.
- d'Angremond, K., J. W. Van der Meer, and R. J. de Jong. 1996. "Wave Transmission at Low-Crested Structures." In *Proceedings 25th International Conference on Coastal Engineering*, Orlando, Florida, USA, ASCE, 2418–2427.
- Davies, A. G., R. L. Soulsby, and H. L. King. 2012. "A Numerical Model of the Combined Wave and Current Bottom Boundary Layer." *Journal of Geophysical Research: Oceans* 93 (C1): 491–508. <https://doi.org/10.1029/JC093iC01p00491>.
- Dawe, Jordan T., and LuAnne Thompson. 2006. "Effect of Ocean Surface Currents on Wind Stress, Heat Flux, and Wind Power Input to the Ocean." *Geophysical Research Letters* 33(9). <https://doi.org/10.1029/2006gl025784>.

- Dean, Robert G., and R. A. Dalrymple. 1984. *Water Wave Mechanics for Engineers and Scientists*. Englewood Cliffs, NJ: Prentice-Hall.
- Department of the Army. 1984. *Shore Protection Manual, 4th Ed., 2 Vol.* Washington, DC: US Government Printing Office. <https://luk.staff.ugm.ac.id/USACE/USACE-ShoreProtectionManual2.pdf>.
- Edinger, J. E., D. K. Brady, and J. C. Greyer. 1974. *Heat Exchange and Transport in the Environment*. Rep. No. 14. Cooling Water Resources Project (RP-49). Palo Alto, CA: Electric Power Research Institute.
- Falconer, R. A. 1980. "Modeling of Planform Influence on Circulation in Harbors. In *Proceedings Coastal Engineering Conference '17*, ASCE, 2726–2744.
- Fredsoe, J. 1984. "Turbulent Boundary Layer in Wave-Current Motion." *Journal of Hydraulic Engineering*, ASCE 110: 1103–1120.
- Gallappatti, R. 1983. "A Depth-Integrated Model for Suspended Transport." *Communications on Hydraulics*, Vol. 83-7. Delft, The Netherlands: Delft University of Technology. <https://repository.tudelft.nl/islandora/object/uuid:2cf67a5b-d2c4-4287-8ed2-16f1b27bdbcc?collection=research>.
- Goda, Y. 1985. *Random Seas and Design of Maritime Structures*. Tokyo: University of Tokyo Press.
- Graf, Walter H., and M. S. Altinakar. 1998. *Fluvial Hydraulics: Flow and Transport Processes in Channels of Simple Geometry*. New York: Wiley.
- Grant, William D., and Ole Secher Madsen. 2012. "Combined Wave and Current Interaction with a Rough Bottom." *Journal of Geophysical Research: Oceans* 84 (C4): 1797–808. <https://doi.org/10.1029/JC084iC04p01797>.
- Hardy, Thomas A. 1993. *The Attenuation of Spectral Transformation of Wind Waves on a Coral Reef*. Queensland, Australia: James Cook University of North Queensland, Townsville.
- Hasselmann, K., T. P. Barnett, E. Bouws, H. Carlson, D. E. Cartwright, K. Enke, J. A. Ewing, H. Gienapp, D. E. Hasselmann, P. Kruseman, A. Meerbrug, P. Muller, D. J. Olbers, K. Richter, W. Sell, and H. Walden. 1973. *Measurements of Windwave Growth and Swell Decay during the Joint North Sea Wave Project (JONSWAP)*. Deutsche Hydrographische Zeitschrift A80(12).
- Hearn, C. J. 1999. "Wave-Breaking Hydrodynamics within Coral Reef Systems and the Effect of Changing Relative Sea Level." *Journal of Geophysical Research* 104 (C12): 30,007–30,019.
- HEC (Hydrological Engineering Center). 2010. *HEC-RAS River Analysis System, Hydraulic Reference Manual, Version 4.1*. Davis, CA: HEC, US Army Corps of Engineers.

- Hirano, Muneo. 1971. "River-Bed Degradation with Armoring." In *Proceedings of the Japan Society of Civil Engineers* 1971 (195): 55–65. https://doi.org/10.2208/jscej1969.1971.195_55.
- Hsu, S. A. 2003. "Coastal Meteorology." *Encyclopedia of Physical Science and Technology*, 155–73. <https://doi.org/10.1016/b0-12-227410-5/00114-9>.
- Iwagaki, Y., T. Asano, Y. Yamanaka, and F. Nagai. 1980. "Wave Breaking Due to Currents." *Annual Journal of Coastal Engineering* 27: 30–34.
- Jenkins, A. D., and O. M. Phillips. 2001. "A Simple Formula for Nonlinear Wave-Wave Interaction." *International Journal of Offshore and Polar Engineering* 11 (2): 81–86.
- Johnson, Bradley, and Alison Grzegorzewski. 2011. "Modeling Nearshore Morphological Evolution of Ship Island During Hurricane Katrina." In *Proceedings of the Coastal Sediments 2011*, 1797–810. https://doi.org/10.1142/9789814355537_0136.
- Johnson, Hakeem K., and Julio A. Zyserman. 2002. "Controlling Spatial Oscillations in Bed Level Update Schemes." *Coastal Engineering* 46 (2): 109–26.
- Jonsson, Ivar G. 1966. "Wave Boundary Layers and Friction Factors." *Coastal Engineering Proceedings* (10): 127–48. <https://doi.org/10.9753/icce.v10.9>.
- Kadlec, R. H., and R. L. Knight. 1996. *Treatment Wetlands*. Boca Raton: Lewis Publishers.
- Karim, M. F., and J. F. Kennedy. 1982. *IALLUVIAL: A Computer-Based Flow-and Sediment-Routing Model for Alluvial Streams and Its Application to the Missouri River*. Iowa Institute of Hydraulic Research IIHR Report No. 250. Iowa City, IA: University of Iowa.
- Kobayashi, Nobuhisa, and Bradley D. Johnson. 2001. "Sand Suspension, Storage, Advection, and Settling in Surf and Swash Zones." *Journal of Geophysical Research: Oceans* 106 (C5): 9363–6. <https://doi.org/10.1029/2000jc000557>.
- Komar, Paul D. 1998. *Beach Processes and Sedimentation*. 2nd ed. Upper Saddle River, NJ: Prentice-Hall, Inc.
- Lamb, H. 1932. *Hydrodynamics*. 6th ed. New York: Dover Publications.
- Li, H., and M. E. Brown. 2017. *Temperature Calculations in the Coastal Modeling System*. ERDC/CHL CHETN-IV-110. Vicksburg, MS: US Army Engineer Research and Development Center, Coastal and Hydraulics Laboratory. <https://dx.doi.org/10.21079/11681/21666>.

- Li, H., and M. E. Brown. 2019. *Modeling Sea Level Change Using the Coastal Modeling System*. ERDC/CHL CHETN-IV-119. Vicksburg, MS: US Army Engineer Research and Development Center, Coastal and Hydraulics Laboratory. <https://dx.doi.org/10.21079/11681/33204>.
- Li, Honghai, Lihwa Lin, Chia-Chi Lu, Christopher W. Reed, and Arthur T. Shak. 2015. "Modeling Study of Dana Point Harbor, California: Littoral Sediment Transport around a Semi-Permeable Breakwater." *Journal of Ocean Engineering and Marine Energy* 1 (2): 181–92. <https://doi.org/10.1007/s40722-015-0018-2>.
- Li, H., and N. J. MacDonald. 2012. *Use of the PTM with CMS Quadtree Grids*. ERDC/CHL CHETN IV-82. Vicksburg, MS: US Army Engineer Research and Development Center, Coastal and Hydraulics Laboratory.
- Li, Honghai, Christopher W. Reed, and Mitchell E. Brown. 2012. *Salinity Calculations in the Coastal Modeling System*. ERDC/CHL CHETN-IV-80. Vicksburg, MS: US Army Engineer Research and Development Center, Coastal and Hydraulics Laboratory. <https://hdl.handle.net/11681/1981>.
- Li, H., A. Sánchez, W. Wu, and C. W. Reed. 2013a. *Implementation of Structures in the CMS: Part I, Rubble Mound*. ERDC/CHL CHETN-IV-93. Vicksburg, MS: US Army Engineer Research and Development Center, Coastal and Hydraulics Laboratory. <https://hdl.handle.net/11681/1989>.
- Li, H., A. Sánchez, W. Wu, and C. W. Reed. 2013b. *Implementation of structures in the CMS: Part II, Weir*. ERDC/CHL CHETN-IV-94. Vicksburg, MS: US Army Engineer Research and Development Center, Coastal and Hydraulics Laboratory. <https://hdl.handle.net/11681/1991>.
- Li, H., A. Sánchez, W. Wu, and C. W. Reed. 2013c. *Implementation of structures in the CMS: Part III, Culvert*. ERDC/CHL CHETN-IV-94. Vicksburg, MS: US Army Engineer Research and Development Center, Coastal and Hydraulics Laboratory. <https://hdl.handle.net/11681/1983>.
- Li, H., A. Sánchez, W. Wu, and C. W. Reed. 2013d. *Implementation of structures in the CMS: Part IV, Tide Gate*. ERDC/CHL CHETN-IV-94. Vicksburg, MS: US Army Engineer Research and Development Center, Coastal and Hydraulics Laboratory. <https://hdl.handle.net/11681/2000>.
- Lin, B. N. 1984. "Current Study of Unsteady Transport of Sediment in China." In *Proceedings Japan-China Bilateral Seminar on River Hydraulics and Engineering Experience*, July, 337–42. Tokyo-Kyoto-Saporo, Japan.
- Lin, Lihwa, and Zeki Demirbilek. 2012. *Modeling Combined Diffraction-Refraction in a Coastal Spectral Wave Model*. In *Proceedings 22nd International Offshore and Polar Engineering Conference*, June 2012, Rhodes, Greece.
- Lin, Lihwa, Zeki Demirbilek, and Hajime Mase. 2011. *Recent Capabilities of CMS-Wave: A Coastal Wave Model for Inlets and Navigation Projects*. Symposium to honor Dr. Nicholas Kraus. *Journal of Coastal Research Special Issue* 59: 7–14.

- Lin, Lihwa, Zeki Demirbilek, Hajime Mase, Jinhai Zheng, and Fumihiko Yamada. 2008. *CMS-Wave: A Nearshore Spectral Wave Processes Model for Coastal Inlets and Navigation Projects*. ERDC/CHL TR-08-13. Vicksburg, MS: US Army Engineer Research and Development Center, Coastal and Hydraulics Laboratory. <https://hdl.handle.net/11681/7653>.
- Lin, Lihwa, Zeki Demirbilek, Robert C. Thomas, and James Rosati. 2011. *Verification and Validation of the Coastal Modeling System; Report 2: CMS-Wave*. ERDC/CHL-TR-11-10. Vicksburg, MS: US Army Engineer Research and Development Center, Coastal and Hydraulics Laboratory. <https://hdl.handle.net/11681/7662>.
- Lin, Lihwa, Zeki Demirbilek, Jinhai Zheng, and Hajime Mase. 2010. *Rapid Calculation of Nonlinear Wave-Wave Interactions in Wave-action Balance Equation*. In *Proceedings 32nd International Conference on Coastal Engineering*, Shanghai, China.
- Lin, Lihwa, Honghai Li, Mitchell E. Brown, Frank Wu, and Lisa C. Andes. 2013. *Pilot Study Evaluating Nearshore Sediment Placement Sites, Noyo Harbor, CA*. ERDC/CHL TR-13-2. Vicksburg, MS: US Army Engineer Research and Development Center, Coastal and Hydraulics Laboratory.
- Lin, Lihwa, and Ray-Qing Lin. 2004. "Wave Breaking Function." In *Proceedings 8th International Workshop on Wave Hindcasting and Prediction*. North Shore, Hawaii. <http://www.waveworkshop.org/8thWaves/Papers/L3.pdf>.
- Lin, Lihwa, Ray-Qing Lin, and J. P. Y. Maa. 2006. "Numerical Simulation of Wind Wave Field." In *9th International Workshop on Wave Hindcasting and Prediction*, September, Victoria, British Columbia, Canada.
- Lin, Lihwa, James Rosati, and Zeki Demirbilek. 2012. *CMS-Wave Model Part 5: Full-Plane Wave Transformation and Grid Nesting*. ERDC/CHL CHETN-IV-81. Vicksburg, MS: US Army Engineer Research and Development Center, Coastal and Hydraulics Laboratory. <https://hdl.handle.net/11681/1996>.
- Lin, Ray-Qing, and Lihwa Lin. 2004. "Wind Input Function." In *Proceedings 8th International Workshop on Wave Hindcasting and Prediction*, November, North Shore, Hawaii, United States.
- Longuet-Higgins, M. S., and R. W. Stewart. 2006. "The Changes in Amplitude of Short Gravity Waves on Steady Non-Uniform Currents." *Journal of Fluid Mechanics* 10 (04): 529–49. <https://doi.org/10.1017/s0022112061000342>.
- Lowe, R. J., J. L. Falter, M. D. Bandet, G. Pawlak, M. J. Atkinson, S. G. Monismith, and J. R. Koseff. 2005. "Spectral Wave Dissipation over a Barrier Reef." *Journal of Geophysical Research* 110:(C04001). doi:10.1029/2004JC002711.
- Macagno, E. O. 1953. "Houle Dans un can Presentent un Passage en Charge." *La Houille Blanche* 9 (1): 10–37.

- MacDonald, Neil J., Michael H. Davies, Alan K. Zundel, John D. Howlett, Zeki Demirbilek, Joseph Z. Gailani, Tahirih C. Lackey, and S. Jarrell Smith. 2006. *PTM: Particle Tracking Model; Report 1: Model Theory, Implementation, and Example Applications*. ERDC/CHL-TR-06-20. Vicksburg, MS: US Army Engineer Research and Development Center, Coastal and Hydraulics Laboratory. <https://hdl.handle.net/11681/7695>.
- Mase, Hajime, H. Amamori, and T. Takayama. 2005. "Wave Prediction Model in Wave-current Coexisting Field." In Proceedings 12th Canadian Coastal Conference.
- Mase, Hajime, Kazuya Oki, Terry S. Hedges, and Hua Jun Li. 2005. "Extended Energy-Balance-Equation Wave Model for Multidirectional Random Wave Transformation." *Ocean Engineering* 32 (8–9): 961–85. <https://doi.org/10.1016/j.oceaneng.2004.10.015>.
- Mei, C. 1989. *The Applied Dynamics of Ocean Surface Waves*. New York: John Wiley.
- Militello, Adele, Christopher W. Reed, Alan K. Zundel, and Nicholas C. Kraus. 2004. *Two-Dimensional Depth-Averaged Circulation Model M2D: Version 2.0, Report 1, Technical Documentation and User's Guide*. ERDC/CHL TR-04-2. Vicksburg, MS: US Army Engineer Research and Development Center, Coastal and Hydraulics Laboratory. <https://hdl.handle.net/11681/7640>.
- Nicholson, John, and Brian A. O'Connor. 1986. "Cohesive Sediment Transport Model." *Journal of Hydraulic Engineering* 112 (7): 621–40. [https://doi.org/10.1061/\(asce\)0733-9429\(1986\)112:7\(621\)](https://doi.org/10.1061/(asce)0733-9429(1986)112:7(621)).
- Nielsen, P. 1992. *Coastal Bottom Boundary Layers and Sediment Transport*. "Advanced Series on Ocean Engineering." <https://doi.org/10.1142/1269>.
- NOAA. n.d. "NOAA Shoreline Website." <https://shoreline.noaa.gov/data/datasheets/cusp.html>.
- NOAA. n.d. "NOAA Tides and Currents." <https://tidesandcurrents.noaa.gov/>.
- Pacanowski, R. C. 1987. "Effect of Equatorial Currents on Surface Stress." *Journal of Physical Oceanography* 17 (6): 833–38. [https://doi.org/10.1175/1520-0485\(1987\)017<0833:Eoecos>2.0.Co;2](https://doi.org/10.1175/1520-0485(1987)017<0833:Eoecos>2.0.Co;2).
- Parker, Gary, Peter C. Klingeman, and David G. McLean. 1983. "Bedload and Size Distribution in Paved Gravel-Bed Streams." *Journal of Hydraulic Engineering* 109 (5): 793–93. [https://doi.org/10.1061/\(asce\)0733-9429\(1983\)109:5\(793\)](https://doi.org/10.1061/(asce)0733-9429(1983)109:5(793)).
- Phillips, O. M. 1957. "On the Generation of Waves by Turbulent Wind." *Journal of Fluid Mechanics* 2:417–445.
- Phillips, O. M. 1977. "The Dynamics of the Upper Ocean, 2nd Edition." *Journal of Fluid Mechanics* 88 (4): 793–94. <https://doi.org/10.1017/s0022112078212396>.

- Powell, Mark D., Peter J. Vickery, and Timothy A. Reinhold. 2003. "Reduced Drag Coefficient for High Wind Speeds in Tropical Cyclones." *Nature* 422 (6929): 279–83. <https://doi.org/10.1038/nature01481>.
- Raudkivi, A. J. 1998. *Loose Boundary Hydraulics*. London, UK: CRC Press. <https://doi.org/10.1201/9781003077800>.
- Reed, Christopher, and Mitchell Brown. 2019. *Coastal Modeling System: Dredging Module Simulation with Multiple Grain Sizes*. ERDC/CHL CHETN-I-98. Vicksburg, MS: US Army Engineer Research and Development Center, Coastal and Hydraulics Laboratory. <https://dx.doi.org/10.21079/11681/33664>.
- Reed, Christopher W., Mitchell E. Brown, Alejandro Sánchez, Weiming Wu, and Adele M. Buttolph. 2011. "The Coastal Modeling System Flow Model (CMS-Flow): Past and Present." *Journal of Coastal Research* 59: 1–6. <https://doi.org/10.2112/si59-001.1>.
- Reed, Christopher W., and Lihwa Lin. 2011. "Analysis of Packery Channel Public Access Boat Ramp Shoreline Failure." *Journal of Coastal Research* 59: 150–55. <https://doi.org/10.2112/si59-015.1>.
- Reed, Christopher W., and Alejandro Sánchez. 2016. *Coastal Modeling System: Dredging Module*. ERDC/CHL CHETN-I-90. Vicksburg, MS: US Army Engineer Research and Development Center, Coastal and Hydraulics Laboratory. <https://hdl.handle.net/11681/20266>.
- Rhie, C., and W. L. Chow 1983. "A Numerical Study of the Turbulent Flow Past an Isolated Airfoil with Trailing Edge Separation." *AIAA Journal* 21: 1525–1532.
- Rosati, James, Ashley E. Frey, Mitchell E. Brown, and Lihwa Lin. 2011. *Analysis of Dredged Material Placement Alternatives for Bottleneck Removal, Matagorda Ship Channel, Texas*. ERDC/CHL-TR-11-2. Vicksburg, MS: US Army Engineer Research and Development Center, Coastal and Hydraulics Laboratory. <https://hdl.handle.net/11681/7718>.
- Sakai, S., N. Kobayashi, and K. Koike. 1989. "Wave Breaking Criterion with Opposing Current on Sloping Bottom: An Extension of Goda's Breaker Index." *Annual Journal of Coastal Engineering* 36: 56–59.
- Sánchez, Alejandro, and Weiming Wu. 2011. "A Non-Equilibrium Sediment Transport Model for Coastal Inlets and Navigation Channels." *Journal of Coastal Research* 59: 39–48. <https://doi.org/10.2112/si59-005.1>.
- Sánchez, Alejandro, Weiming Wu, and Tanya M. Beck. 2016. "A Depth-Averaged 2D Model of Flow and Sediment Transport in Coastal Waters." *Ocean Dynamics* 66 (11): 1475–95. <https://doi.org/10.1007/s10236-016-0994-3>.

- Sánchez, Alejandro, Weiming Wu, Tanya M. Beck, Honghai Li, Julie Dean Rosati, Zeki Demirbilek, and Mitchell E. Brown. 2011. *Verification and Validation of the Coastal Modeling System; Report 4: CMS-Flow Sediment Transport and Morphology Change*. ERDC/CHL TR-11-10. Vicksburg, MS: US Army Engineer Research and Development Center, Coastal and Hydraulics Laboratory. <https://hdl.handle.net/11681/7658>.
- Sánchez, Alejandro, Weiming Wu, Tanya M. Beck, Honghai Li, James Rosati, Robert C. Thomas, Julie Dean Rosati, Zeki Demirbilek, Mitchell E. Brown, and Christopher W. Reed. 2011. *Verification and Validation of the Coastal Modeling System; Report 3: CMS-Flow Hydrodynamics*. ERDC/CHL TR-11-10. Vicksburg, MS: US Army Engineer Research and Development Center, Coastal and Hydraulics Laboratory. <https://hdl.handle.net/11681/7657>.
- Sánchez, Alejandro, Weiming Wu, Honghai Li, Mitchell E. Brown, Christopher W. Reed, Julie Dean Rosati, and Zeki Demirbilek. 2014. *Coastal Modeling System: Mathematical Formulations and Numerical Methods*. ERDC/CHL TR-14-2. Vicksburg, MS: US Army Engineer Research and Development Center, Coastal and Hydraulics Laboratory. <https://hdl.handle.net/11681/7361>.
- Sidiropoulou, Melina G., Konstadinos N. Moutsopoulos, and Vassilios A. Tsihrintzis. 2006. "Determination of Forchheimer Equation Coefficients A and B." *Hydrological Processes* 21 (4): 534–54. <https://doi.org/10.1002/hyp.6264>.
- Smagorinsky, J. 1963. "General Circulation Experiments with the Primitive Equations." *Monthly Weather Review* 91 (3): 99–164. [https://doi.org/10.1175/1520-0493\(1963\)091<0099:Gcewtp>2.3.Co;2](https://doi.org/10.1175/1520-0493(1963)091<0099:Gcewtp>2.3.Co;2).
- Son, Huynh-Thanh, and Temperville André. 1991. "A Numerical Model of the Rough Turbulent Boundary Layer in Combined Wave and Current Interaction." *Coastal Engineering* 1990: 853–66. <https://doi.org/10.1061/9780872627765.067>.
- Soulsby, R. L. 1995. Bed shear-stresses due to combined waves and currents. in *Advanced in Coastal Morphodynamics*, ed M.J.F Stive, H.J. de Vriend, J. Fredsoe, L. Hamm, R.L. Soulsby, C. Teisson, and J.C. Winterwerp, Delft Hydraulics, Netherlands. 4-20 to 4-23 pp.
- Soulsby, R. L. 1997. *Dynamics of Marine Sands*. London: Thomas Telford.
- Soulsby, R. L., and R. J. S. W. Whitehouse. 1997. "Threshold of Sediment Motion in Coastal Environment." In *Proc. Pacific Coasts and Ports '97 Conference*, 149–54. Christchurch, New Zealand: University of Canterbury.
- Stark, J. 2012. "The Influence of Dredging on the Morphological Development of the Columbia River Mouth." Masters thesis. Delft, The Netherlands: Delft University of Technology. <https://repository.tudelft.nl/islandora/object/uuid:e5d65bb4-5aef-432e-b6a2-871fb22f0de4?collection=education>.
- Svendsen, I. A. 2006. *Introduction to Nearshore Hydrodynamics*. Singapore: World Scientific.

- Swart, D. H. 1977. "Predictive Equations Regarding Coastal Transports." In *Coastal Engineering 1976*, 1113–32. <https://doi.org/10.1061/9780872620834.066>.
- USACE (US Army Corps of Engineers). 2002. *Coastal Engineering Manual*. EM 1110-2-1100. Washington, DC: US Army Corps of Engineers.
- USACE (US Army Corps of Engineers). 2018. *Dredging Cost Analysis–2017*. US Army Corps of Engineers Institute for Water Resources, Navigation Data Center–Dredging Information Section. Washington, DC: US Army Corps of Engineers. <https://usace.contentdm.oclc.org/digital/collection/p16021coll2/id/2659/>.
- van Doormaal, J. P., and G. D. Raithby. 1984. "Enhancements of the Simple Method for Predicting Incompressible Fluid Flows." *Numerical Heat Transfer* 7 (2): 147–163. <https://doi.org/10.1080/01495728408961817>.
- van Rijn, Leo C. 1984a. "Sediment Transport, Part I: Bed Load Transport." *Journal of Hydraulic Engineering* 110 (10): 1431–56. [https://doi.org/10.1061/\(asce\)0733-9429\(1984\)110:10\(1431\)](https://doi.org/10.1061/(asce)0733-9429(1984)110:10(1431)).
- van Rijn, Leo C. 1984b. "Sediment Transport, Part II: Suspended Load Transport." *Journal of Hydraulic Engineering* 110 (11): 1613–41. [https://doi.org/10.1061/\(asce\)0733-9429\(1984\)110:11\(1613\)](https://doi.org/10.1061/(asce)0733-9429(1984)110:11(1613)).
- van Rijn, Leo C. 1984c. "Sediment Transport, Part III: Bed Forms and Alluvial Roughness." *Journal of Hydraulic Engineering* 110 (12): 1733–54. [https://doi.org/10.1061/\(asce\)0733-9429\(1984\)110:12\(1733\)](https://doi.org/10.1061/(asce)0733-9429(1984)110:12(1733)).
- van Rijn, Leo C. 2007a. "Unified View of Sediment Transport by Currents and Waves. I: Initiation of Motion, Bed Roughness, and Bed-Load Transport." *Journal of Hydraulic Engineering* 133 (6): 649–67. [https://doi.org/10.1061/\(asce\)0733-9429\(2007\)133:6\(649\)](https://doi.org/10.1061/(asce)0733-9429(2007)133:6(649)).
- van Rijn, Leo C. 2007b. "Unified View of Sediment Transport by Currents and Waves. II: Suspended Transport." *Journal of Hydraulic Engineering* 133 (6): 668–89. [https://doi.org/10.1061/\(asce\)0733-9429\(2007\)133:6\(668\)](https://doi.org/10.1061/(asce)0733-9429(2007)133:6(668)).
- Walstra, D. J. R., J. A. Roelvink, and J. Groeneweg. 2001. "Calculation of Wave-Driven Currents in a 3D Mean Flow Model." In *Coastal Engineering 2000*, 1050–63. [https://doi.org/10.1061/40549\(276\)81](https://doi.org/10.1061/40549(276)81).
- Wang, Ping, Tanya M. Beck, and Tiffany M. Roberts. 2011. "Modeling Regional-Scale Sediment Transport and Medium-Term Morphology Change at a Dual-Inlet System Examined with the Coastal Modeling System (CMS): A Case Study at Johns Pass and Blind Pass, West-Central Florida." *Journal of Coastal Research* 59: 49–60. <https://doi.org/10.2112/si59-006.1>.
- Ward, J. C. 1964. "Turbulent Flow in Porous Media." *Journal of the Hydraulics Division* 90 (5): 1–12. <https://doi.org/10.1061/jyceaj.0001096>.

- Watanabe, A. 1987. "3-Dimensional Numerical Model of Beach Evolution." In *Proceedings Coastal Sediments '87*, 802–17.
- Wu, W. 1991. *The Study and Application of 1-D, Horizontal 2D and Their Nesting Mathematical Models for Sediment Transport*. PhD dissertation. Wuhan University of Hydraulic and Electrical Engineering.
- Wu, W. 2004. "Depth-Averaged Two-Dimensional Numerical Modeling of Unsteady Flow and Nonuniform Sediment Transport in Open Channels." *Journal of Hydraulic Engineering* 130 (10): 1013–24. [https://doi.org/10.1061/\(asce\)0733-9429\(2004\)130:10\(1013\)](https://doi.org/10.1061/(asce)0733-9429(2004)130:10(1013)).
- Wu, W. 2007. *Computational River Dynamics*. Milton Park, Abingdon-on-Thames, Oxfordshire United Kingdom: Taylor & Francis.
- Wu, W., M. Altinakar, and S. S. Y. Wang. 2006. "Depth-Averaged Analysis of Hysteresis between Flow and Sediment Transport under Unsteady Conditions." *International Journal of Sediment Research* 21 (2): 101–12.
- Wu, W., and Q. Lin. 2011. *Extension of the Lund-CIRP Formula for Multiple-Sized Sediment Transport under Currents and Waves*. Oxford, MS: The University of Mississippi, National Center for Computational Hydroscience and Engineering.
- Wu, Weiming, Alejandro Sánchez, and Mingliang Zhang. 2011a. "An Implicit 2D Depth-Averaged Finite-Volume Model of Flow and Sediment Transport in Coastal Waters." *Coastal Engineering Proceedings* 1(32). <https://doi.org/10.9753/icce.v32.sediment.23>.
- Wu, W., Alejandro Sánchez, and Mingliang Zhang. 2011b. "An Implicit 2D Shallow Water Flow Model on Unstructured Quadtree Rectangular Mesh." *Journal of Coastal Research* 59: 15–26. <https://doi.org/10.2112/si59-003.1>.
- Wu, W., P. Wang, and N. Chiba. 2004. "Comparison of Five Depth-Averaged 2D Turbulence Models for River Flows." *Archives of Hydro-Engineering and Environmental Mechanics* 51 (2): 183–200. <https://www.infona.pl/resource/bwmeta1.element.baztech-article-BAT3-0011-0022>.
- Wu, Weiming, Sam S. Y. Wang, and Yafei Jia. 2010. "Nonuniform Sediment Transport in Alluvial Rivers." *Journal of Hydraulic Research* 38 (6): 427–34. <https://doi.org/10.1080/00221680009498296>.
- Zarillo, Gary A., and Florian G. A. Brehin. 2007. "Hydrodynamic and Morphologic Modeling at Sebastian Inlet, FL." In *Coastal Sediments '07*, 1297–310. [https://doi.org/10.1061/40926\(239\)100](https://doi.org/10.1061/40926(239)100).
- Zheng, Jinhai, H. Mase, Z. Demirebilek, and L. Lin. 2008. "Implementation and Evaluation of Alternative Wave Breaking Formulas in a Coastal Spectral Wave Model." *Ocean Engineering* 35 (11–12). <https://www.sciencedirect.com/science/article/pii/S0029801808001157>.

Abbreviations

ADCIRC	Advance Circulation
CIRP	Coastal Inlets Research Program
CMS	Coastal Modeling System
CSHORE	Cross-SHORE
CUSP	Continually Updated Shoreline Product
DM	Dredging module
ERDC	US Army Engineer Research and Development Center
GIS	Geographic Information System
GMRES	Generalized Minimal Residual
HLPA	Hybrid Linear/Parabolic Approximation
ICCG	Incomplete Cholesky Conjugate Gradient
JONSWAP	Joint North Sea Wave Project
MLLW	Mean lower-low water
MLW	Mean low water
MSL	Mean sea level
MTL	Mean tide level
NAD83	North American Datum of 1983
OpenMP	Open Multiprocessing
PTM	Particle Tracking Model
QUAD	Quadratic
SIMPLEC	Semi-Implicit Method for Pressure Linked Equations Consistent
SIP	Strongly Implicit Procedure
SMS	Surface-water Modeling System

SWL	Still water level
TMA	Texel Marsen Arsloe
2DH	Two-dimensional horizontal
WSE	Water surface elevation
USACE	US Army Corps of Engineers

REPORT DOCUMENTATION PAGE

1. REPORT DATE Month 2024		2. REPORT TYPE Final Special Report (SR)		3. DATES COVERED	
				START DATE FY23	END DATE FY24
4. TITLE AND SUBTITLE Coastal Modeling System User's Manual					
5a. CONTRACT NUMBER		5b. GRANT NUMBER		5c. PROGRAM ELEMENT	
5d. PROJECT NUMBER		5e. TASK NUMBER		5f. WORK UNIT NUMBER	
6. AUTHOR(S) Honghai Li, Mitchell E. Brown, Lihwa Lin, Yan Ding, Tanya M. Beck, Alejandro Sánchez, Weiming Wu, Christopher W. Reed, and Alan K. Zundel					
7. PERFORMING ORGANIZATION NAME(S) AND ADDRESS(ES) See reverse.				8. PERFORMING ORGANIZATION REPORT NUMBER ERDC/CHL SR-24-??	
9. SPONSORING/MONITORING AGENCY NAME(S) AND ADDRESS(ES) US Army Engineer Research and Development Center Coastal and Hydraulics Laboratory 3909 Halls Ferry Road Vicksburg, MS 39180-6199			10. SPONSOR/MONITOR'S ACRONYM(S)		11. SPONSOR/MONITOR'S REPORT NUMBER(S)
12. DISTRIBUTION/AVAILABILITY STATEMENT Distribution Statement A. Approved for public release: distribution is unlimited.					
13. SUPPLEMENTARY NOTES Funding Account Code U4391283; AMSCO Code 060000					
14. ABSTRACT The Coastal Modeling System (CMS) is a suite of coupled 2D numerical models for simulating nearshore waves, currents, water levels, sediment transport, morphology change, and salinity and temperature. Developed by the Coastal Inlets Research Program of the US Army Corps of Engineers, the CMS provides coastal engineers and scientists a PC-based, easy-to-use, accurate, and efficient tool for understanding of coastal processes and for designing and managing of coastal inlets research, navigation projects, and sediment exchange between inlets and adjacent beaches. The present technical report acts as a user guide for the CMS, which contains comprehensive information on model theory, model setup, and model features. The detailed descriptions include creation of a new project, configuration of model grid, various types of boundary conditions, representation of coastal structures, numerical methods, and coupled simulations of waves, hydrodynamics, and sediment transport. Pre- and postmodel data processing and CMS modeling procedures are also described through operation within a graphic user interface—the Surface Water Modeling System.					
15. SUBJECT TERMS Coasts--Wetlands; Dredging spoil--Reuse; Mangrove forests; Mangrove restoration; Sea level					
16. SECURITY CLASSIFICATION OF:			17. LIMITATION OF ABSTRACT		18. NUMBER OF PAGES
a. REPORT Unclassified	b. ABSTRACT Unclassified	c. THIS PAGE Unclassified	SAR		180
19a. NAME OF RESPONSIBLE PERSON Honghai Li			19b. TELEPHONE NUMBER (include area code) (601)-634-2840		

7. PERFORMING ORGANIZATION NAME(S) AND ADDRESS(ES) (continued)

US Army Engineer Research and Development Center
Coastal and Hydraulics Laboratory
3909 Halls Ferry Road
Vicksburg, MS 39180-6199

Hydrologic Engineering Center, US Army Corps of Engineers
609 Second Street
Davis, CA 95616-4687

Department of Civil and Environmental Engineering
Wallace H. Coulter School of Engineering
Clarkson University
8 Clarkson Avenue
Potsdam, New York 13699

Reed and Reed Consulting, LLC
1400 Village Square Blvd Unit 3-146
Tallahassee, FL 32312

Aquaveo, LLC
3210 N. Canyon Road
Provo, UT 84604